DEVELOPMENT AND VALIDATION OF A FINITE ELEMENT DUMMY MODEL FOR AEROSPACE AND SPACEFLIGHT SAFETY APPLICATIONS

Jacob B. Putnam

Thesis Submitted to the Faculty of Virginia Polytechnic Institute and State University in partial fulfillment of the requirements for the degree of

MASTER OF SCIENCE
In
Biomedical Engineering

Costin D. Untaroiu, Chair
Stefan M. Duma
Warren N. Hardy
Martin S. Annett

June 17, 2014
Blacksburg, VA

Keywords:

Keywords: *finite element modeling, impact biomechanics, dummy model, optimization, sensitivity analysis.*

Development and Validation of a Finite Element Dummy Model for Aerospace and Spaceflight Safety Applications

Jacob B. Putnam

ABSTRACT

Anthropometric test devices (ATDs), commonly referred to as crash test dummies, are tools used to conduct aerospace and spaceflight safety evaluations. Finite element (FE) analysis provides an effective complement to these evaluations. In this work a FE model of the Test Device for Human Occupant Restraint (THOR) dummy was developed, calibrated, and validated for use in aerospace and spaceflight impact analysis.

A previously developed THOR FE model was first evaluated under spinal loading. The FE model was then updated to reflect recent updates made to the THOR dummy. A novel calibration methodology was developed to improve both kinematic and kinetic responses of the updated model in various THOR dummy certification tests. The updated THOR FE model was then calibrated and validated under spaceflight loading conditions and used to asses THOR dummy biofidelity.

Results demonstrate that the FE model performs well under spinal loading and predicts injury criteria values close to those recorded in testing. Material parameter optimization of the updated model was shown to greatly improve its response. The validated THOR-FE model indicated good dummy biofidelity relative to human volunteer data under spinal loading, but limited biofidelity under frontal loading.

The calibration methodology developed in this work is proven as an effective tool for improving dummy model response. Results shown by the dummy model developed in this study recommends its use in future aerospace and spaceflight impact simulations. In addition the biofidelity analysis suggests future improvements to the THOR dummy for spaceflight and aerospace analysis.

ACKNOWLEDGEMENTS

I would first like to thank my advisor, Costin Untaroiu for his continual guidance and support. I would like to thank my committee members, Stefan Duma, Warren Hardy, and Martin Annett for their insight and help in completing this work. I would like to thank Jeff Somers of Wyle Laboratories his valuable support throughout this work. I am indebted to all the members of the Virginia Tech Center for Injury Biomechanics for sharing their knowledge and expertise with me. Finally, I would like to thank my family and friends for all of their guidance and support throughout the years.

ATRIBUTION

Several colleagues aided in the writing and research behind chapters presented as part of this dissertation. A brief description of their contribution is included here.

Chapter 2: FINITE ELEMENT MODEL OF THE THOR-NT DUMMY UNDER VERTICAL IMPACT LOADING FOR AEROSPACE INJURY PREDICTION: MODEL EVALUATION AND SENSITIVITY ANALYSIS

Chapter 2 was accepted for publication in the Journal of the American Helicopter Society.

Costin D. Untaroiu, (Center for Injury Biomechanics, School of Biomedical Engineering), is currently an associate professor in biomedical engineering at Virginia Tech. Dr. Untaroiu was a co-author on this paper, principle investigator for the contracts supporting the research, and contributed editorial comments.

Justin Littell, (Landing and Dynamics Impact Research Facility, NASA Langley Research Center), is currently a test engineer at the NASA Langley Research Center. Dr. Littell was a co-author on this paper and conducted the physical tests used in the study.

Martin Annette, (Landing and Dynamics Impact Research Facility, NASA Langley Research Center), is currently a research aerospace engineer at the NASA Langley Research Center. Mr. Annette was a co-author on this paper and conducted the physical tests used in the study.

Chapter 3: THE DEVELOPMENT, CALIBRATION, AND VALIDATION OF A HEAD-NECK COMPLEX OF THOR MOD KIT FINITE ELEMENT MODEL

Chapter 3 was accepted for publication in Traffic Injury Prevention

Jeff T. Somers, (NASA Human Research Program, Wyle Integrated Science and Engineering Group), is currently a project engineer at Wyle laboratories. Mr. Somers was a co-author on this paper and contributed editorial comments.

Costin D. Untaroiu, (Center for Injury Biomechanics, School of Biomedical Engineering), is currently an associate professor in biomedical engineering at Virginia Tech. Dr. Untaroiu was a co-author on this paper, principle investigator for the contracts supporting the research, and contributed editorial comments.

Chapter 4: THE DEVELOPMENT, CALIBRATION, AND VALIDATION OF A HEAD-NECK COMPLEX OF THOR MOD KIT FINITE ELEMENT MODEL

Chapter 4 was submitted for publication in Accident Analysis & Prevention

Jeff T. Somers, (NASA Human Research Program, Wyle Integrated Science and Engineering Group), is currently a project engineer at Wyle laboratories. Mr. Somers was a co-author on this paper and helped conduct the physical tests used in the study.

Costin D. Untaroiu, (Center for Injury Biomechanics, School of Biomedical Engineering), is currently an associate professor in biomedical engineering at Virginia Tech. Dr. Untaroiu was a co-author on this paper, principle investigator for the contracts supporting the research, and contributed editorial comments.

Table of Contents

Development and Validation of a Finite Element Dummy Model for Aerospace and Spaceflight Safety Applications i

Abstract ii

Acknowledgements iii

Atribution iv

Table of Contents vi

List of Figures ix

List of Tables xii

1. Introduction and Background 1

1.1. Aerospace and Spaceflight Impacts Injuries 1

1.2 Use of Crash Dummies in Safety Analysis 2

1.3. Finite Element Analysis 3

1.4. Brief Summaries of Chapters 4

1.5. References 6

2. Finite Element Model of the THOR-NT Dummy under Vertical Impact Loading for Aerospace Injury Prediction: Model Evaluation and Sensitivity Analysis 7

2.1 Abstract 8

2.2 Introduction 8

2.3 Methods 10

2.3.1 THOR Model Updates 10

2.3.2 Modeling Test Conditions 11

2.3.3 Finite Element (FE) Simulations 12

2.3.4 Quantitative Model Evaluation: CORA Rating System 14

2.3.5 Injury Criteria Comparisons 15

2.3.6 Positioning Sensitivity Analysis 16

2.4 Results 17

2.4.1 Kinematic (Acceleration) Response 17

2.4.2 Kinetic (Loading) Response 20

2.4.3 Overall Model Response 22

2.4.4 Injury Criteria 23

2.4.5 Sensitivity Study of Pre-Impact Dummy Position 24

2.5 Discussion 25
2.5.1 Model Response 26
2.5.2 Injury Criteria 29
2.5.3 Sensitivity Study of Pre-Impact Dummy Position 30
2.6 Conclusions 32
2.7 References 33
3. The Development, Calibration, and Validation of a Head-Neck Complex of THOR Mod Kit Finite Element Model 35
3.1 Abstract 36
3.2 Introduction 37
3.3 Methods 38
3.3.1 Development of the head-neck dummy FE model 38
3.3.2 Model rating system and optimization techniques 41
3.3.3 Calibration of the head-neck dummy FE model 45
3.3.4 Validation of the head-neck dummy FE model 53
3.3.5. Sensitivity Analysis of the Head-Neck Model relative to Pre-Impact Dummy Position in a Frontal Crash 54
3.4 Results 56
3.4.1 Model Calibration 56
3.4.2 Model Validation 61
3.4.3 Sensitivity Analysis 63
3.5 Discussion 64
3.6 Conclusions 67
3.7 Acknowledgments 68
3.8 References 68
4. Development and Evaluation of a Dummy Finite Element Model for Occupant Protection of Spaceflight Crewmembers 71
4.1 Abstract 72
4.2 Introduction 73
4.3 Methods 75
4.3.1 Development/updating of THOR Dummy Model 75
4.3.2 Model Calibration 76

4.3.3 Model Validation 83
4.3.4 Comparison of Dummy-to-Human responses under Spinal and Frontal Impact Loadings 84
4.4 Results and Discussion 86
4.4.1 Model Calibration 86
4.4.2 Validation of Dummy FE Model 90
4.4.3 Comparison to human response 92
4.5 Discussion 94
4.5.1 THOR-k FE Model Calibration and Validation 95
4.5.2 Biofidelity Analysis 96
4.6 Acknowledgments 99
4.7 References 99
5. Conclusion 102
5.1 Future Work 103

List of Figures

Figure 1-1. Loading paths of (a) aerospace crash[6] and (b) spaceflight water landing [7]. 2

Figure 1-2. Spine shape comparison of HIII typically used in (a) frontal impact analysis [10] [11] and (b) spinal impact analysis [11]. 3

Figure 2-1. Comparison between pretest conditions of experiment (a) and FEM (b). 12

Figure 2-2. Deceleration pulses. 2010-1 (A), 2012-1 (B) and 2012-3 (C) 13

Figure 2-3**.** Time histories of local head vertical acceleration. 2010-1 (A), 2012-1 (B), 2012-3 (C). 18

Figure 2-4**.** Time histories of local horizontal head CG acceleration. 2010-1 (A), 2012-1 (B), 2012-3 (C). 18

Figure 2-5**.** Time histories of local vertical T1 acceleration. 2010-1 (A), 2012-1 (B), 2012-3 (C). 19

Figure 2-6**.** Time histories of local vertical T12 acceleration. 2010-1 (A), 2012-1 (B), 2012-3 (C). 19

Figure 2-7**.** Time histories of local vertical upper neck load. 2010-1 (A), 2012-1 (B), 2012-3 (C). 20

Figure 2-8. Time histories of local sagittal upper neck moment. 2010-1 (A), 2012-1 (B), 2012-3 (C). 20

Figure 2-9**.** Time histories of local vertical lower neck load. 2010-1 (A), 2012-1 (B), 2012-3 (C). 21

Figure 2-10. Time histories of local sagittal lower neck moment. 2010-1 (A), 2012-1 (B), 2012-3 (C). 22

Figure 2-11**.** Time histories of local vertical lumbar spine load. 2010-1 (A), 2012-1 (B), 2012-3 (C). 22

Figure 2-12**.** Variation of HIC_{15} values relative to head and thorax rotations. 2010-1 (A), 2012-1 (B), 2012-3 (C)..... 25

Figure 2-13**.** Variation of maximum vertical lumbar load relative to head and thorax rotations. 2010-1 (A), 2012-1 (B), 2012-3 (C). 25

Figure 3-1**.** Comparison between the FE models of: (a) THOR-NT and (b) THOR-k. 39

Figure 3-2**.** (a) Cross-section of Head THOR-k FE model through the updated parts of THOR (b) Models of THOR-k dummy instrumentation. 40

Figure 3-3**.** (a) The updated OC-joint (rotational spring-based joint) and (b) the angular stiffness assigned to OC-joint. 41

Figure 3-4**.** Schematic of developed calibration method. 42

Figure 3-5**.** CORA Rating System: Corridor Method. 43

Figure 3-6**.** CORA rating system: correlation method factors – (a) phase shift, (b) progression, (c) 44

Figure 3-7**.** (a) The main components related to the head-neck response used in calibration process and (b) the schematic of calibration/validation process. 46

Figure 3-8**.** NBDL test model (lateral) – (a) simulation setup, (b) acceleration pulse. 48

Figure 3-9**.** Pendulum test model (flexion and extension) – (a) simulation setup, (b) rotational acceleration pulse. 50

Figure 3-10**.** Example head spring stiffness optimization curves – (a) loading, (b) unloading. ... 51

Figure 3-11**.** Frontal head impact test setup – (a) physical test (GESAC 2005), (b) FE-simulation. 52

Figure 3-12**.** NBDL test setup (frontal flexion) – (a) model setup, (b) acceleration pulse. 53

Figure 3-13**.** Pendulum lateral simulation – (a) simulation setup, (b) rotational acceleration pulse. 54

Figure 3-14**.** Frontal crash simulation setup: (a) pre impact positioning, (b) sled acceleration pulse. 55

Figure 3-15**.** Positioning sensitivity setup: (a) belt translation, (b) upper body rotation. 56

Figure 3-16**.** Model Calibration: NBDL lateral time history CORA rating comparison: (a) upper neck lateral force, (b) upper neck vertical force, (c) upper neck coronal moment, (d) lower neck lateral force, (e) lower neck vertical force, (f) lower neck coronal moment, (g) head lateral displacement, (h) head vertical displacement, (i) head coronal rotation angle, (j) total CORA rating (original | calibrated)..... 57

Figure 3-17**.** Model Calibration: Pendulum extension time history comparison: (a) upper neck horizontal force, (b) upper neck vertical force, (c) upper neck sagittal moment, (d) front spring force, (e) OC-joint rotation angle, (f) total CORA rating (original | calibrated). 59

Figure 3-18. Model Calibration: Pendulum flexion time history comparison: (a) upper neck horizontal force, (b) upper neck vertical force, (c) upper neck sagittal moment, (d) rear spring force, (e) OC-joint rotation angle, (f) total CORA rating (original | calibrated). 60

Figure 3-19**.** Head impact time history comparison: (a) head impact force (b) total CORA rating (original | calibrated). 61

Figure 3-20. Model Validation: NBDL frontal time history comparison: (a) upper neck horizontal force, (b) upper neck vertical force, (c) upper neck sagittal moment, (d) lower neck lateral force, (e) lower neck vertical force, (f) lower neck sagittal moment, (g) head lateral displacement, (h) head vertical displacement, (i) head sagittal l rotation angle, (j) rear spring force, (k) OC-joint rotation angle, (l) total CORA rating. 62

Figure 3-21. Model Validation: Pendulum lateral time history comparison: (a) upper neck lateral force, (b) upper neck vertical force, (c) upper neck coronal moment, (d) CORA score. 63

Figure 3-22. Sensitivity Results: (a) Sobol global sensitivities, (b) HIC_{36} response surface, (c) N_{IJ} response surface. 64

Figure 4-1**. (**a) Schematic of the calibration & validation of the THOR-k FE Model with (b) diagram of calibrated parts..... 77

Figure 4-2**.** Pelvis flesh quasi-static compression setup: FE simulation. 78

Figure 4-3. THOR-k dummy and test setup: (a) physical, (b) FE-Models, (c) belt stiffness curves. 79

Figure 4-4. Model Calibration: Acceleration pulses used in the THOR-k simulations. (a) The spinal (vertical) direction, (b) the frontal (horizontal) direction. 80

Figure 4-5. Schematic of CORA rating methodology. 81

Figure 4-6. Schematic of the calibration method. 82

Figure 4-7. (a) Stress-strain curves of pelvis flesh model. Force displacement curves of spinal column rubber: (b) loading and (c) unloading. 83

Figure 4-8. Model Validation: Acceleration pulses used in the THOR-k simulations. (a) The spinal (vertical) direction and (b) the frontal (horizontal) direction. 84

Figure 4-9. Physical test vs. FE model: (a) frontal test setup (test # 200301) and (b) spinal test setup (test #199906). 85

Figure 4-10. Pelvis flesh quasi static force vs. displacement response: (a) pre optimization, (b) post optimization. 87

Figure 4-11. Model Spinal Calibration – pulse 10g @ 70 ms impact time history comparison in vertical direction: (a) head CG acceleration, (b) chest acceleration, (c) pelvis acceleration, (d) upper neck force, (e) lower neck force, (f) lumbar spine force, (g) total CORA rating. 89

Figure 4-12. Model Frontal Calibration – pulse 10g @ 70 ms impact time history comparison in horizontal direction: (a) head CG acceleration, (b) chest TRACC displacement, (c) pelvis acceleration, (d) upper neck force, (e) upper neck moment, (f) lower neck force, (g) lower neck moment, (h) total CORA rating. 90

Figure 4-13. Model Spinal Validation – pulse 10g @ 40 ms impact time history comparison in spinal direction: (a) head CG acceleration, (b) chest acceleration, (c) pelvis acceleration, (d) upper neck force, (e) lower neck force, (f) lumbar spine force, (g) total CORA rating. 91

Figure 4-14. Model Frontal Validation – pulse 8g @ 100 ms impact time history comparison in horizontal direction: (a) head CG acceleration, (b) chest TRACC displacement, (c) pelvis acceleration, (d) upper neck force, (e) upper neck moment, (f) lower neck force, (g) lower neck moment, (h) total CORA rating. 92

Figure 4-15. Dummy FE model vs. Human volunteer Comparison: Kinematic responses under spinal loading: (a) head acceleration, (b) chest acceleration, (c) total CORA rating, (d) total bio-fidelity rating. 93

Figure 4-16. Dummy FE model vs. Human volunteer Comparison: Kinematic responses under frontal loading: (a) head acceleration, (b) chest acceleration, (c) total CORA rating, (d) total bio-fidelity rating. 94

List of Tables

Table 2-1. Total CORA Rating 23

Table 2-2. HIC_{15} and HIC_{36} Values: Comparison Test vs. Simulation. 23

Table 2-3. BC Values: Comparison Test vs. Simulation 24

Table 2-4. Lumbar Load (LL) and its Ratio relative of LL injury limit (1,500 lbs): Comparison Test vs. Simulation 24

Table 3-1. Calibrated Values of Spring Stiffness Parameters 58

Table 3-2. Calibrated Values of Head-Skin Material Parameters 60

Table 4-1. The Age and Anthropometric Information of WPAFB Male Volunteer subjects 84

Table 4-2. Pelvis Flesh Quasi-Static Stiffness 87

Table 4-3. The parameters of Calibrated Material Models 88

1. INTRODUCTION AND BACKGROUND

1.1. Aerospace and Spaceflight Impacts Injuries

According to the Air Safety Institute, in 2012 there were a total of 1,375 aerospace crashes in the US (both fixed-wing and rotary) resulting in 376 fatalities[1]. Additionally, approximately 1,000 patients are admitted to the hospital each year in the US with aviation mishap related injuries. Primary regions of injury include lower limb, head, and spine [2-4].

During a space flight, increased injury risk to occupants could occur as both takeoff and landing phases of flight impart significant accelerative loads on the human body [5]. In both aerospace crashes and spaceflight landings the occupant is subjected to multidirectional loading. This presents a complex issue for developing new safety standards and protective measures, as previous biomechanics research has primarily focused on unidirectional loading paths (e.g. FMVSS 208 –frontal crash test).

Primary occupant loading during aerospace crashes in addition to planned multipurpose crew spaceflight vehicle landings is along both the frontal g_x (eyeballs in-out) and spinal g_z (eyeballs up-down) directions (Fig. 1-1) [5]. Though these individual loading directions have been studied extensively (frontal-automotive & spinal-seat ejection), resulting in defined testing standards and devices for both, analysis of combined loading in these directions still lacking. To improve safety in the aeronautic transportation field it is essential to develop a test device which can accurately predict human response in both directions simultaneously. Finite Element (FE) modeling provides an effective tool for improving the efficiency of this process. In order for FE modeling to be used as an effective scientific tool the model must first be validated in conditions similar to its intended use.

a) b)

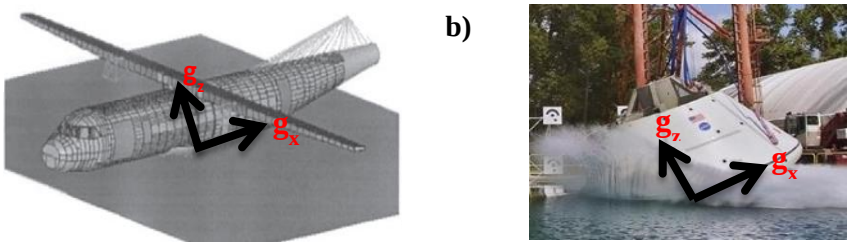

Figure 1-1. Loading paths of (a) aerospace crash[6] and (b) spaceflight water landing [7].

[6] Jackson, K.E., Y.T. Fuchs, and S. Kellas, Overview of the National Aeronautics and Space Administration Subsonic Rotary Wing Aeronautics Research Program in Rotorcraft Crashworthiness. Journal of Aerospace Engineering, 2009. 22(3): p. 229-239. (Used under fair use, 2014)
[7] Vieru, T. Orion Capsule Test Article Completes Its Final Drop Tests.2012 (Used under fair use, 2014)

1.2 Use of Crash Dummies in Safety Analysis

In all sectors of vehicular transport, anthropomorphic test devices (ATDs), commonly referred to as crash test dummies, have been the standard tool for performing crash safety analysis. The current standard for most crash safety requirements is the Hybrid III ATD [8]. This dummy traditionally has a curved lumbar spine region for best dummy response in the frontal impact direction. For spinal impact analysis, this is typically replaced with a straight part (e.g. Hybrid II spine) to better predict spinal response and better align the ATD in the upright posture for crew seats (Fig. 1-2) [9]. Though these configurations of the Hybrid III have proven effective in providing crashworthiness criteria in these individual testing directions, they do not present an option for most accurately capturing a combined loading response.

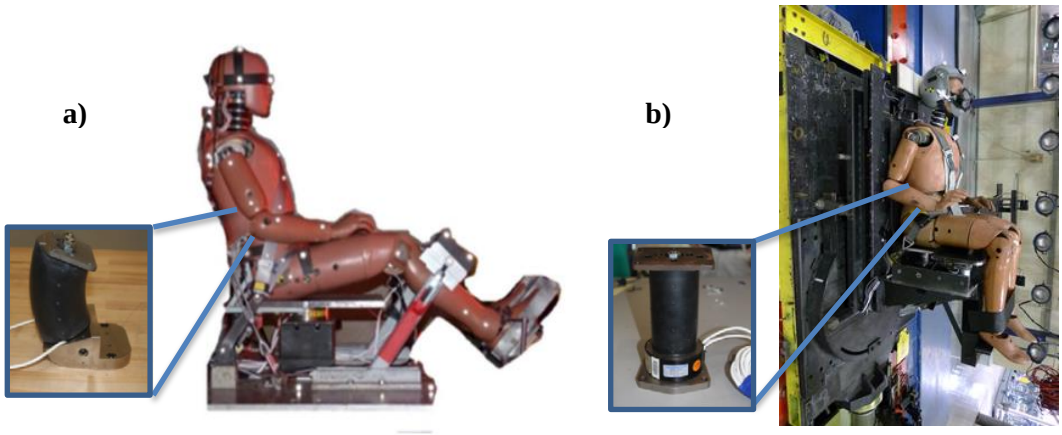

Figure 1-2. Spine shape comparison of HIII typically used in (a) frontal impact analysis [10] [11] and (b) spinal impact analysis [11].

[10] Shaw, C., et al. Response Comparison for the Hybrid III, THOR Mod Kit with SD-3 Shoulder, and PMHS in a Simulated Frontal Crash. in 23rd ESV Conference, Paper. 2013. (Used under fair use, 2014)
[11] Polanco, M.A. and J.D. Littell, Vertical Drop Testing and Simulation of Anthropomorphic Test Devices, in 67th AHS Forum. 2011: Virginia Beach, VA. (Used under fair use, 2014)

The latest ATD developed by the National Highway Safety Administration, the Test Device for Human Occupant Restraint (THOR), has come recently under investigation to bridge the biofidelity gap in both impact directions. The THOR has demonstrated improved biofidelity over the Hybrid III in automotive testing [12]. The THOR was developed to exhibit improved spine and neck kinematics compared to previous ATD's, so improved response is expected in THOR under vertical loading [13]. With this in mind the National Aeronautics and Space Administration (NASA) has undertaken the mission to assess the multidirectional biofidelity of THOR for possible development and implementation of new safety standards for spaceflight.

1.3. Finite Element Analysis

Numerical analysis provides an essential complement to impact testing, demonstrated by its use in crash safety field over the past 50 years [14]. ATD testing has proven to improve vehicle safety, but remains very limited by access to testing facilities, dummy availability, cost, and time of testing. These limitations usually lead to a reduced number of feasible impact tests, which makes the development of new advanced safety standards difficult. Finite Element (FE)

modeling is an advanced numerical tool which allows for the analysis of full scale crash scenarios as well as simulation of testing conditions with much fewer limitations. FE simulations allow for in depth analysis of both ATD and human response in various impact configurations. This presents an opportunity to evaluate dummy response in a wide variety of conditions without the cost and time of extensive testing. In addition, it provides an opportunity for sensitivity analysis and vehicle design optimization, which requires large number of tests not reasonable for physical testing.

A FE model has previously been developed to represent the ATD version THOR-NT. The model was developed in the FE code LS-DYNA (LSTC, Livermore, CA) to match the ATD design specifications. This model was previously calibrated and validated in the horizontal impact direction for use in the automotive industry [15, 16]. In order to be used in the aerospace and spaceflight fields the THOR FE model additionally had to be further validated in the vertical direction. In this work the baseline THOR-NT FE model was evaluated in a series of drop test conditions to assess the validity of its spinal response. The FE model was then updated to match changes recently made to the ATD (THOR Mod Kit). The newly developed THOR FE model (THOR-k model) was then calibrated and validated in both the frontal and spinal loading directions under conditions approximate of a spaceflight landing. The final THOR-k model was simulated under conditions of human volunteer tests performed in both frontal and spinal loading directions and its response compared to test data to assess the THOR biofidelity. In addition, the developed THOR FE model was used to evaluate the sensitivity of dummy response to pre-impact positioning.

1.4. Brief Summaries of Chapters

The subsequent chapters of this work, including title and summary are:

Chapter 2: **Finite Element Model of the THOR-NT Dummy under Vertical Impact Loading for Aerospace Injury Prediction: Model Evaluation and Sensitivity Analysis**

The previously developed THOR-NT FE model was updated for use in the spinal loading environment and its response is evaluated in terms of kinematic, kinetic, and injury criteria predictions. Sensitivity analysis was performed using the updated model to determine sensitivity of injury to pre impact position.

Chapter 3: **The Development, Calibration, and Validation of a Head-Neck Complex of THOR Mod Kit Finite Element Model**

The head neck region of the THOR-NT FE model, essential to dummy mechanics in both frontal and spinal impacts, was updated to the latest specifications of modification made to the THOR-NT by NHTSA. This model was then calibrated to accurately match test data response. Lastly it was validated against a separate test series.

Chapter 4: **Development and Evaluation of a Dummy Finite Element Model for Occupant Protection of Spaceflight Crew Members**

An updated THOR FE model was assembled and calibrated to accurately predict dummy response in both frontal and spinal impacts simultaneously. The resulting model was used to assess THOR biofidelity for aerospace and spaceflight crash safety analysis.

1.5. References

1. A.O.P.A, *2011-2012 GA Accident Scorecard*, 2012: Fredrick, Maryland.
2. Baker, S.P., et al., *Aviation-related injury morbidity and mortality: data from US health information systems.* Aviation, space, and environmental medicine, 2009. **80**(12): p. 1001-1005.
3. Lillehei, K.O. and M.N. Robinson, *A critical analysis of the fatal injuries resulting from the Continental flight 1713 airline disaster: evidence in favor of improved passenger restraint systems.* Journal of Trauma-Injury, Infection, and Critical Care, 1994. **37**(5): p. 826-830.
4. Scullion, J., S. Heys, and G. Page, *Pattern of injuries in survivors of a helicopter crash.* Injury, 1987. **18**(1): p. 13-14.
5. Newby, N., et al., *Assessing Biofidelity of the Test Device for Human Occupant Restraint (THOR) Against Historic Human Volunteer Data.* Stapp Car Crash J, 2013. **57**: p. 469-505.
6. Jackson, K.E., Y.T. Fuchs, and S. Kellas, *Overview of the National Aeronautics and Space Administration Subsonic Rotary Wing Aeronautics Research Program in Rotorcraft Crashworthiness.* Journal of Aerospace Engineering, 2009. **22**(3): p. 229-239.
7. Vieru, T. *Orion Capsule Test Article Completes Its Final Drop Tests*. 2012.
8. Transportation, U.S.D.o., *Federal Motor Vehicle Safety Standards and Regulations*, 1998, National Highway Traffic Safety Administration: Washington, DC.
9. Gowdy, V., et al., *A lumbar spine modification to the hybrid iii atd for aircraft seat tests*, 1999, SAE Technical Paper.
10. Shaw, C., et al. *Response Comparison for the Hybrid III, THOR Mod Kit with SD-3 Shoulder, and PMHS in a Simulated Frontal Crash*. in *23rd ESV Conference, Paper*. 2013.
11. Polanco, M.A. and J.D. Littell, *Vertical Drop Testing and Simulation of Anthropomorphic Test Devices*, in *67th AHS Forum*2011: Virginia Beach, VA.
12. Shaw, G., J. Crandall, and J. Butcher, *Comparative evaluation of the THOR advanced frontal crash test dummy.* International Journal of Crashworthiness, 2002. **7**(3): p. 239-253.
13. Haffner, M., et al. *Foundations and elements of the NHTSA THOR alpha ATD design*. in *Proc. 17th ESV Conference, Amsterdam*. 2001.
14. Yang, K.H., et al., *Development of numerical models for injury biomechanics research: a review of 50 years of publications in the Stapp Car Crash Conference.* Stapp car crash journal, 2006. **50**: p. 429-490.
15. Untaroiu, C., et al., *Evaluation of a finite element of the Thor-NT dummy in frontal crash environment*, in *ESV Conference*2009: Stuttgart, Germany.
16. Untaroiu, C. and Y.-C. Lu, *A Simulation-Based Calibration and Sensitivity Analysis of a Finite Element Model of THOR Head-Neck Complex*, in *SAE 2011 World Congress & Exhibition*, SAE, Editor 2011: Detroit, USA.

2. FINITE ELEMENT MODEL OF THE THOR-NT DUMMY UNDER VERTICAL IMPACT LOADING FOR AEROSPACE INJURY PREDICTION: MODEL EVALUATION AND SENSITIVITY ANALYSIS

Jacob B. Putnam, Costin D. Untaroiu, Justin Littell, Martin Annett

Manuscript accepted for publication in *Journal of the American Helicopter Society* on May 31, 2014
(Currently in press)

2.1 Abstract

Anthropometric test devices (ATDs), commonly referred to as crash test dummies, are tools used to conduct aerospace safety evaluations. In this study, the latest finite element (FE) model of the Test Device for Human Occupant Restraint (THOR) dummy was simulated under vertical impact conditions based on data recorded in a series of drop tests conducted at the NASA Langley Research Center (LaRC). The purpose of this study was threefold. The first was to improve and then evaluate this FE model for use in a vertical loading environment through kinematic and kinetic response comparisons. The second was to evaluate dummy injury criteria under variable impact conditions. The last was to determine the response sensitivity of the FE model with respect to its pre-impact postural position. Results demonstrate that the updated FE model performs well under vertical loading and predicts injury criteria values close to those recorded in testing. In the postural sensitivity study, the head injury criteria (HIC) response and peak lumbar load (LL) are primarily sensitive to the pre-impact head angle and thorax angle, respectively. Results shown by the dummy model are promising for conducting impact simulations with vertical deceleration pulses. In addition, it is believed that assigning accurate viscoelastic material properties to the deformable parts of the model may further increase the model fidelity for a larger range of impacts.

2.2 Introduction

The safety of aerospace transport is evaluated primarily through testing of anthropometric test devices (ATDs), commonly known as crash test dummies. These evaluations are essential to the development of improved aerospace technology in both the military and civilian sectors, as safety remains the priority in all sectors of vehicular transport. Historically, the Hybrid II,

Aerospace Hybrid III, and FAA Hybrid III dummies have been the most commonly used crash dummies in aerospace crashworthiness testing.

Recently, researches at National Aeronautics and Space Administration (NASA) have been investigating the development of aerospace occupant protection standards specific to the Test Device for Human Occupant Restraint (THOR) dummy. The THOR dummy, developed and continuously improved by National Highway Traffic Safety Administration (NHTSA) [1], exhibits improved biofidelity over the current automotive industry standard Hybrid III dummy [2]. Impact tests have been conducted on the THOR-NT dummy under automotive collision conditions [3]. Unlike during the majority of automotive collisions, the crewmembers are subjected to a combined frontal and spinal loading during aerospace crashes as well as spaceflight launch and landings. To be recommended for use within the aerospace industry, the performance of this dummy in vertical impact conditions must first be evaluated. A series of drop tests were performed using the THOR-NT dummy at the NASA Langley Research Center (LaRC) [4]. The THOR response was evaluated in comparison to other dummies tested under similar conditions [5].

Dummy testing provides an effective method for vehicular safety evaluation. However, the high cost and limited availability of dummies makes performing large numbers of impact tests in a multitude of aerospace configurations difficult. Numerical simulations may provide an important complement to testing through the evaluation of dummy model response as they are not constrained by these limitations. Currently available finite element (FE) codes such as LS-DYNA are capable of modeling accurate vehicle structural response during a crash impact [6]. However, validation of test dummy models in relevant impact scenarios is necessary in order to confidently employ FE analyses in both the design and safety evaluation phase of rotorcraft.

In this study, the current THOR-NT FE model [7] is evaluated in terms of both kinematic and kinetic response as well the predicted injury risk in comparison to the test data recorded during recent dummy tests performed at NASA LaRC [4]. Finally, the effect of pre-impact postural position on dummy response is investigated in a model sensitivity evaluation.

2.3 Methods

2.3.1 THOR Model Updates

The latest available version of THOR-NT dummy FE model [7] was used in this study. The model contains a total of 239,031 nodes and 453,094 elements. Preliminary simulations of a subset of tests from the test series were conducted on this model to obtain confidence in model performance. Based on the results of these preliminary simulations, a series of refinements were applied to improve this model and accurately simulate the test series.

Defined locking joints were created at the lower neck and lumbar spine load cell locations on the model, in order to accurately calculate loading at these locations. The upper neck loads were calculated using a defined cross section through the middle of the upper neck load cell. Local coordinate systems and/or accelerometers were defined for all model outputs.

The stiffness of the original OC (Occipital Condoyle)-joint was controlled by contact friction defined between the OC-cam and stoppers. This technique was unstable at high rotation rates due to high deformations of stopper elements. Therefore, this contact-based joint was replaced by a defined joint between the upper neck and the head. A defined moment vs. rotation angle stiffness curve was applied to this joint based on test data provided by NHTSA. Both THOR FE models, with the original and modified OC-Joints, showed similar response in THOR pendulum flexion simulations, modeled in accordance with the pendulum certification test described in the THOR

certification manual [8]. In addition, the stiffness of the pelvis material model also was tuned to improve the model fidelity under vertical loading.

To improve positioning ability for vertical impact conditions, the positioning tree of the THOR FE model was updated. A rotational axis was added at the neck and lower thoracic spine pitch change mechanisms. This allowed the model to be positioned in an upright manner matching that of the simulated vertical loading scenario. This addition to the THOR FE model is essential for future use in aerospace testing. All results presented in this paper are produced with the updated model described in this section.

2.3.2 Modeling Test Conditions

In the vertical impact tests, the THOR-NT dummy was placed in an upright seated position and restrained to a rigid seat by minimally tensioned straps on the legs and chest. Then, the seat was dropped from a specified height onto a cardboard honeycomb block which generated a specific deceleration pulse upon impact [4].

A seat model was developed to the specifications of the physical seat used in the tests [4]. Cardboard padding, placed between the dummy and the seat, was modeled in LS-PREPOST (LSTC, Livermore, CA) based on dimensions of the padding used in testing. The material properties of this padding were assigned based on data found in literature (20 GPa elastic modulus) [9]. The straps were modeled as using a combination of seat belt shell elements, with the belt elements pretensioned to 70 N around the dummy model.

The THOR-NT FE model was positioned within the seat model based on photogrammetric imagery of the dummy recorded prior to testing (Fig. 2-1). Landmark locations were measured

relative to a point centered at the base of the seat. Using LS-PREPOST the model was adjusted to match landmark locations to corresponding locations recorded on the physical dummy.

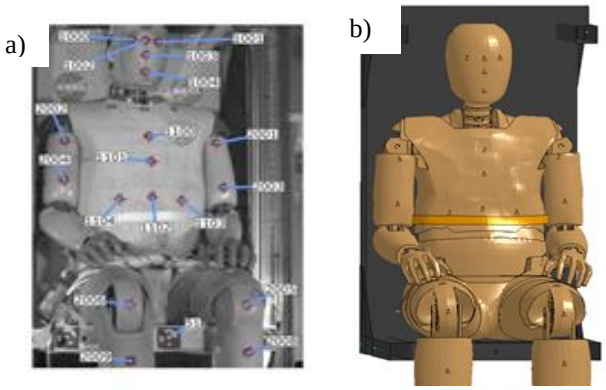

Figure 2-1. Comparison between pretest conditions of experiment (a) and FEM (b).

2.3.3 Finite Element (FE) Simulations

FE simulations were run in LS-DYNA FE software (LSTC, Livermore, CA, USA) on a desktop PC with an Intel® Core™ i7-2600 CPU @ 3.4 GHz processor. The simulation time step was 0.63 μs with an average computation time of approximately 30 hours per a complete simulation of a vertical impact test. Kinematic conditions of the seat were replicated in the FE simulation using the pre-impact velocity and crash pulse deceleration data measured during testing. In this study three deceleration pulses were examined (Fig. 2-2). The first pulse, 2010-1, had been used in previous vertical drop testing of the Hybrid II and III dummies [5]. The 2012-1 pulse closely approximates the rotorcraft impact pulse outlined in 14 CFR xx.562 regulations. Lastly the 2012-3 pulse, similar to the predicted landing acceleration pulse of the Orion Multipurpose Crew Vehicle for space flight, was evaluated [4, 5] . The acceleration waveform shape from the 2012-3 test condition is much different than the response from the other two test conditions. The first two nominal pulses are trapezoid shaped pulses while the 2012-1 pulse is half-sine [4].

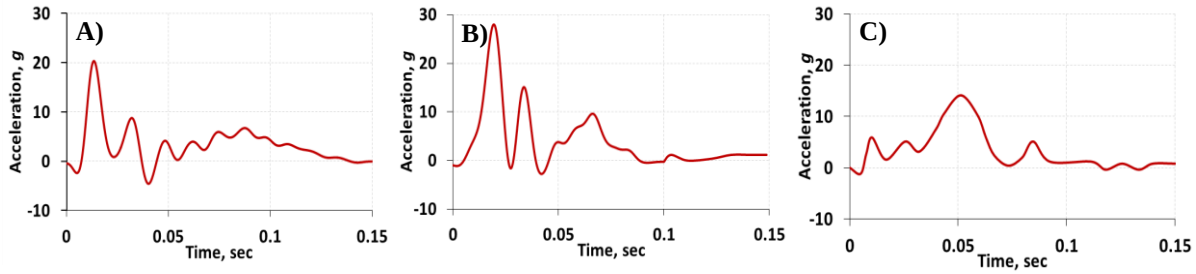

Figure 2-2. Deceleration pulses. 2010-1 (A), 2012-1 (B) and 2012-3 (C)

These impact tests were chosen to best encompass the range of testing conditions for comparison. Initial velocity was prescribed on all dummy and seat model parts based on the test pre-impact velocity. The acceleration time history of the seat, recorded in testing and filtered in accordance with guidelines set forth by SAE J211[10], was assigned to the seat model. Gravitational acceleration (9.81 m/s^2) was applied to all dummy parts in the FE simulation. Dummy kinematics and loading data were calculated during the simulations in their respective local coordinate systems, defined based on the local coordinate systems of physical dummy accelerometers and load cells. As in testing, simulation data were sampled at 10 kHz. Acceleration response during simulation was calculated at the head center of gravity (CG), thorax, pelvis, T1 vertebrae, and T12 vertebrae locations on the dummy model. Force and moment response were calculated at the upper neck, lower neck, and lumbar spine load cell locations. All simulation output was filtered in accordance with the recommended practices established in SAE J211[10]. Comparisons of the time history data between test and simulation response were performed for accelerations in the head CG, T1 vertebrae, and T12 vertebrae. Vertical load was compared at the upper neck, lower neck, and spine. In addition, the sagittal moment at the upper and lower neck load cells were compared.

2.3.4 Quantitative Model Evaluation: CORA Rating System

In the safety analysis, dummy/human models have been traditionally evaluated against test data by comparing the peak values, evaluating entire time histories qualitatively, or through certification guidelines [11]. These methods are limited as they do not provide a standard method for evaluating a wide range of instrumented signals in a complete manner. Peak comparisons provide quantitative evaluation of peak response, but provide no insight to the quality of the whole response. Qualitative evaluations can provide some insight into the overall response quality but are inherently subjective. Certification guidelines are only available for specific tests and signals. To amend these limitations the Technical Specification and Standard for the TC22/SC10/SC12/WG4 "Virtual Testing" Working Group as well as others organizations [12] have been focused on developing a systematic methodologies for model evaluations [13-17], particularly for impact tests where a large number of channels must be compared. Though the final system has yet to be released [17], the system currently being proposed for the International Organization for Standardization (ISO) is based primarily on the CORA (CORelation and Analysis) and EEARTH(Enhanced Error Assessment of Response Time Histories) [18] software packages. For this reason, the CORA system was used to quantitatively evaluate the THOR FE model in this study.

The FE model was quantitatively evaluated using the CORA software vers. 3.6[19]. CORA is an objective rating tool, which employs a combination of two sub-rating systems, corridor and cross-correlation[20], to evaluate total correlation between two time history curves. All rating scores are averaged using several weighting factors to give the total score for a certain signal. The corridor method calculates the deviation between a model time history and a reference curve (usually the corresponding test time history) by means of corridor fitting. The cross-correlation

system rates the correlation of the curves based on three characteristics: phase shift, size, and shape. Each system gives a score between 0 and 1 which is averaged to the total CORA rating for that signal [20]. The original values recommended by the Partnership for Dummy Technology and Biomechanics (PDB) were used to define the corridor and correlation rating metrics for all signals compared. The interval of evaluation of each signal was set to the total simulation time (0.15 sec) for each specific test pulse. A total model rating score was developed for each simulation by averaging the individual scores of all recorded signals.

2.3.5 Injury Criteria Comparisons

Three commonly accepted injury criteria were compared between the FE model and physical dummy. The first was the Head Injury Criterion (HIC); an injury criterion widely accepted and used in safety regulations and consumer tests [21]:

$$HIC_{\Delta t} = \max_{t_2 - t_1 \le \Delta t} \left\{ \frac{1}{(t_2 - t_1)^{3/2}} \left[\int_{t_1}^{t_2} a(t)dt \right]^{5/2} \right\}, \tag{2.1}$$

The magnitude of the linear acceleration observed at the head CG is described by *a(t)*. Time intervals (Δt) of 15 milliseconds (ms) and 36 ms were used to calculate the HIC_{15} and HIC_{36}, respectively. Established injury thresholds for a mid-size male dummy are 700 and 1000 for the HIC_{15} and HIC_{36}, respectively [1]. One drawback of this criterion is that it is developed to determine injury primarily due to head impacts. Though no head impacts occurred in testing or simulation, HIC does still provide application comparing total head acceleration response between dummy and dummy model.

The next metric evaluated was the Lower Neck Beam Criterion (BC). This criterion was chosen over Nij [22] due to a higher prevalence of lower neck injuries (C5/T1) than upper neck

injuries (C1) observed in vertical Post Mortem Human Surrogate PMHS impact tests [23, 24]. BC was originally developed to quantify the risk of injury in helicopter pilots during controlled 30° nose-in crashes[24]. The BC is calculated based on maximum vertical load (F_z) and anterior/posterior flexion moment of the lower neck ($M_{y)}$ with respect to defined critical values as follows.

$$BC = \frac{F_z}{F_{zc}} + \frac{M_y}{M_{yc}} \tag{2.2}$$

F_{zc} and M_{yc} are critical values specific to the 50th male dummy: 1,220 lbs. (5,430 N) compression and 1248 lb.-in (141 N-m) flexion. BC is used to predict probability of a lower neck injury using the abbreviated injury scale (AIS) [25], where a BC value of 1 indicates a 50% risk of an AIS 2+ neck injury. BC is limited as it mathematically approximates the head-neck region as a uniform beam, and thus its accuracy depends on the flexion-extension bending properties of the head-neck evaluated. In this case because the criterion is used as a comparison of similarity between two test objects rather than a determination of injury it is considered a reasonable approximation.

The final metric evaluated in this study was the Lumbar Load (LL) Criterion. This is defined as the peak vertical load between the pelvis and the lumbar spine. Because there is currently no defined injury threshold specific to the THOR dummy, the defined injury threshold for the Hybrid III 50th male dummy, 1,500 lbs. (6,672 N), was used in this study. In both testing and simulation, the lumbar load values were recorded at the lower spine load cell.

2.3.6 Positioning Sensitivity Analysis

A sensitivity analysis was performed to investigate the effects of the position variation of particular THOR components on vertical impact response under each impact pulse. The first

variable was the pretest position of the head, rotated around the OC-Joint. This variable was chosen because the head may slightly rotate during the pre-impact phase which was not simulated in this study. The pre-impact head angle was examined in a range from -5 to 5 degrees of rotation. The second variable examined was the position of the thorax rotated around the lumbar spine. Though vertical impacts are typically tested in an upright position, the dummy or an actual occupant could potentially be leaning forward prior to impact. The thorax angle was examined in the range of 0 to 5 degrees of rotation. Further rotation was improbable due to interference between the chest jacket and internal structure of the pelvis region. A Latin Hypercube Design of Experiment (DOE) scheme was used in LS-Opt (LSTC, Livermore, CA, USA) to select the head and thorax angles corresponding to 20 pre-test dummy model configurations. The sensitivities of HIC_{15} values and peak lumbar load values were investigated based on the dummy model response extracted from these simulations.

2.4 Results

2.4.1 Kinematic (Acceleration) Response

The FE model exhibits a similar response in head CG local vertical acceleration to the physical dummy (Fig. 2-3). The 2010-1 and 2012-1 simulations show the highest correlation to test response. Both are shown to have closely matching peaks followed by an increased acceleration drop in simulation and a return to matched response towards the end of simulation. The 2012-3 simulation exhibits slightly lower peak acceleration than seen in the test results. Both 2012-1 and 2012-3 simulations exhibit a negative acceleration spike of approximately 20 g (gravitational acceleration - 9.81 m/s^2) as the head approaches zero vertical acceleration. These negative spikes have little effect on the CORA rating scores due mostly of their short durations.

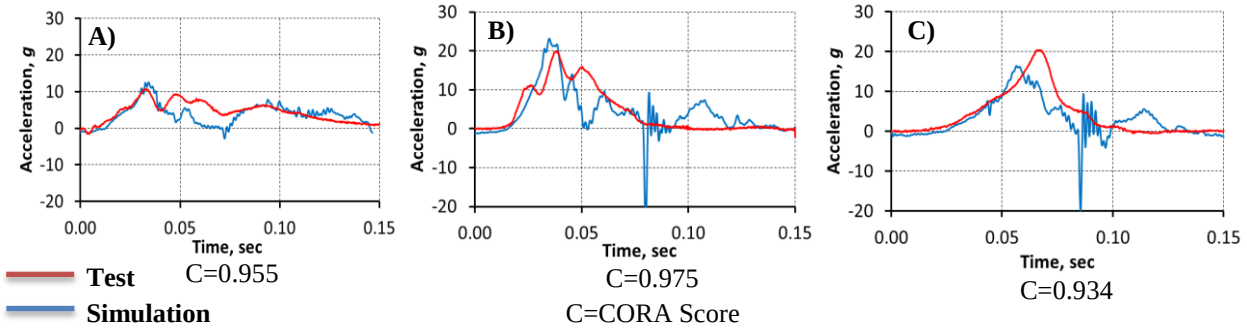

Figure 2-3**.** Time histories of local head vertical acceleration. 2010-1 (A), 2012-1 (B), 2012-3 (C).

Overall, local horizontal acceleration responses in FE simulations matched well with the corresponding responses measured in testing (Fig. 2-4). However, some inherent differences were observed. For example, an increased horizontal acceleration was observed towards the end of 2010-1 simulation, in comparison to the physical test. In the 2012-1 response the greatest difference occurred at the time of peak negative acceleration. The 2012-3 simulation response oscillates about the test response, with the greatest difference occurring towards the middle of the time history curve.

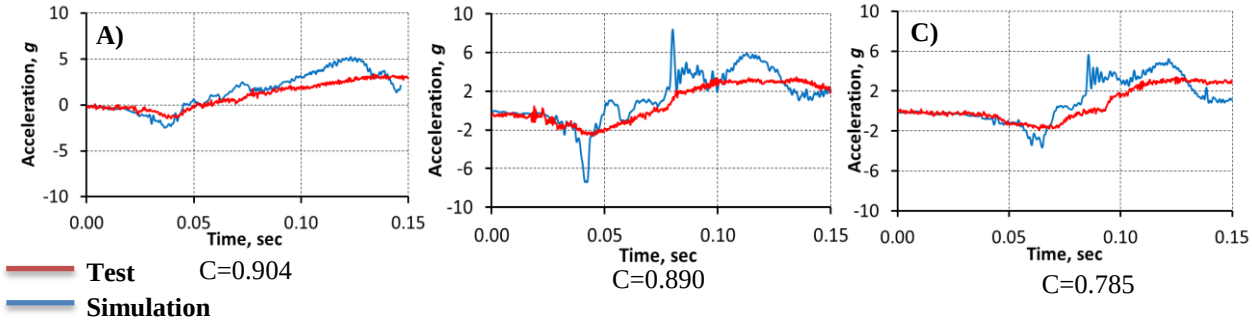

Figure 2-4**.** Time histories of local horizontal head CG acceleration. 2010-1 (A), 2012-1 (B), 2012-3 (C).

The local vertical acceleration responses at the T1 location exhibited a high correlation between simulation and testing curves (Fig. 2-5). The differences observed correspond with differences described in the head CG vertical acceleration. The largest difference is observed in

the 2012-1 simulation. Larger peak acceleration occurred in simulation, followed by a greater drop off.

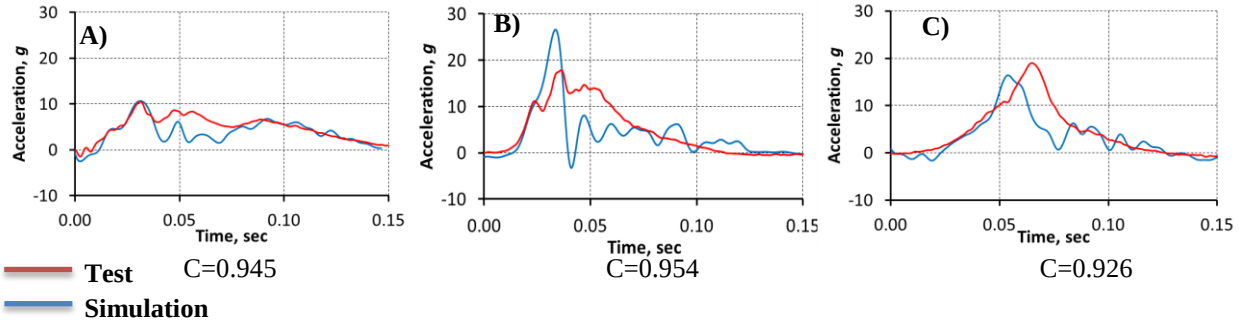

Figure 2-5**.** Time histories of local vertical T1 acceleration. 2010-1 (A), 2012-1 (B), 2012-3 (C).

In both tests and simulations, the shape of local vertical T12 acceleration response is similar to that of T1 (Fig. 2-6). The acceleration peaks in 2010-1 simulation matched the testing data, but relatively larger values were recorded in the other two simulations. The acceleration pulse 2010-1 test does have a higher initial peak than the corresponding peak of 2012-3, but it has a much smaller acceleration plateau. These shape differences in acceleration pulses result in a higher energy transfer to dummy in the 2012-3 test than in the 2010-1 tests which explain the higher acceleration peaks in the dummy responses observed in both testing and FE simulations in 2010-1 test versus 2012-3.

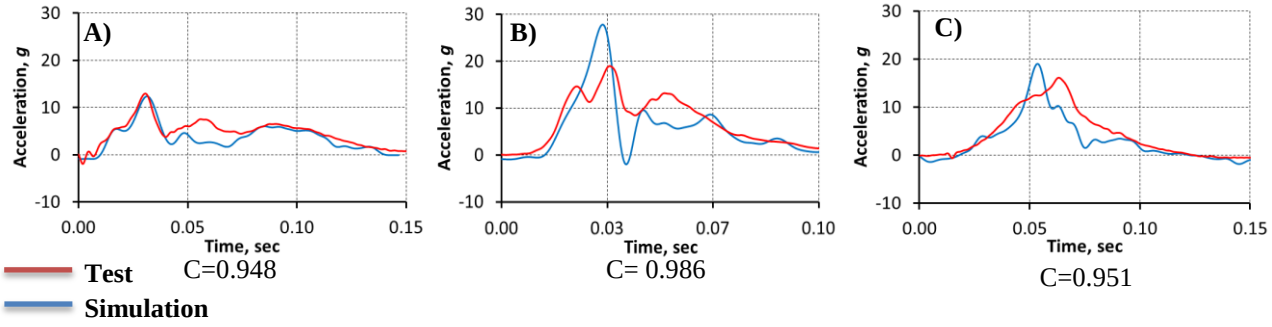

Figure 2-6**.** Time histories of local vertical T12 acceleration. 2010-1 (A), 2012-1 (B), 2012-3 (C).

2.4.2 Kinetic (Loading) Response

Local vertical load responses at the upper neck are shown in Figure 2-7. The 2012-1 simulation exhibits the highest correlation to the test results. The 2012-3 simulation exhibits lower initial peak load while the other tests exhibit higher. Both 2012-1 and 2012-3 simulations exhibit a tensile load spike at the time of the negative head CG vertical acceleration spike. All simulations exhibit a short rise in compressive load following unloading.

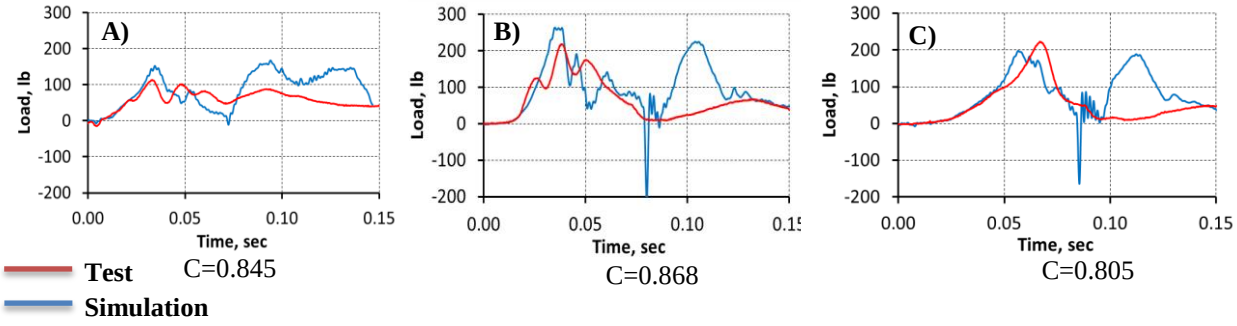

Figure 2-7. Time histories of local vertical upper neck load. 2010-1 (A), 2012-1 (B), 2012-3 (C).

Similar initial peak moments at local upper neck location between test and simulation are exhibited during the initial impact phase (Fig. 2-8). All simulations exhibit a rapid rise as the moment becomes positive. This rise occurs simultaneously with the dramatic rise observed in the upper neck vertical load time history.

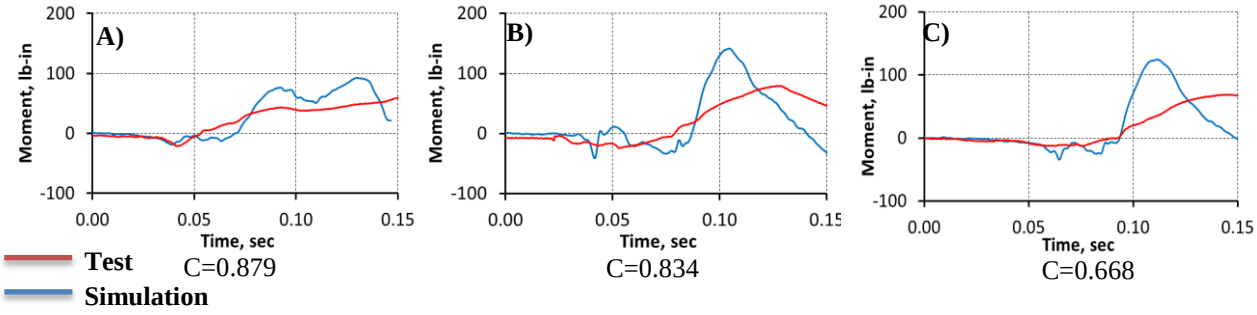

Figure 2-8. Time histories of local sagittal upper neck moment. 2010-1 (A), 2012-1 (B), 2012-3 (C).

The FE model lower neck response correlation varies between the three simulations (Fig. 2-9). Overall a similar initial peak response is observed in all simulations. This is followed by a dramatic increase in FE load response after approximately 70 ms. Low values of CORA scores corresponding to vertical lower neck load are observed for all pulses, the lowest score was calculated for the pulse 2010-1 simulation (0.68). This score was primarily caused by the corridor component of CORA score which penalized the high differences between simulation and test data after about 70 ms. Although the 2012-1 and 2012-3 demonstrate non-physical spikes the duration of the peak differences between test and simulation are much smaller than the 2010-1 pulse, resulting in a smaller penalization.

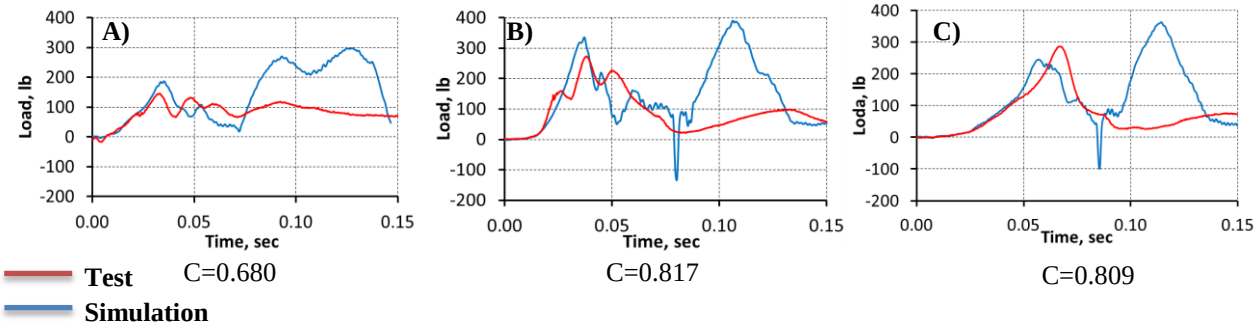

Figure 2-9**.** Time histories of local vertical lower neck load. 2010-1 (A), 2012-1 (B), 2012-3 (C).

In each simulation, similar response is observed towards the beginning and end of the time history of the lower neck moment (Fig. 2-10). A larger moment is observed in the FE model throughout the rest of the simulation. The largest discrepancy is observed in the 2012-1 simulation.

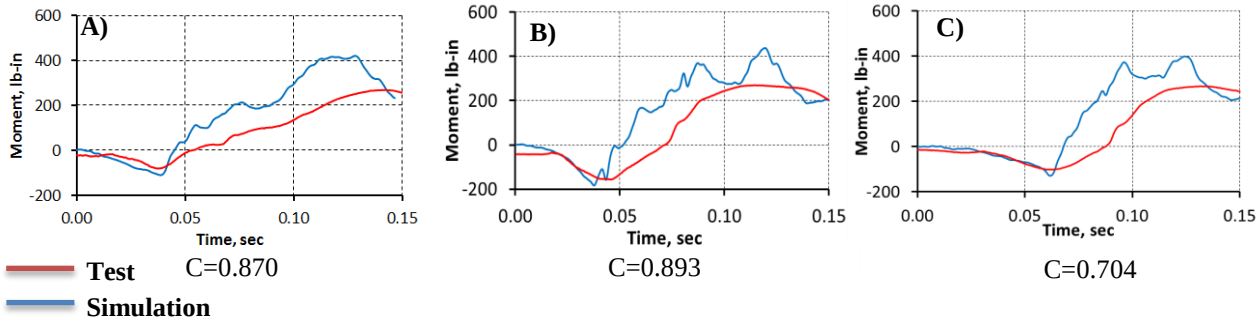

Figure 2-10. Time histories of local sagittal lower neck moment. 2010-1 (A), 2012-1 (B), 2012-3 (C).

The vertical load response at the lumbar spine exhibits similar shape to the physical tests in all simulations (Fig. 2-11). The model predicts dummy response with a high degree of accuracy in the 2010-1 simulation. The differences that do occur are consistent with results throughout the dummy model. All simulations exhibit a faster drop off after peak load. In the 2010-1 and 2012-1 simulations the load drop off is larger than in testing. The 2012-3 simulation exhibits a faster initial rise towards the load peak. The 2012-1 simulation exhibits the highest divergence from test data with a 30% over prediction of peak force. The CORA rating is still above 0.9 in this case because the response is still within the automatic corridors calculated for this response along with similar event timing.

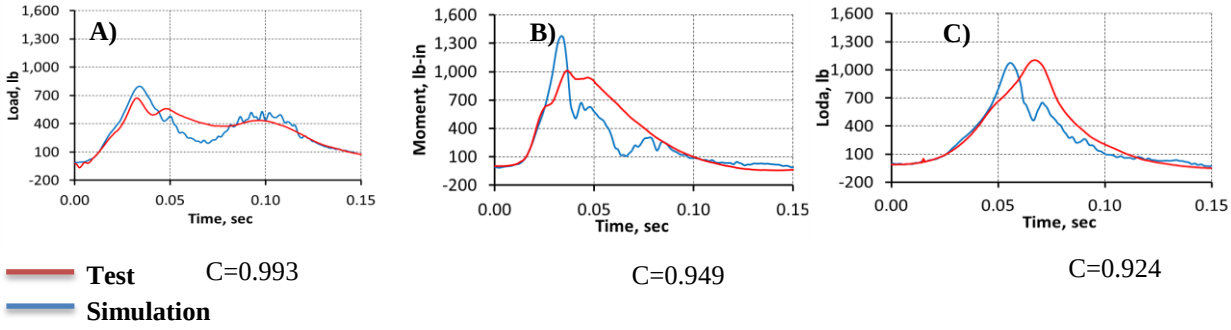

Figure 2-11**.** Time histories of local vertical lumbar spine load. 2010-1 (A), 2012-1 (B), 2012-3 (C).

2.4.3 Overall Model Response

Even though some regions (e.g. neck) showed modest rating scores, the overall FE model response (the average score) correlated relatively well with the test data recorded in all three test

pulses evaluated. Overall, the FE model scored very similar in all three simulations, approximately 0.85-0.9 of 1, with the most well correlated pulse being 2012-1(Table 2-1).

Table 2-1**.** Total CORA Rating

Deceleration Pulse	CORA Rating
2010-1	0.891
2012-1	0.907
2012-3	0.845

2.4.4 Injury Criteria

HIC values at both intervals calculated from test and simulation results are well below the injury thresholds (Table 2-2). The largest test value of HIC_{15} (18.28), seen during the 2012-3 pulse, is 2.61% of the injury limit. In addition, the largest simulation value of HIC_{15} (16.26) exhibited during the 2012-1 pulse is 2.32% of the injury limit (700). Similarly, lower HIC_{36} values than the injury limit (1,000) were observed in both test and simulation. The HIC values observed in these test conditions are well below the peak value because no head impacts occurred under these testing conditions. Generally, larger HIC_{15} values were observed in the FE simulations than in testing, while the test exhibits larger HIC_{36} values.

Table 2-2. HIC_{15} and HIC_{36} Values: Comparison Test vs. Simulation.

Deceleration Pulse	HIC_{15}		HIC_{36}	
	Test	Sim.	Test	Sim.
2010-1	2.24	3.89	4.80	3.65
2012-1	15.18	16.26	24.43	14.08
2012-3	18.28	10.32	19.93	10.51

The values of BC injury criterion calculated from the simulation data are larger than those calculated from test data (Table 2-3). The largest difference was observed in the 2010-1 pulse, while the slightest difference was observed under the 2012-3 pulse.

Table 2-3. BC Values: Comparison Test vs. Simulation

Deceleration Pulse	BC	
	Test	Sim.
2010-1	0.2341	0.3764
2012-1	0.2167	0.3497
2012-3	0.2366	0.3652

Larger Lumbar Load (LL) values were observed in the simulations than in testing for the first two pulses (Table 2-4). However, under the 2012-3 pulse, slightly lower LL value was observed in simulation than in testing. The largest LL value (1,333.7) calculated in the 2012-1 simulation represents 88.91% of the limit for injury threshold (1500 lbs). Similar to the HIC_{15} criteria, the test and simulation LL criteria exhibit different conclusions as to the more injury prone pulse: the test suggests the 2012-3 pulse, while the simulation suggests the 2012-1 pulse.

Table 2-4. Lumbar Load (LL) and its Ratio relative of LL injury limit (1,500 lbs): Comparison Test vs. Simulation.

Deceleration Pulse	LL		LL/LL_{lim} (%)	
	Test	Sim.	Test	Sim.
2010-1	675.0	797.4	44.8	53.2
2012-1	1010.9	1333.7	67.4	88.9
2012-3	1104.5	1073.8	73.6	71.6

2.4.5 Sensitivity Study of Pre-Impact Dummy Position

HIC_{15} values are shown to be primarily sensitive to head rotation angle in all three simulations (Fig. 2-12). HIC_{15} values are shown to increase when the initial head angle increases in both flexion and extension. Changes in HIC_{15} values reach up to 68% of the initial value (head angle $=0^0$). The HIC_{15} sensitivity to thorax rotation angle is smaller and is seen to be dependent on the impact strength of the test pulse (based on peak lumbar load values). The 2010-1 pulse (lowest peak lumbar load value) exhibits almost no dependence (0.9% maximum change due to thorax rotation) while the 2012-3 pulse (largest peak lumbar load value) shows slight dependence (14% maximum change due to thorax rotation).

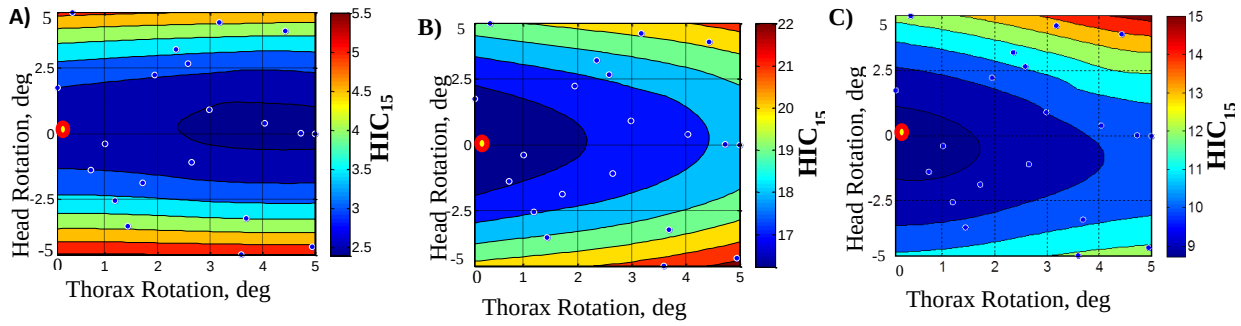

Figure 2-12**.** Variation of HIC_{15} values relative to head and thorax rotations. 2010-1 (A), 2012-1 (B), 2012-3 (C).

Head angle is shown to have a minimal effect on LL values compared to thorax rotation (Fig. 2-13). LL values are primarily sensitive to thorax rotation; the average maximum change in LL values with maximum thorax rotation (5 degrees) is 13%. An increase in thorax angle is shown to cause a general decrease in lumbar load. Similar to the trend observed in HIC_{15}, the sensitivity of LL values to thorax rotation is higher for the pulses which impart larger lumbar load forces (2012-1 and 2012-3).

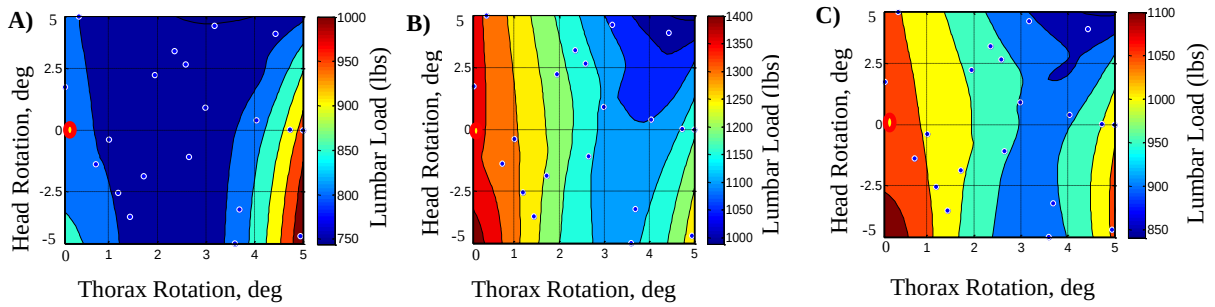

Figure 2-13**.** Variation of maximum vertical lumbar load relative to head and thorax rotations. 2010-1 (A), 2012-1 (B), 2012-3 (C).

2.5 Discussion

A previously developed FE model of THOR-NT by NHTSA and their collaborators was improved in this study to facilitate vertical impact simulations. The OC joint model was simplified relative to the previous model, but its response was preserved and the current model

exhibits better stability. In addition, the updated positioning tree developed in the current study allows an easier and faster setup of the dummy model posture to match the aerospace straight spine configuration. In the preliminary simulations (pulse 2010-1), the dummy model was found to exhibit a stiffer response and several parametric studies were performed to discern the cause of these differences. The influence of pelvis preloading, seat belt position and pre-tensioning, both global and local (T1 vertebrae puck, upper neck load cell, and lumbar spine) part damping, and pelvis material stiffness were investigated. Only the pelvic foam material properties were shown to have major influence on dummy response. Since material testing data for THOR pelvic material are not currently available, the stress-strain curves of its LS-DYNA material model (Mat 83) were scaled. For a more accurate representation of the model and consequently better overall response, parameter identification of its material model from material testing and through model optimization techniques [16, 26, 27], is strongly recommended in the future.

2.5.1 Model Response

The THOR FE model exhibited responses close to physical THOR dummy in most upper body kinematics and kinetics under various vertical impact conditions. The highest average kinematic and kinetic correlations are demonstrated at the T12 vertebrae and in the lumbar load with an average score of 0.963 and 0.958, respectively. Upper and lower neck kinetics exhibits the poorest correlation with average scores of 0.854 and 0.825 respectively. Overall, the average CORA score for all three simulations was 0.894. Though the overall CORA rating proved relatively high there were some discrepancies between individual quantitative analysis and qualitative inspection of the model response. The clearest example of this is found in the head vertical acceleration as well as neck loads. In the 2012-1 and 2012-3 pulses, a ringing type

response is observed in the FE model not seen in the test data. The minimal effect this has on the CORA rating is due to the short duration. The difference is not carried over multiple sections and although that minute section may receive a low score it is washed out in the rest of the curve. This feature of CORA is developed to minimize the effects of noise on the rating but in this case it is a limitation. In addition, the automatic bounds for the corridor evaluation seem to be on occasion too wide for this analysis. This results in a liberal rating score, particularly observed in the lumbar spine for the 2012-1 pulse. Another limitation of CORA is the overall meaning of the calculated scores. While it is possible to discriminate a better model between different variants of the model if the same CORA parameter set is used, the score ranges corresponding to a good/reasonable/poor model were not defined yet. The CORA rating system is currently in the process of being repackaged into a more effective rating standard which may clarify this issue in the future.

Overall the initial peak response between FE model and the THOR dummy were generally similar in magnitude and duration. However, some large oscillations in simulation data compared to test data were observed. These may suggest some inaccuracies in terms of modeling the damping properties of physical dummy. Damping is usually associated with the dissipation of vibration energy through the materials, joints, and sliding contacts. Assigning viscoelastic material models to elastomeric dummy parts based on material characterization tests performed at various rates may significantly improve the material damping characteristics of the model. Damping of joints is defined by moment vs. angular rotation rate curves. Thus, rate dependent testing is recommended on the main dummy joints, such as the OC-joint, to obtain an estimation of joint damping. A Coulomb formulation is used in LS-DYNA to define contact sliding friction.

Friction decreases during the simulation from primarily static friction (μ_s) to dynamic friction(μ_d): $\mu = \mu_s + (\mu_d - \mu_s)e^{-cv_r}$, where c and v_r are the relative velocity between parts in contact and a decay coefficient, respectively. While the values of these parameters are unknown, structural testing may help in providing better estimations of their values. Applying simulation-based identification techniques could help to better calibrate the model[28] based on new test data by providing the best estimation of multiple model parameters.

Vertical accelerations and lumbar load in FE simulations drop considerably after the initial peak, compared to the test results. This response is indicative of the model exhibiting a slight "bounce" in the seat after the initial impact, in a manner not observed in testing. Pre-loading of the model within the seat as well as adjustments of the belt load were performed in attempt to fix this issue, but were found to have little effect on the results. During the slow deceleration rise of the 2012-3 pulse the simulation seams to reach a maximum impact peak faster than the test. In addition initial peak loads and accelerations are generally lower, opposite of the results exhibited by the 2010-1 and 2012-1 pulses. The primary difference between these tests is the pulse duration, 2010-1 and 2012-1 exhibit fast rising and falling short duration peaks while the 2013-3 pulse exhibits a slow rising and falling long duration peak. These observed response differences, shown to be acceleration rate dependent, are likely due to viscoelastic material differences between the physical dummy and the model. Therefore, assigning viscoelastic material properties of dummy components based on material test data followed by a dummy model re-calibration under certification impact tests is recommended in the future.

2.5.2 Injury Criteria

The larger HIC_{15} values exhibited by simulation during the 2010-1 and 2012-1 are due to the slightly higher peak acceleration observed in simulation. The opposite is seen during the 2012-3 pulse due to a lower peak initial acceleration. A larger difference is exhibited in the HIC_{36} values between simulation and test at each pulse. This is likely due to specific shape differences between head acceleration time histories. During the 2010-1 and 2012-1 tests the acceleration drop is slow and steady after the initial peak. This causes the HIC_{36} value, measured over a longer time interval, to increase in comparison to the simulation in which acceleration drop is more dramatic. This effect is not as prevalent in the 2012-3 pulse, as the acceleration shape seems to match more closely during the slower rising and falling deceleration pulse. Though both simulation and test HIC values conclude no head injury risk, the described differences should not be ignored. The difference is shown to increase with sharper and higher impact decelerations and could become of consequence when modeling more violent impact scenarios. In addition, these tests only assess HIC predictions of the FE model due to inertial loading while injuries associated with HIC are typically due to head impacts. Impact test evaluation is necessary to determine the accuracy of the model in determining injury in these scenarios. While the THOR-NT head model was calibrated against a frontal impact (pendulum test and head drop test) in a previous study [7], future work is necessary to assess its prediction in a combined frontal-vertical impact corresponding to aerospace loading conditions with and without head contact.

The FE dummy model is shown to predict higher LL values at higher impact rates. This difference is associated with increased stiffness exhibited in the FE model, causing a larger over-prediction of load response with increased force of impact. Similar to the HIC criterion, this

difference should be taken into account during simulation of more forceful vertical loading scenarios, as it could lead to a difference in pass/fail outcomes between testing and simulation. Additionally, the 1500 lb. threshold defined for 170 lb. ATD's in 14 CFR 27.562 was developed based on testing of the Hybrid II dummy. There are differences between THOR-NT and Hybrid II spine structures and future investigations should be performed for identification of THOR spine injury threshold. In the lower neck region simulation exhibited larger BC values, though the differences were not shown to be pulse dependent. The large secondary spike observed in simulated lower neck load is likely attributed with this difference. The THOR head- neck model was previously calibrated [7] under frontal (flexion) loading corresponding to Naval Biodynamic Laboratory (NBDL) tests [29], which are included in the THOR biomechanical response requirements [8]. However, during the vertical loading, the head-neck complex has a combined flexion-extension behavior caused by inertia forces along vertical direction and the OC loading-unloading joint properties. Therefore, future work is necessary to improve the response of the FE model neck region, especially under vertical loading, before full confidence can be had in its prediction of BC. As with the lumbar load criterion, future work should be performed to identify appropriate THOR Injury Assessment Reference Values (IARVs) of neck injury criteria for aerospace and spaceflight conditions [30].

2.5.3 Sensitivity Study of Pre-Impact Dummy Position

Overall HIC_{15} values are shown to be primarily sensitive to head rotation. In the original (non-rotated) head position, the head CG lies closely along the axis of the neck that contains the origin of OC-joint. A rotation of the head around OC-joint causes an increase of the distance from the head CG to neck axis. During impact, this increased distance (lever arm) leads to an

increased torque of the head inertia force at the OC-joint, which consequently leads to increased rotation causing higher levels of head CG accelerations and HIC_{15} values. Since the stiffness of OC-joint is almost symmetric [28], the sensitivity of HIC_{15} values to head rotation is almost symmetrical as well (Fig. 2-12). The forward rotation of the thorax changes the loading pathway within the thorax (e.g. reduce the spinal load), which results in changes in the thorax kinematics and consequently in the head kinematics. While an increased acceleration of head CG and HIC_{15} is observed (Fig. 2-12) due the pre-test thorax rotation, this increase is much lower than that produced by the head pre-test rotation.

On the contrary, LL shows an increased sensitivity to the thorax rotation than to head rotation. The abdomen of the THOR-NT dummy is split into two parts, the upper abdomen (attached above the lumbar load cell) and the lower abdomen (attached to the pelvis). A forward pre-test rotation of the thorax tilts the upper and lower abdominal parts come in contact earlier in simulation. This causes a larger degree of energy to transfer through the abdomen, resulting in lower lumbar spine loading (Fig. 2-13). Since the two separate abdomen parts do not correctly represent the human abdomen, future dummy modifications to improve its biofidelity under vertical loading should consider designing of one-piece dummy abdomen. This could be better analyzed and better designed through comparison studies using human FE models (e.g. Total Human Model for Safety-THUMS model and Global Human Body Modeling Consortium-GHBMC model).

While the position sensitivity study performed on the FE model may provide insights regarding the influence of pre-impact posture on the values of injury criteria, tests in some of these conditions would be useful to further validate these results and consequently the dummy model. More severe impact simulations along with body contact scenarios are necessary to gain

greater confidence in the FE model for crash injury analysis. In addition, validation testing in a mixed impact (horizontal & vertical) scenario, as that observed in aerospace and spaceflight impacts, may improve the confidence in the model. Additional future work may include improvements of the FE pelvis model, involving both testing of the physical part as well as parameter identification based on material test data. A comparison study between the response of a THOR dummy model and a FE human body model under vertical loading may also provide insight for improving the bio-fidelity of the THOR dummy for future aerospace safety assessment.

2.6 Conclusions

1 The FE model of THOR-NT dummy was evaluated for vertical loading against test data using an objective rating system. While some differences were observed especially in the neck response, the overall CORA scores of dummy model corresponding to three unique impact scenarios were between 0.845 and 0.907 on a scale from 0 to 1 (the best).

2 Pre-impact positioning is shown to have a moderate effect on overall model response. The head and thorax pre-test rotations lead to increased values of HIC and lumbar force, consequently.

3 Further model improvements may consider more accurate material and structural properties of dummy model's deformable parts and defined OC-joint for both loading and unloading phase, respectively.

4 The model predicts relatively close values of injury criteria in the scenarios tested, but future work should be focused on defining the appropriate THOR IARVs for aerospace and spaceflight impact conditions.

2.7 References

1. U.S. Department of Transportation, N., *Federal Motor Vehicle Safety Party 571. Standard 208 – Occupant Crash Protection*, 2003. p. 46539 -46546.
2. Shaw, G., J.R. Crandall, and J. Butcher, *Biofidelity Evaluation of the Thor Advanced Frontal Crash Test Dummy*, in *IRCOBI Conference Proceedings*2000: Montpellier France.
3. Untaroiu, C., et al., *Evaluation of a finite element of the Thor-NT dummy in frontal crash environment*, in *21st ESV Conference*2009: Stuttgart, Germany.
4. Littell, J. and M. Annett, *The Evaluation of a Test Device for Human Occupant Restraint (THOR) Under Vertical Loading Conditions: Experimental Setup and Results*, in *69 AHS Forum*2013: Pheonix, AZ.
5. Polanco, M.A. and J.D. Littell, *Vertical Drop Testing and Simulation of Anthropomorphic Test Devices*, in *67th AHS Forum*2011: Virginia Beach, VA.
6. Jackson, K.E., Y.T. Fuchs, and S. Kellas, *Overview of the National Aeronautics and Space Administration Subsonic Rotary Wing Aeronautics Research Program in Rotorcraft Crashworthiness.* Journal of Aerospace Engineering, 2009. 22(3): p. 229-239.
7. Untaroiu, C. and Y.-C. Lu, *A Simulation-Based Calibration and Sensitivity Analysis of a Finite Element Model of THOR Head-Neck Complex*, in *SAE 2011 World Congress & Exhibition*2011, SAE: Detroit, USA.
8. GESAC, *Biomechanical Response Requirements of the Thor NHTSA Advanced Frontal Dummy*, 2005.
9. Eekhout, M., *Cardboard in architecture*. 2008: IOS Press.
10. SAE, *Surface Vehicle Recommended Practice: Instrumentation for Impact Test-Part 1-Electronic Instrumentation*, 2007.
11. Yu, H., et al., *Head-neck finite element model of the crash test dummy THOR.* International Journal of Crashworthiness, 2004. 9(2): p. 175-186.
12. Pellettiere, J. and D. Moorcroft, *Occupant calibration and validation methods*, in *Advances in Applied Human Modeling and Simulation*, V.G. Duffy, Editor. 2012, CRC Press: Boca Raton, FL. p. 307-316.
13. Jacob, C., et al., *Mathematical models integral rating.* International Journal of Crashworthiness 2000. 5(4): p. 417-432.
14. Hovenga, P.E., H.H. Spit, and M. Uijldert, *Rated facet Hybrid-III 50th model with improved user-friendliness introduced*, in *10th International MADYMO Users Meeting*2004.
15. Sarin, H., et al., *A Comprehensive Metric for Comparing Time Histories in Validation of Simulation Models with Emphasis on Vehicle Safety Applications.* Detc 2008: Proceedings of the Asme International Design Engineering Technical Conferences and Computers and Information in Engineering Conference, Vol 1, Pts a and B, 2009: p. 1275-1286.
16. Untaroiu, C.D., J. Shin, and Y.C. Lu, *Assessment of a dummy model in crash simulations using rating methods.* International Journal of Automotive Technology, 2013. 14(3): p. 395-405.
17. Barbat, S., et al., *Objective rating metric for dynamic systems*, in *Proceedings of the 23rd International Technical Conference on the Enhanced Safety of Vehicles (ESV)*2013.
18. Zhan, Z., Y. Fu, and R.-J. Yang, *Enhanced Error Assessment of Response Time Histories (EEARTH) Metric and Calibration Process*, in *SAE 2011 World Congress*, SAE, Editor 2011: Detroit, MI, USA.
19. Thunert, C., *CORA Release 3.6, User's Manual*, 2012.

20. **Gehre, C., H. Gades, and P. Wernicke, *Objective Rating of Signals using Test and Simulation Responses*, in *ESV Conference*2009: Stuttgart, Germany.**
21. **Versace, J., *A Review of the Severity Index*, 1971.**
22. **Kleinberger, M., et al., *Development of Improved Injury Criteria for the Assessment of Advanced Automotive Restraint Systems*, 1998, NHTSA: Washington, DC.**
23. **Bass, C.R., et al. *A New Neck Injury Criterion in Combined Vertical/Frontal Crashes with Head Supported Mass*. in *International IRCOBI Conference on the Biomechanics of Impact*. 2006. Madrid, Spain.**
24. **Salzar, R.S., et al., *Ejection injury to the spine in small aviators: sled tests of manikins vs. post mortem specimens.* Aviat Space Environ Med, 2009. 80(7): p. 621-8.**
25. **Civil, I.D. and C.W. Schwab, *The Abbreviated Injury Scale, 1985 Revision - a Condensed Chart for Clinical Use.* Journal of Trauma-Injury Infection and Critical Care, 1988. 28(1): p. 87-90.**
26. **Untaroiu, C.D., et al., *Crash reconstruction of pedestrian accidents using optimization techniques.* International Journal of Impact Engineering, 2009. 36(2): p. 210-219.**
27. **Untaroiu, C.D. and Y.C. Lu, *Material characterization of liver parenchyma using specimen-specific finite element models.* J Mech Behav Biomed Mater, 2013. 26: p. 11-22.**
28. **Putnam, J.B., J.T. Somers, and C.D. Untaroiu, *Development, Calibration, and Validation of a Head-Neck Complex of THOR Mod Kit Finite Element Model.* Traffic Injury Prevention, 2014.**
29. **Ewing, C.L., et al., *Dynamic Response of the Head and Neck of the Living Human to -Gx Impact Acceleration*, in *12th Stapp Car Crash Conference*, SAE, Editor 1968.**
30. **Somers, J.T., et al., *Investigation of the THOR Anthropomorphic Test Device for Predicting Occupant Injuries during Spacecraft Launch Abort and Landing.* Frontiers in Bioengineering and Biotechnology, 2014. 2.**

3. THE DEVELOPMENT, CALIBRATION, AND VALIDATION OF A HEAD-NECK COMPLEX OF THOR MOD KIT FINITE ELEMENT MODEL

Jacob B. Putnam, Jeff T. Somers, Costin D. Untaroiu

Manuscript accepted for publication in *Traffic Injury Prevention* on January 5, 2014

(Currently in press- DOI)

3.1 Abstract

In an effort to continually improve upon the design of the Test Device for Human Occupant Restraint (THOR) dummy, a series of modifications have recently been applied. The first objective of this study was to update the THOR head-neck finite element (FE) model to the specifications of the latest dummy modifications. The second objective was to develop and apply a new optimization-based methodology to calibrate the FE head-neck model based on experimental test data. The calibrated head-neck model was validated against both frontal and lateral impact test data. Finally, the sensitivities of the model, in terms of head and neck injury criteria, to pre-test positioning conditions were evaluated in a frontal crash test simulation.

The updated parts of the head-neck THOR FE model were re-meshed from CAD geometries of the modified parts. In addition, further model modifications were made to improve the effectiveness of the model (e.g., model stability). A novel calibration methodology, which incorporates the CORA (CORelation and Analysis) rating system with an optimization algorithm implemented in Isight software, was developed to improve both kinematic and kinetic responses of the model in various THOR dummy certification and biomechanical response tests. A parametric study was performed to evaluate head and neck injury criteria values in the calibrated head-neck model, during a 40 km/h frontal crash test, with respect to variation in the THOR model upper body and belt pre-test position.

Material parameter optimization was shown to greatly improve the updated model response by increasing the average rating score from 0.794 ± 0.073 to 0.964 ± 0.019. The calibrated neck showed the biggest improvement in the pendulum flexion simulation from 0.681 in the original model up to 0.96 in the calibrated model. The fully calibrated model was effective at predicting dummy response in frontal and lateral loading conditions during the validation phase (0.942

average score). Upper body position has a greater effect on head-neck response than belt position. The pre-test positioning variation resulted in a 10% maximum change in HIC_{36} values and 14% maximum change in N_{IJ} values.

The optimization-based calibration methodology markedly improved model performance. The calibrated head-neck model demonstrated application in a crash safety analysis, showing slight head-neck injury sensitivity to pre-test positioning in a frontal crash impact scenario.

3.2 Introduction

More than 1.2 million people die each year in road accidents worldwide and as many as 50 million others are injured and disabled[1]. To reduce traffic road fatalities, consumer organizations and the government proposed and implemented safety regulations determined from data recorded during laboratory crash tests with new vehicle models. Anthropometric test devices (ATD), otherwise known as crash test dummies, are frequently employed in these crash tests to evaluate injury risk for vehicle occupants [2-5] and pedestrians [6-8].

The THOR (Test Device for Human Occupant Restraint), a dummy exhibiting advanced biofidelity, has been developed and continuously improved by the National Highway Traffic Safety Administration (NHTSA) to provide an advanced crash test dummy for crash safety analysis[9]. Rapid advances in both computational power and crash simulation technology enables the use of a computational component complementary to experimental testing, especially in the optimization of vehicle components or restraint systems during the manufacturer's design process [10-12]. However, to provide maximum utility of the dummy computational model, the biofidelity of its components should be assessed against the test data recorded from the physical dummy and the data corridors obtained from PMHS and volunteer tests.

The main goal of this study was to update the components of the head and neck finite element (FE) dummy model to the specifications of the most recent version of dummy, called THOR Mod Kit[13, 14]. This update was performed corresponding to the new dummy components based on their CAD data. To ensure the effectiveness of this update, the model was calibrated using a novel optimization-based approach, which employed a rating score as the objective function. Post calibration simulations validated the developed model as well as the effectiveness of the optimization-based approach used. In an effort to prove the applicability of the model in safety studies, the developed head-neck model was coupled with other body parts of the THOR dummy model and the sensitivity of its prediction of head-neck injury criteria was investigated relative to the pre-impact position of THOR dummy in a frontal crash simulation.

3.3 Methods

3.3.1 Development of the head-neck dummy FE model

The THOR Mod Kit (THOR-k) head-neck FE model was developed in LS-DYNA (LSTC, Livermore, CA) from the THOR-NT FE model[15]. The CAD drawings of the THOR-k dummy were reviewed and FE models were developed for the updated parts. The most significant change was found in the head skin, which has a uniform scalp thickness in THOR-k opposed to a tapered thickness in the THOR-NT (Fig. 3-1). All parts were meshed in Hypermesh (Altair, Troy, MI, USA) with mixed hexa-tetra elements. To mitigate possible simulation instability, the head skin model was developed with a multi-element thickness mesh, rather than the single element mesh previously used.

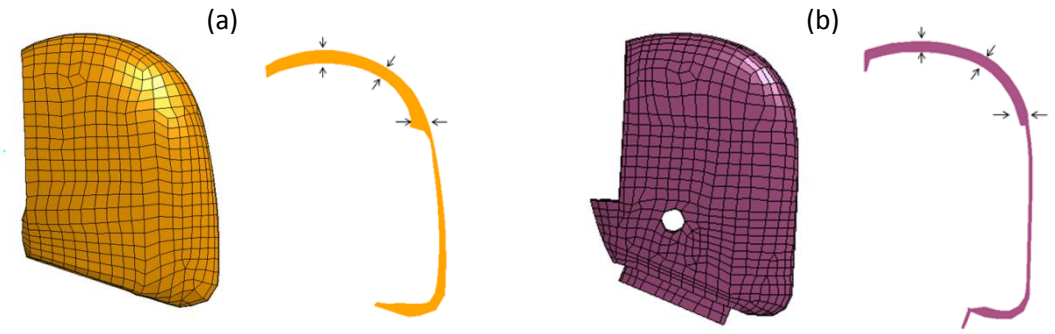

Figure 3-1. Comparison between the FE models of: (a) THOR-NT and (b) THOR-k.

No significant changes were observed in the geometry of the head casting between the THOR-NT and THOR-k models, but to maintain a shared node contact with the THOR-k head skin this part was re-meshed as well. A shared-node approach was used between these parts to avoid the use of a defined contact, which may increase the computational time. Elements adjacent to the head skin were adjusted, with minimal geometry change, to match the node count of the head skin interior.

To account for the geometry changes of the new head skin, the foam insert and front face plate were also re-meshed based on a THOR-k geometry CAD model (NHTSA) (Fig. 3-2a). The initial mesh was manually altered to fit between the head skin and head plate. This manual adjustment is representative of compression of the foam, necessary to fit these parts within the head skin, during the assembly of the dummy face. Similar to the head casting, the foam inserts and face plates were meshed to have a shared-node contact with the head skin. The head ballast was updated to account for a significant difference in geometry between the THOR-NT and THOR-k (Fig. 3-2a).

The instrumentation of the physical THOR-k dummy was reviewed and corresponding models were defined in the THOR-k FE model (Fig. 3-2b). Load cells were modeled using two approaches: (a) cross-section through a deformable part (upper-neck load cell) and (b) locking

joints (lower-neck and face-load cells). Rear-neck spring force, front-neck spring force, and Occipital Condoyle joint (OC-joint) rotational displacement was calculated within corresponding spring models. Head kinematics were calculated at a point representative of the head center of gravity (CG).

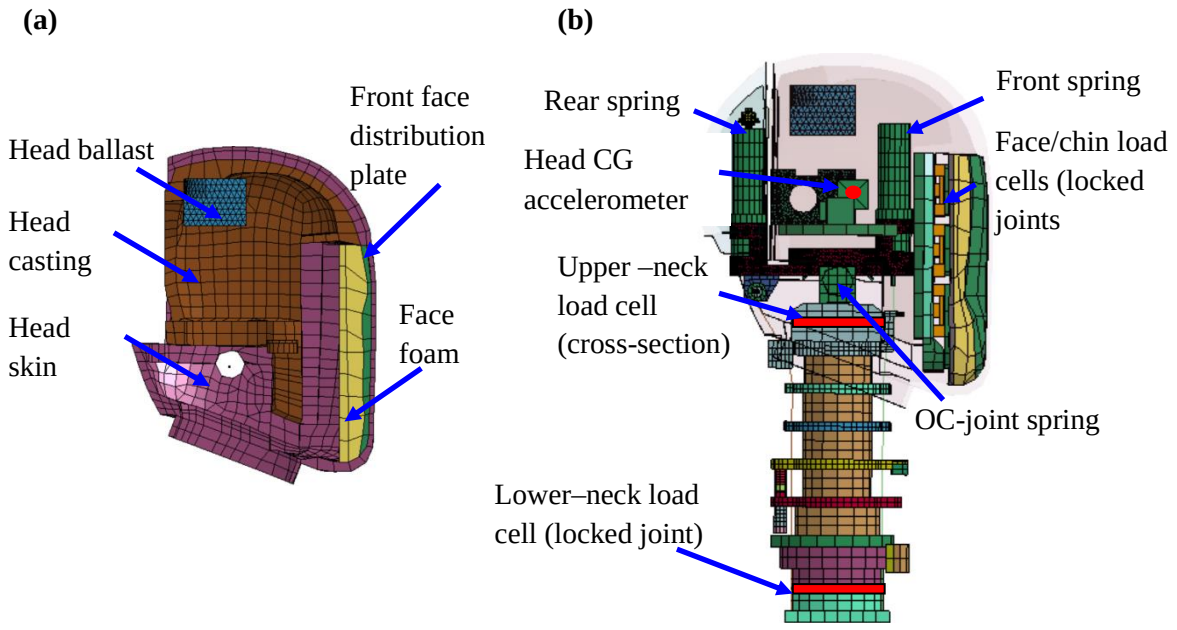

Figure 3-2**.** (a) Cross-section of Head THOR-k FE model through the updated parts of THOR (b) Models of THOR-k dummy instrumentation.

The majority of deformable solid elements were modeled using a fully integrated selectively reduced (S/R) scheme[16]. The face foam and neck stoppers (rubber and Delrin) were modeled using a one-point integration scheme with constant stress. Hourglass control was used in all three parts. The LS-DYNA hourglass type Flanagan-Belytschko stiffness form with exact volume integration [16] for solid elements was used to control the face foam. Flanagan-Belytschko viscous form with exact volume integration [16] for solid elements was used for both neck stops. Hourglass energy was negligible (under 0.1%) compared to internal energy in all simulations.

The OC-joint mechanics of the THOR-k FE model was also updated. Previously the rotation at the OC-joint was controlled by a friction contact between an OC-cam part rigidly attached to the neck and stoppers attached to the head mounting bracket [15]. This method for generating the rotation stiffness can result in excessive deformation of stoppers in impact simulations, causing instability issues. In the new model this contact based stiffness was replaced with a spring model set to define rotational stiffness between the upper neck load cell and the head mounting bracket (Fig. 3-3a). The rotational stiffness curve was defined based on moment versus angle data from the OC-joint Quasi Static rotation test curves provided by NHTSA (Fig. 3-3b). Positive and negative rotation stop angles were also applied based on the bounds of this data.

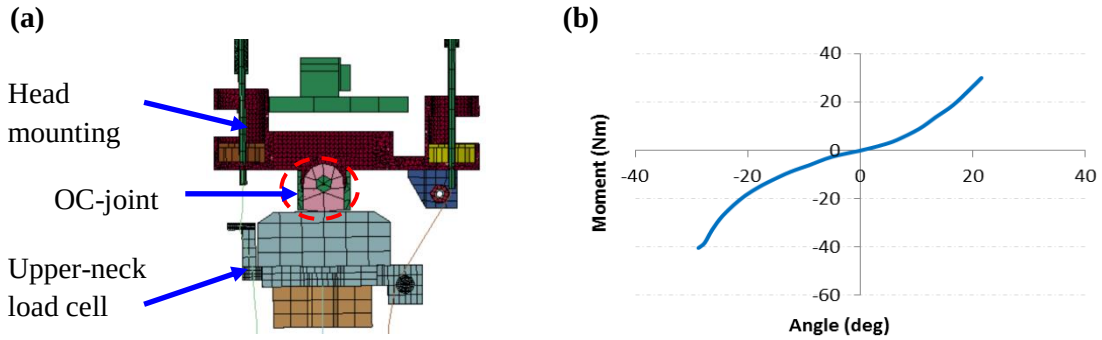

Figure 3-3**.** (a) The updated OC-joint (rotational spring-based joint) and (b) the angular stiffness assigned to OC-joint.

3.3.2 Model rating system and optimization techniques

Traditionally, model evaluations in safety applications have been performed by comparing the peak values of test and simulation data, by evaluating the overall curve shapes qualitatively, or by satisfying several certification guidelines [17]. Recently, there have been several efforts focused on developing systematic methodologies for model evaluations [18-23], especially in impact tests where a large number of channels must be compared. These approaches evaluate the response of the model in comparison to test data based on defined correlation metrics, which allow a quantitative evaluation of the model response. A calibration methodology was developed

to utilize this emerging systematic evaluation capability. The focus of this calibration method was to optimize the total model rating, developed using CORrelation and Analysis (CORA) signal rating software [24], through the adjustment of FE model parameters. An optimization hierarchy was developed within Isight™ software vers. 5.7. [25] (Fig. 3-4). LS-Dyna simulations were run with the model parameters selected iteratively by the optimization algorithm until the value of the CORA total model rating, defined as the objective function, was maximized.

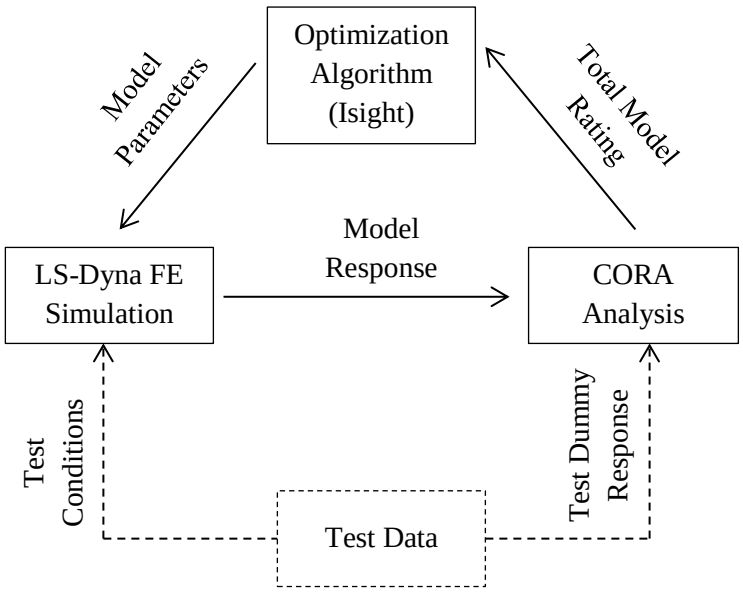

Figure 3-4. Schematic of developed calibration method.

3.3.2.1 Model Rating System: CORA

The CORA rating system uses a combination of two different rating systems, corridor and cross-correlation, to evaluate the similarity between two curves [20]. In the case that multiple signals are used in evaluation, the rating of each curve comparison is combined to a final score based on a weighting factor assigned to each signal. If no weighting factor is assigned all comparisons are weighted equally.

This system automatically evaluates only the main portion of curves, calculated by an algorithm based on the maximum absolute value of the test curve: Y_{max}. The start and end time

(t_a and t_b) are calculated as the first and last time at which the test curve exceeds an absolute value greater than a percentage of Y_{max} defined as $a_{tres}*Y_{max}$ and $b_{tres}*Y_{max,}$ respectively (a_{tres} = 0.05 and b_{tres} = 0.07). The final evaluation interval limits are defined by these parameters, an optional enlarging factor (α_{eval}=1), and the test/simulation bound times (t_{start} and t_{end}).

$$t_{\min} = \max\left[t_a - \alpha_{eval}(t_b - t_a), t_{start}\right],\ t_{\max} = \min\left[t_b + \alpha_{eval}(t_b - t_a), t_{end}\right],\ 0 \le \alpha_{eval} \le 1 \quad (1)$$

The corridor method scores the simulation curve based on its position with respect to defined boundary corridors (Fig. 3-5). The widths of inner and outer corridor are calculated as: $d_{inn} = \alpha_{inn} Y_{\max}$ and $d_{out} = \alpha_{out} Y_{\max}$ (α_{inn}= 0.7 and α_{out} = 0.9). Discrete scores are assigned based on the location of the simulation curve relative to these corridors at evenly distributed points. A score of 1 is given within the inner corridor, a score of 0 is given outside of the outer corridor, and a score between 0 and 1 is calculated by interpolation for the region between inner and outer corridors. Finally, these discrete scores are averaged to produce the final corridor score.

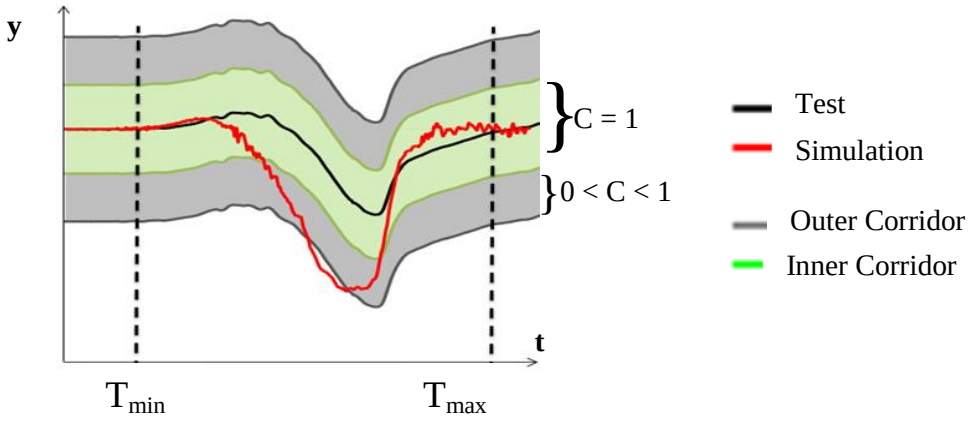

Figure 3-5. CORA Rating System: Corridor Method.

The correlation method is based on three correlation factors of the compared curves: phase shift, progression, and size (Fig. 3-6). Each of these is given a rating of between 0 and 1 which is combined to create the total cross correlation rating. A set of defined algorithms are used in the

calculation of each factor value [24]. The weight of each correlation factor can be defined individually to place a higher importance on certain factors. In this study all factors were weighted equally.

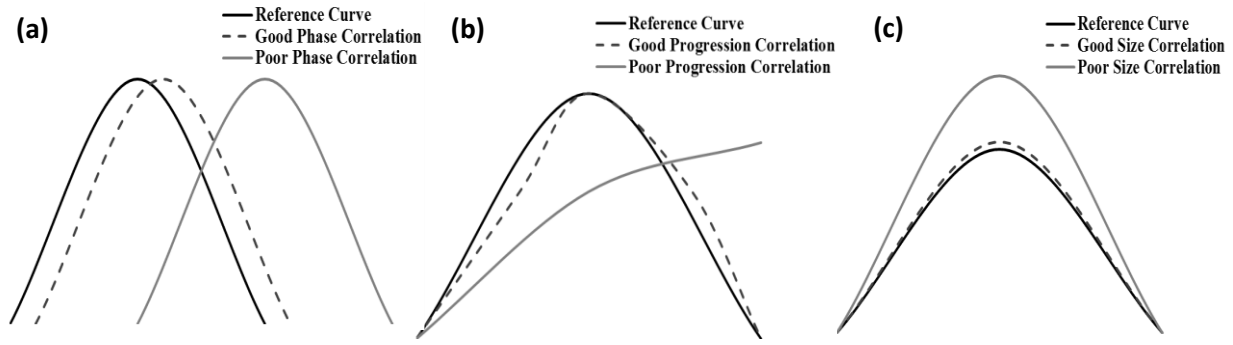

Figure 3-6**.** CORA rating system: correlation method factors – (a) phase shift, (b) progression, (c)

With the exception of t_{start} and t_{end}, which are simulation dependent, the parameter values used in the definition of the interval calculation, corridor method, and correlation methods were the original values recommended by the Partnership for Dummy Technology and Biomechanics (PDB). These system values were used in all evaluations to ensure a meaningful comparison during the optimization process. When the number of kinematic and kinetic signals was not equal the signals were manually weighted so to have equal (kinematic and kinetic) influence on the total rating. Each signal was weighted based on the formula: $W_{factor}= 0.5/N$, were N is the total number of similar signals (kinematic or kinetic) compared.

3.3.2.2 Optimization Algorithm

Archive–based Micro Genetic Algorithm (AMGA) implemented within Isight^{TM} was used to maximize the total rating score of the model. This genetic algorithm uses a small population size and creates an external archive, updated iteratively, with the best solutions obtained. The parent population is obtained from the archive based on the concept of the non-dominance ranking [26]. It should be mentioned that AMGA is a heuristic optimization algorithm, so it cannot guarantee

an optimal solution, only a solution close to the global optimum by examining a large discrete space in a reasonable amount of time. AMGA, an improved genetic algorithm, was chosen in this study based on its superior performance demonstrated in our previous studies where various types of heuristic algorithms were compared (e.g. simulated annealing, simplex, or particle-swarm optimization algorithms [27, 28].

3.3.3 Calibration of the head-neck dummy FE model

A protocol was developed to calibrate each component identified as key to the kinematic and kinetic response of the THOR-k head-neck dummy FE model (Fig. 3-7a). Calibration was performed in a step-wise manner to reduce confounding effects between these components using the data from four of six impact tests available. The other two impact tests: one under frontal loading and one under lateral loading were employed during the model validation. All available data relevant to each test direction were employed in the derivation of CORA scores.

The head neck cables and springs were seen to have insignificant influence on the model response during lateral flexion response, thus the stiffness of the neck pucks were first calibrated in a lateral flexion simulation. Of the two lateral tests available, the NBDL lateral test was used during the lateral calibration due to the higher number of kinetic and kinematic signals available for comparison.

The friction coefficient of the slip-rings defined between each neck plate and the neck cables as well as the stiffness properties of the head springs were calibrated in simultaneously run pendulum extension and pendulum flexion simulations. Similar friction coefficients were assumed for both front and rear neck cables. The addition and calibration of an unloading curve in the rotational stiffness definition of the OC-joint was considered as an optimization parameter. In a preliminary calibration the unloading curve was defined by scaling interior points of the

loading curve from 0.1 to 1, in which 1 resulted in an unloading curve congruent with loading. A scale factor of approximately 1 yielded optimal model response, indicating the separate unloading curve had no positive effect on model response.

The head-skin material was calibrated in a head-impact simulation. Lastly, the fully calibrated head-neck model was validated against a frontal flexion sled test and a lateral flexion pendulum test. The final optimization protocol is outlined in Figure 3.7b. Because no material testing data was available on of the THOR-k dummy parts the updated model had to be calibrated by adjusting material parameters of the THOR-NT model that were originally approximated based on the material properties of similar materials found in literature.

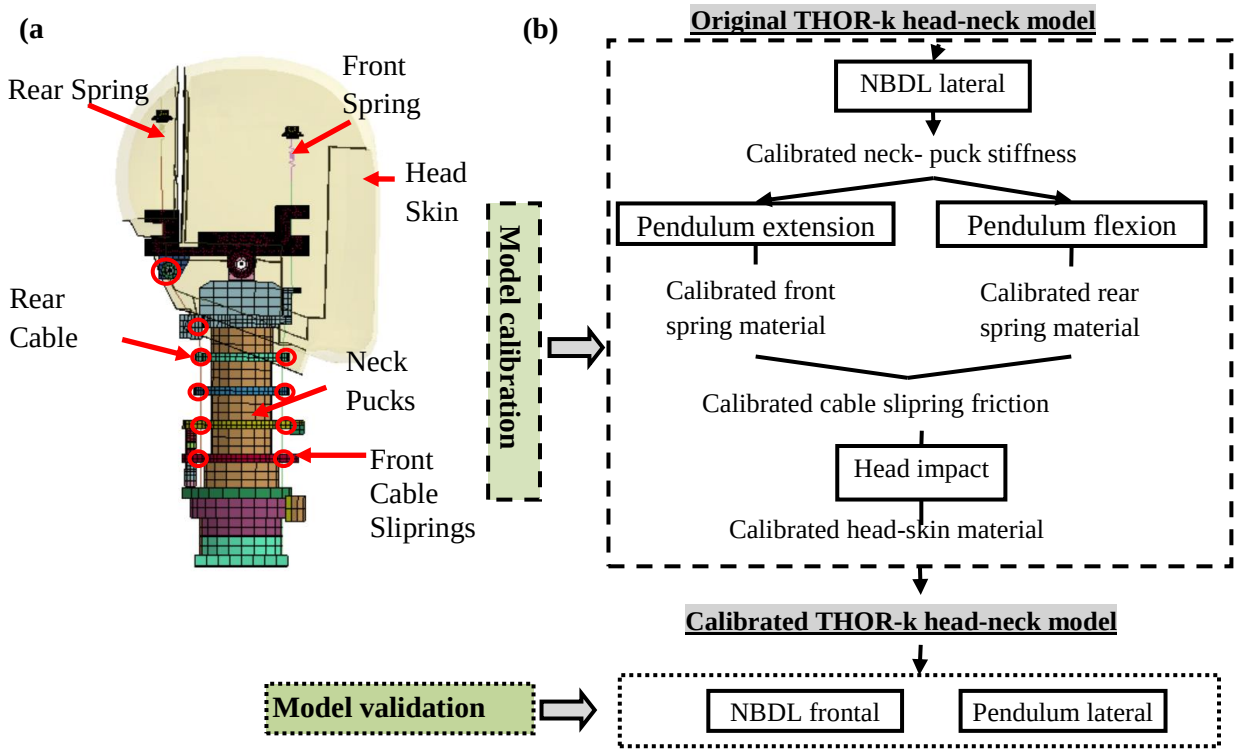

Figure 3-7. (a) The main components related to the head-neck response used in calibration process and (b) the schematic of calibration/validation process.

3.3.3.1 Neck-Puck Calibration: NBDL Lateral Simulation

Frontal, lateral, and oblique sled impact tests were originally performed on a series of human volunteers at the Naval Biodynamics Laboratory (NBDL) in New Orleans [29]. Sagittal, coronal,

and transverse response of the head-neck region were recorded. The 15-g frontal and 7-g lateral impact responses are defined as biomechanical requirements for THOR dummy[30]. These tests are performed only on the head-neck component of the dummy, with the T1 plate attached directly to an impact sled. The dummy head-neck response is typically verified in these tests by head rotation angle as well as the horizontal and vertical displacements of the head CG [15].

The FE simulations of the NBDL tests used in this study were performed based on the sled data recorded by the Japan Automobile Research Institute (JARI). JARI performed 3 NBDL frontal and 3 NBDL lateral tests on the head-neck of a THOR-k dummy (NHTSA Biomechanics Test Database numbers 10999-11001 and 11005-11007). In these tests, force and moment time histories in the upper- and lower-neck load cells and force time histories in the front and rear springs were recorded. In addition, head acceleration and OC-joint rotation were recorded by the head CG accelerometer and OC-joint angular potentiometer. Kinematics of the head motion were additionally calculated from photogrammetric imaging of the dummy taken from markers placed at the exterior representative location of the head CG during testing.

In the lateral FE simulation, the time history of sled acceleration recorded in testing was applied along the lateral direction to the lower-neck load cell, which was constrained in all other directions (Fig. 3-8). Kinetic response was compared in the upper- and lower-neck load cells. Head displacement was compared in the vertical and lateral directions. The coronal plane rotation angle of the head was also compared. The sled acceleration pulse used in FE simulation as well as data used in comparison was taken as an average of the 3 repeated lateral tests.

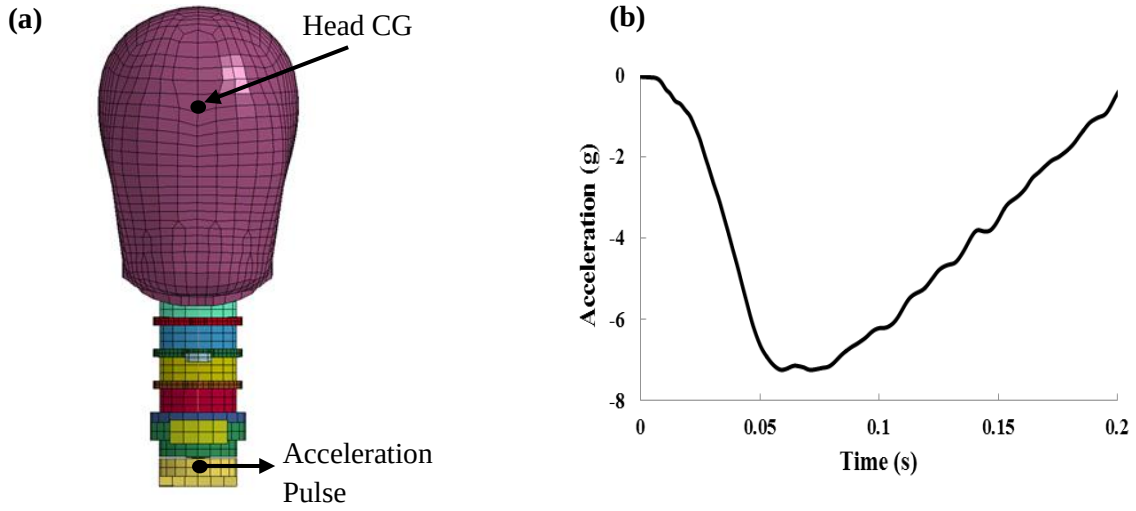

Figure 3-8**.** NBDL test model (lateral) – (a) simulation setup, (b) acceleration pulse.

The NBDL lateral simulation test was employed to calibrate the neck puck stiffness, as other key components (e.g., the front spring, rear spring, and cable friction) had a minimal effect on model response in this test. The stiffness curve of the incompressible rubber material model assigned to the neck pucks of the THOR-k FE model was optimized through scaling to improve the dummy response. The scaling factor, k_{neck}, was optimized within the range of 0.1 to 1. All FE simulations performed in the calibration and validation of the head-neck model were run on a desktop PC with an Intel® Core™ i7-2600 CPU @ 3.4 GHz processor using two CPUs in Shared Memory Parallel Processing (SMP). The run time of this simulation was approximately 3 hours. 25 simulations were run during this optimization process.

3.3.3.2. Cable-Neck Plate Friction Identification and Springs Calibration: Pendulum Extension and Flexion Simulations

The pendulum tests are included in the current certification tests of a 50th percentile male ATD. These tests are employed to evaluate the dynamic response of the head-neck assembly in flexion, extension, and lateral directions. In these tests, the head-neck complex is rigidly mounted to the end plate of a pendulum (as defined in CFR Title 49, Part 572, Subpart E). The

pendulum with head-neck attached is brought to a certain height and released so that it impacts stoppers at a desired velocity (3.7 ± 0.1 m/s). An accelerometer attached to the pendulum measures translational acceleration throughout the test. Forces and moments are measured at the upper-neck load cell. In addition, the force in the front and rear-neck springs is recorded along with rotational displacement of the head around the OC-joint[30].

In FE simulation, the head-neck assembly was attached to the pendulum model which was constrained to rotate only along the sagittal plane (Fig. 3-9). The prescribed angular acceleration time history was calculated based on the pendulum linear acceleration measured during testing. Additionally initial rotational velocity, calculated from the impact velocity measured during testing, was applied to all parts. In both simulations, kinetic response was evaluated in the upper-neck load cell. Lower neck load cell data was not available for all pendulum tests. The rear-spring and front-spring force were evaluated in flexion and extension, respectively. The OC-joint rotation angle was evaluated in each simulation.

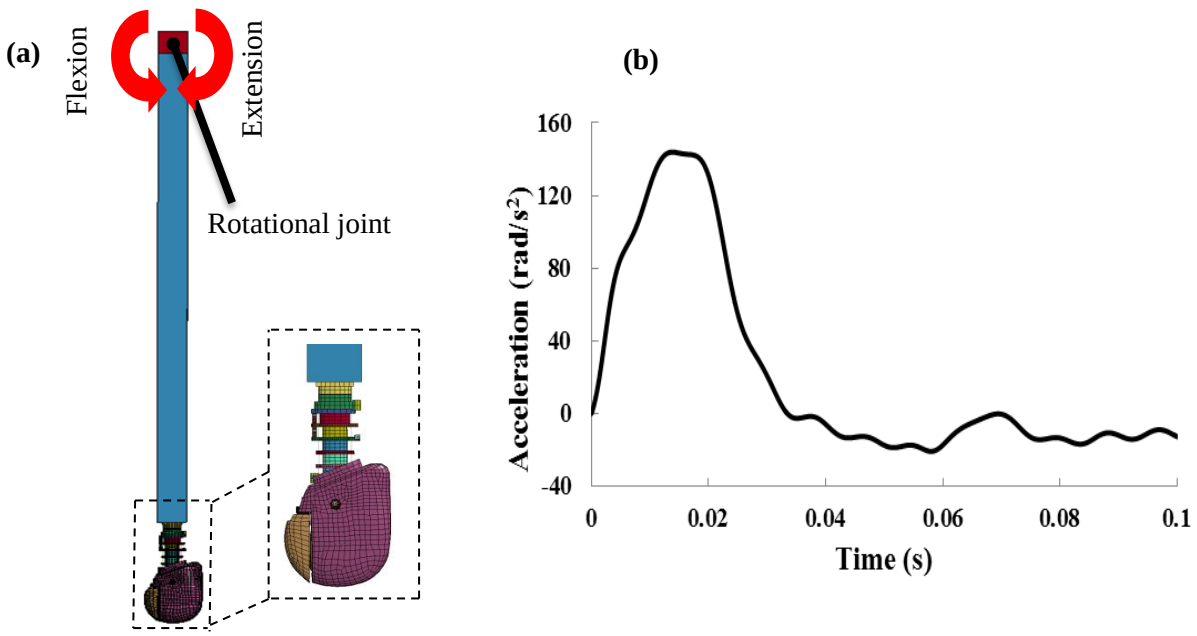

Figure 3-9**.** Pendulum test model (flexion and extension) – (a) simulation setup, (b) rotational acceleration pulse.

Both neck-flexion and neck-extension pendulum impact tests were simultaneously run in optimization to calibrate the stiffness curves of head springs and the friction coefficient between neck cables and neck plates at the slip-ring location. This was done by implementing a single set of optimization parameters, which were input into both test simulations. The simulations were run simultaneously and the CORA score for each simulation was calculated. These two CORA scores were then averaged to attain a single score used as the optimization response variable. The previously calibrated puck stiffness was used in these simulations. In the FE model, the head springs are defined as general nonlinear translational springs with defined loading and unloading stiffness curves (Mat_Spring_General_Nonlinear [16]). The initial three-phase stiffness curves employed in the THOR-NT FE model were approximated by two-phase curves in THOR-k model. The curve parameters (Fig. 3-10), defined as design variables in the optimization process, were: the lengths of the first phase (d_l loading and d_u unloading), the spring force at these points (h_{l1} loading and h_{u1} unloading), and the peak forces in the secondary phase (h_2). Maximum spring displacement was set constant at 40 mm, which showed to be well above the observed

displacements in all certification tests. A total of 162 simulations with 11 variables (10 rear/front spring stiffness parameters and 1 cable-plate friction coefficient) were run in this optimization with an individual run time of 1.5 hours.

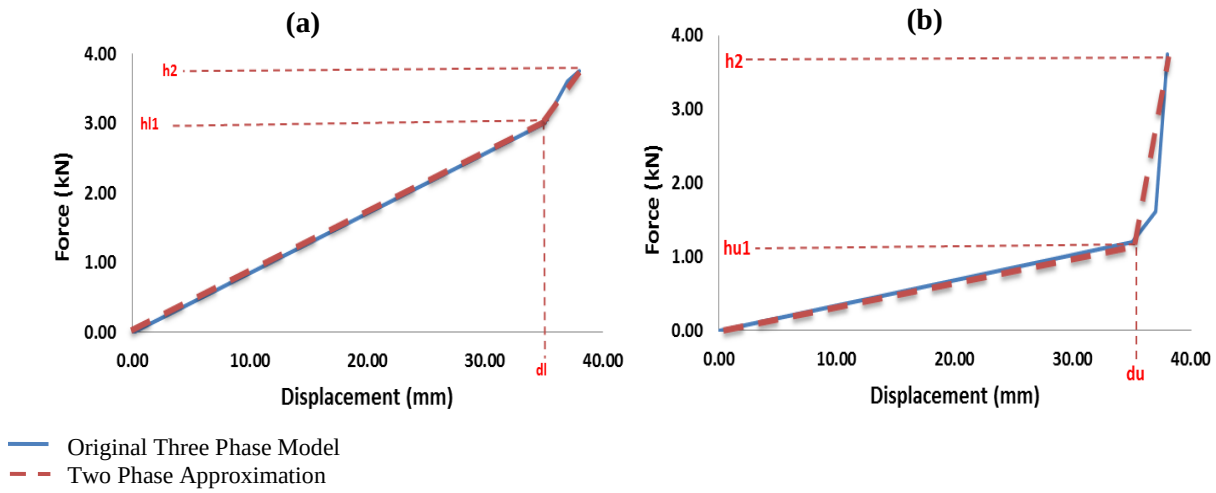

Figure 3-10**.** Example head spring stiffness optimization curves – (a) loading, (b) unloading.

3.3.3.3 Head Skin Calibration: Head Impact Simulation

The material model of head skin was calibrated based on the data recorded in a head impact test. In this certification test, the dummy is placed on a seat with limbs extended horizontally forward. A 152-mm diameter cylindrical impactor with a mass of 23.4 kg is placed with its longitudinal axis at a dummy head point 30 mm above the horizontal line marking the lowest limit of the forehead and on the mid-sagittal plane (Fig. 3-11). The impactor contacts the head at an initial velocity of 2.0 m/s, and the time history of impact force is recorded[30].

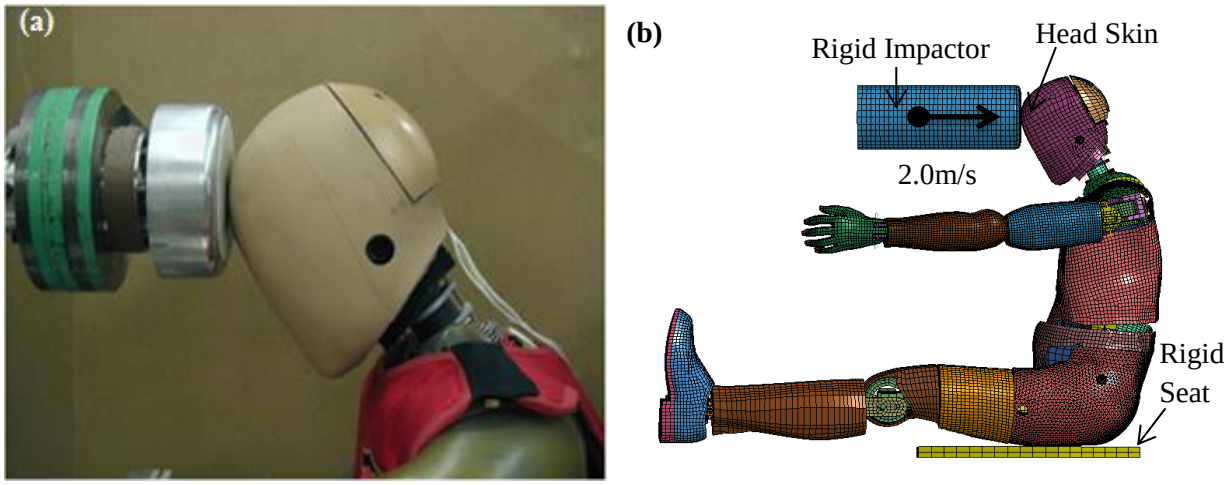

Figure 3-11**.** Frontal head impact test setup – (a) physical test (GESAC 2005), (b) FE-simulation.

The FE test performed on the THOR-k head-neck was set up in accordance to the specifications outlined in the physical test. The head-neck calibrated in previous simulations was connected to other components of THOR model. The dummy was placed upon a rigid steel seat (200 GPa elastic modulus), with defined contact friction between the seat and body (0.53/0.38 static/dynamic coefficients [31]). Initial position of the impactor and head-neck tilt was adjusted until impact specifications were met (the center of the impactor aligned parallel to the 30 mm mark above the horizontal line marking the lowest limit of forehead and on the mid-sagittal plane of the dummy model). The impactor part was assigned a set mass of 23.4 kg and an initial horizontal velocity of 2.0 m/s. The force-time response of the head skin-impactor contact was recorded during FE simulation.

A linear viscoelastic material model was assigned to the head skin. Initial material parameters were taken from a previous optimization performed on the head skin of THOR-NT model[15]. The bulk modulus, short time shear modulus, long-time shear modulus, and decay constant parameters of the head-skin material were defined as design variables during the optimization process. A total of 43 simulations were run in this optimization with a simulation run time of approximately 3 hours.

3.3.4 Validation of the head-neck dummy FE model

To ensure a multidirectional validation, the calibrated head-neck complex of the THOR-k dummy model was validated in a NBDL flexion as well as pendulum lateral simulation. These simulations provided a means of assessing overall model improvement without the effects of test specific calibration. In addition, these tests provided a large number of relevant signals for the model validation.

3.3.4.1 Frontal Validation: NBDL Flexion Simulation

In NBDL flexion FE simulation (Fig. 3-12), the average time history of sled acceleration recorded in testing was applied along the horizontal direction to the lower-neck load cell, which was constrained in all other directions. Kinetic response was compared in the upper- and lower-neck load cells as well as the rear neck cable. OC-joint rotation angle, head displacements along horizontal and vertical directions (sagittal plane), and head rotation kinematics were also compared. Similar to the NBDL lateral simulation, averaged test data was used in simulation and model comparison.

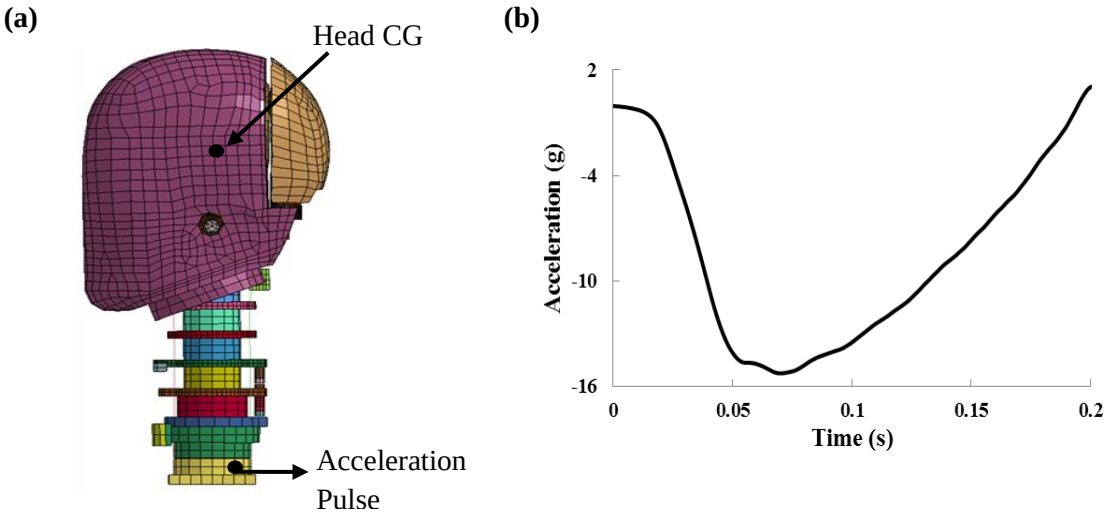

Figure 3-12. NBDL test setup (frontal flexion) – (a) model setup, (b) acceleration pulse.

3.3.4.2. Lateral Validation: Pendulum Lateral Simulation

In the lateral pendulum FE simulation, the pendulum complex was constrained to rotate with the prescribed angular acceleration (Fig. 3-13) only along the coronal plane. The kinetic response was evaluated in the upper neck load cell. The spring forces were not evaluated in this simulation as they were insignificant to the kinematic response of the model in this test. The OC joint is constrained to the sagittal plane rotation, which is very low (under 2 degrees) in this test, and thus was not evaluated in this simulation. No other kinematic data was available for this dummy certification test in the NHTSA database.

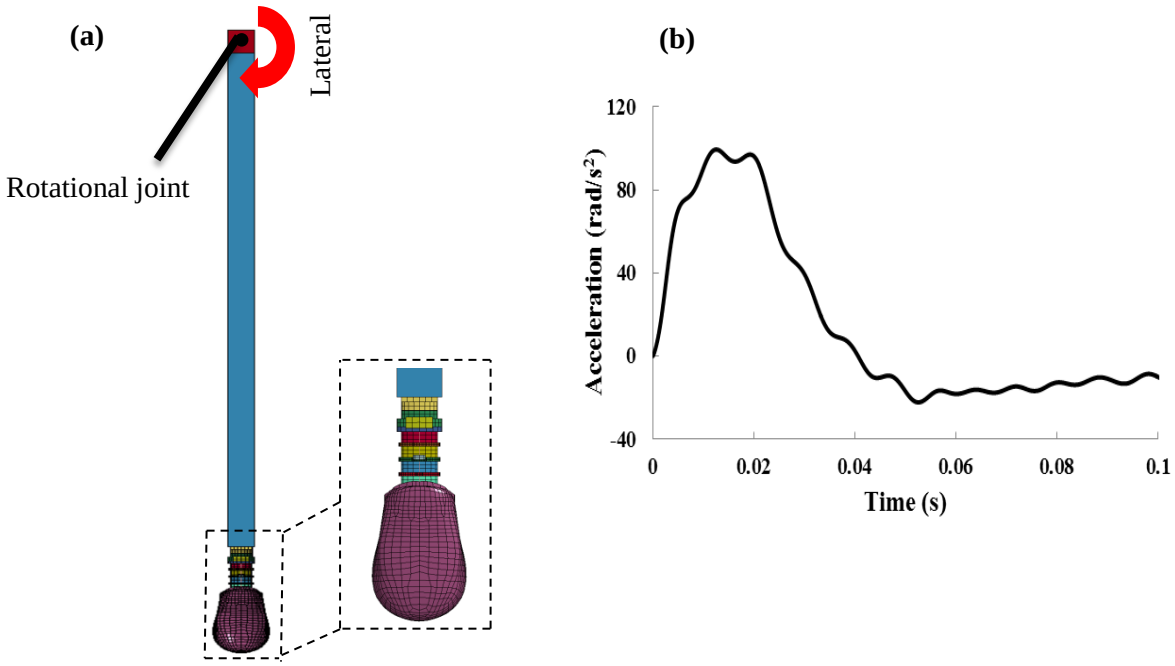

Figure 3-13. Pendulum lateral simulation – (a) simulation setup, (b) rotational acceleration pulse.

3.3.5. Sensitivity Analysis of the Head-Neck Model relative to Pre-Impact Dummy Position in a Frontal Crash

To better understand the sensitivity of head-neck injury criteria relative to inherent variations of the pre-impact dummy position, the fully calibrated head neck model was integrated into the latest available THOR-k full body FE model. A 40 km/h front seat passenger frontal impact sled

test [32], in which the THOR-NT dummy was positioned on a rigid planar seat and restrained using a standard 3-point shoulder and lap belt system, was modeled (Fig. 3-14a). A sled model with belts, knee bolster, and footrest previously developed from the test sled CAD design was used in this study [32]. The updated THOR-k model was positioned to match the position of the original model, which had been positioned based on recorded dummy pre-test positioning specifications, within the sled. Surface to surface contacts were defined between all dummy and sled/belt parts, which come into contact during simulation. Test conditions were simulated by constraining the sled model to the linear acceleration profile of the sled buck recorded during dummy testing (Fig. 3-14b).

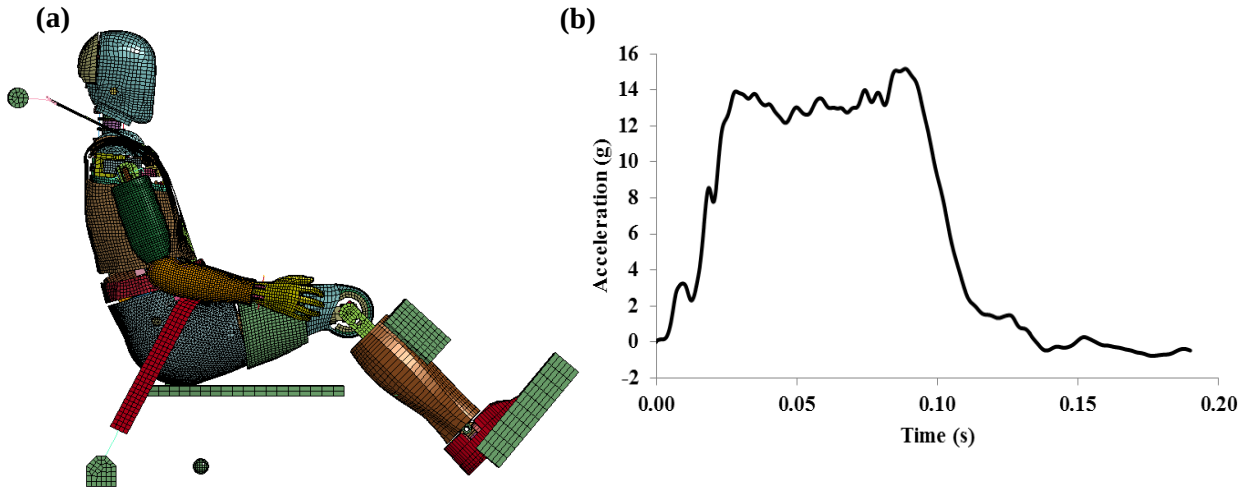

Figure 3-14**.** Frontal crash simulation setup: (a) pre impact positioning, (b) sled acceleration pulse.

A parametric study was performed in LS-Opt (LSTC, Livermore, CA, USA) to quantify the sensitivity of the head neck region to changes in belt and dummy position within the sled. In this study the position of the chest belt was varied between 5 and 10 mm from its initial position to left and right of the dummy model respectively (Fig. 3-15a). The upper body (including the pelvis region) was varied in rotation between 0 and 3 degrees around the center of the dummy hip rotation point (H-point). Both belts were rotated with the body to maintain their position with respect to the dummy model (Fig. 3-15b). These variables were chosen to represent inherent

changes in test condition, which may occur between tests. To evaluate the sensitivity of the updated head neck region to these variables upper neck (N_{IJ}) and head (HIC) injury criterion were evaluated as response variables [33]. A total of 25 design points (pre-impact dummy positions) were fully simulated in massively parallel processing (MPP) on the TRACC Argon Cluster (Argonne National Laboratories) with 16 CPUs per simulation. Total run time for each simulation was approximately 7.5 hours.

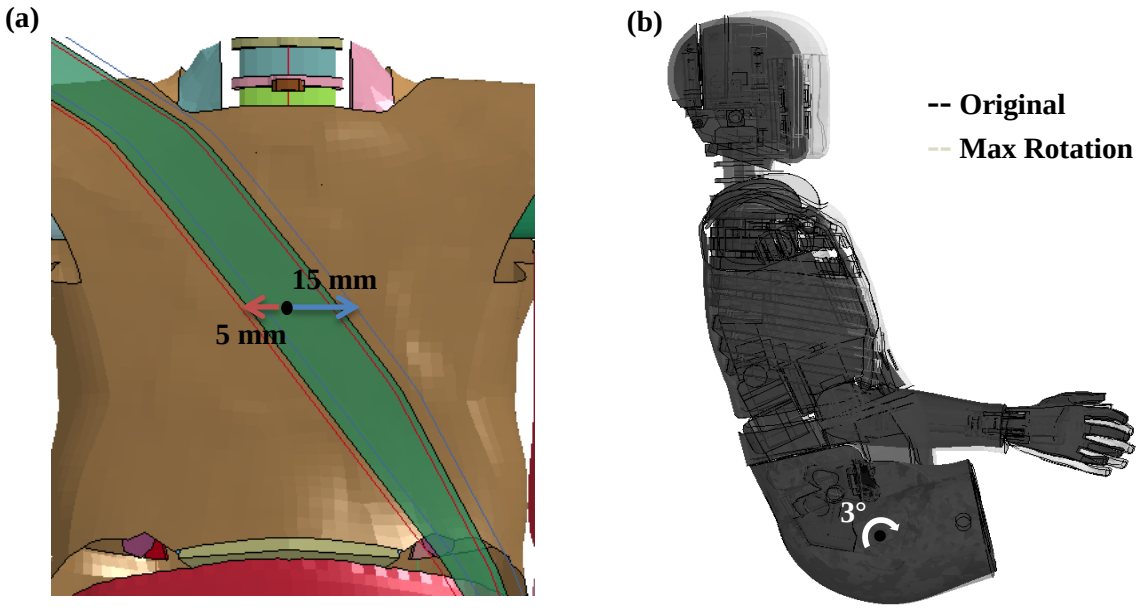

Figure 3-15. Positioning sensitivity setup: (a) belt translation, (b) upper body rotation.

3.4 Results

3.4.1 Model Calibration

3.4.1.1 Neck Puck Calibration: NBDL Lateral Simulation

The calibration of the neck puck material model resulted in a stiffness reduction of 0.623. Both kinetic and kinematic responses of the FE head-neck complex were improved in the NBDL lateral simulation. Horizontal, lateral, and rotational motion all increased with the decrease in

puck stiffness, resulting in a similar motion to the test dummy. The rating score of the model increased from 0.845 in the initial model up to 0.971 in the calibrated model (Fig. 3-16).

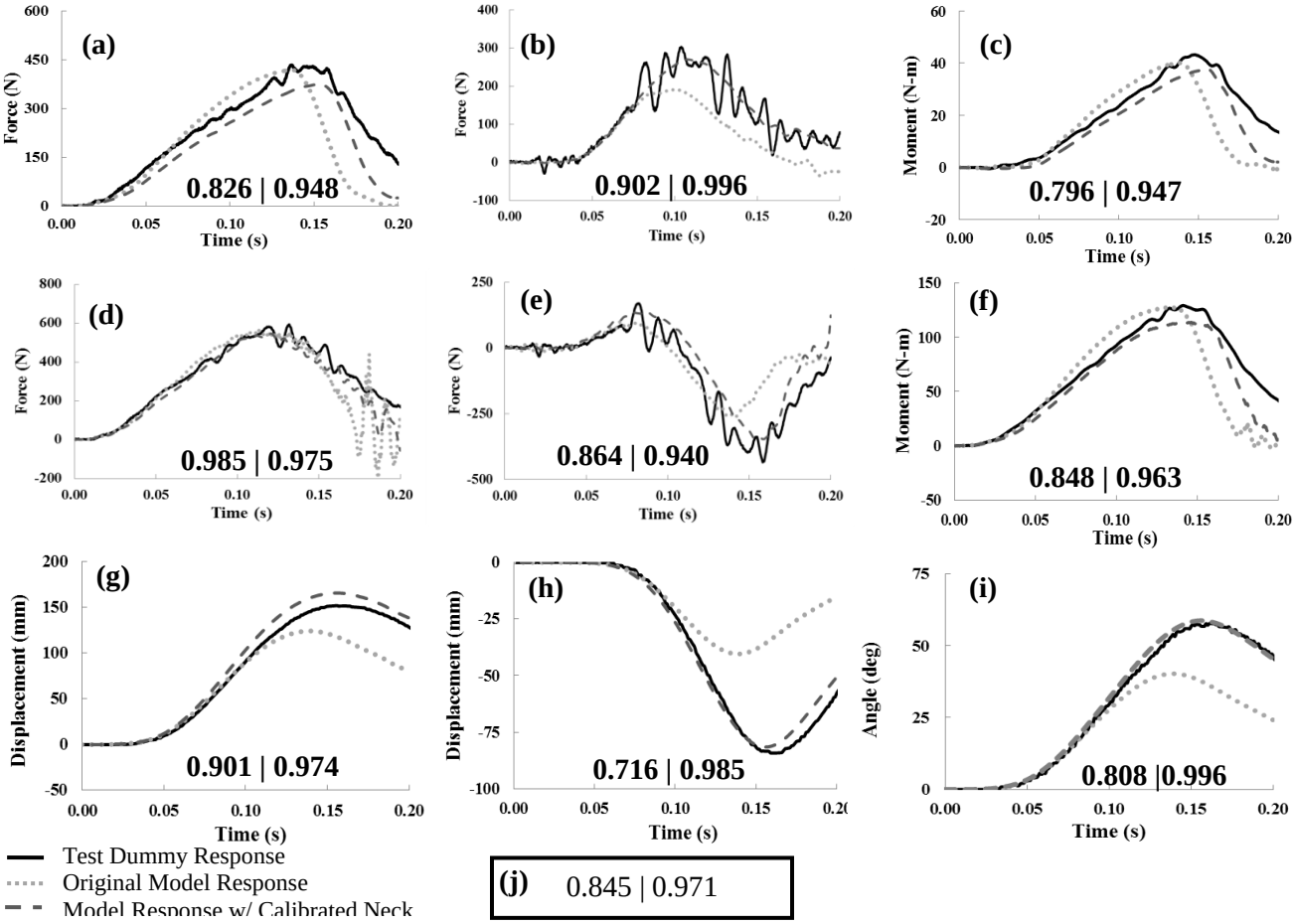

Figure 3-16**.** Model Calibration: NBDL lateral time history CORA rating comparison: (a) upper neck lateral force, (b) upper neck vertical force, (c) upper neck coronal moment, (d) lower neck lateral force, (e) lower neck vertical force, (f) lower neck coronal moment, (g) head lateral displacement, (h) head vertical displacement, (i) head coronal rotation angle, (j) total CORA rating (original | calibrated).

3.4.1.2 Cable-Neck Plate Friction Identification and Springs Calibration: Pendulum Extension and Flexion Simulations

The optimized value of cable friction coefficient was increased from its original value (0.6) to the upper bound of the optimization range (0.99). The first phase of the load-displacement curves increased in slope (stiffness) in the front spring while it decreased in the rear spring. The duration of the first phase was also decreased in both springs. The second phase peak load was

increased in the front spring while decreased in the rear spring. The phase lengths remained similar in the unloading curves. First phase unloading slope was decreased consequently increasing the second phase unloading slope in the front spring. The first phase unloading slope of the rear spring is increased approaching that of the loading curve (Table. 3-1).

Table 3-1. Calibrated Values of Spring Stiffness Parameters

Variable	**Original Value**	**Optimized Values**
Front Spring Coefficients		
dl	25	12.4
du	32	33.3
hl1	0.96	0.74
hu1	0.84	0.34
h2	2.88	5.87
Rear Spring Coefficients		
dl	35	29.35
du	25	29.99
hl1	3	0.38
hu1	0.75	0.38
h2	3.75	2.62

In the pendulum extension simulation (Fig. 3-17), the model improvement is primarily associated with the front cable and spring calibration as the rear spring force has minimal effect in this test. The calibration was shown to most significantly improve the peak response values of the upper neck and rear spring model forces. The OC-joint additionally demonstrates improved initial peak response though the second phase shape remains inconsistent with the physical dummy.

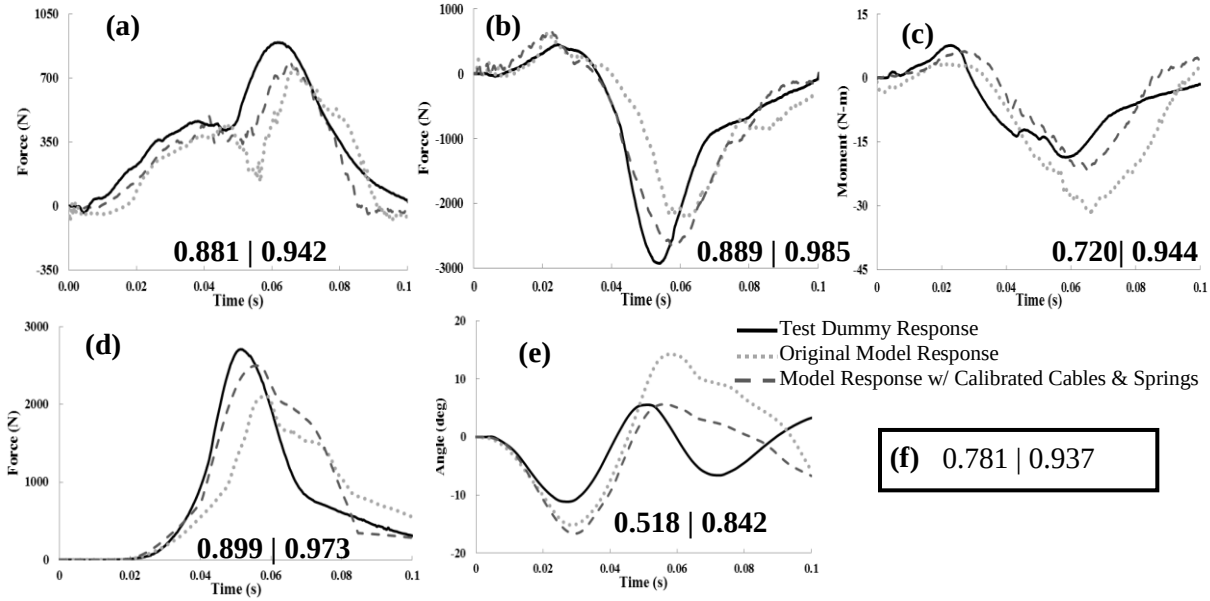

Figure 3-17**.** Model Calibration: Pendulum extension time history comparison: (a) upper neck horizontal force, (b) upper neck vertical force, (c) upper neck sagittal moment, (d) front spring force, (e) OC-joint rotation angle, (f) total CORA rating (original | calibrated).

Model calibration is shown to greatly improve the model response in pendulum flexion, as the CORA rating improved from 0.681 to 0.96 (Fig. 3-18). Horizontal force in the neck is shown to improve significantly as well as the rotational motion around the OC-joint. Though both pendulum extension and flexion simulations were run in parallel to calibrate both front and rear springs simultaneously, the front spring force and the rear spring force showed minimal influence in the flexion test and the extension test, respectively.

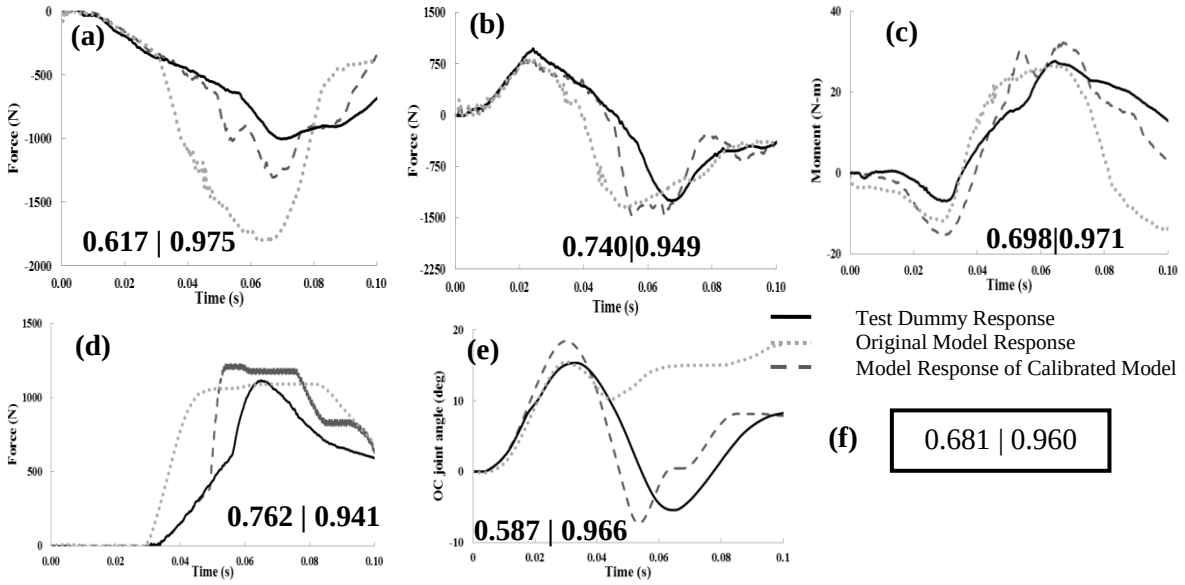

Figure 3-18. Model Calibration: Pendulum flexion time history comparison: (a) upper neck horizontal force, (b) upper neck vertical force, (c) upper neck sagittal moment, (d) rear spring force, (e) OC-joint rotation angle, (f) total CORA rating (original | calibrated).

3.4.1.3 Head Skin Calibration: Head Impact Simulation

In the calibrated model, the long and short time shear moduli in addition to the bulk modulus were decreased (Table 3-2), resulting in a peak force reduction in the FE simulation that more closely matched the test data (Fig. 3-19). To increase the contact time between impactor and dummy head, the material decay constant increased in the calibrated model. Overall, both shape and size of the impact force significantly improve in calibrated model resulting in a higher CORA rating score (0.991 versus 0.87) for this calibrated head skin model.

Table 3-2**.** Calibrated Values of Head-Skin Material Parameters

Visco-Elastic Coefficients	**Baseline Value**	**Optimized Values**
Bulk Modulus (MPa)	160	8.2
Short Time Shear Modulus (MPa)	9.1	1.82
Long Time Shear Modulus (KPa)	0.26	0.05
Decay Constant (ms^{-1})	0.4	0.59

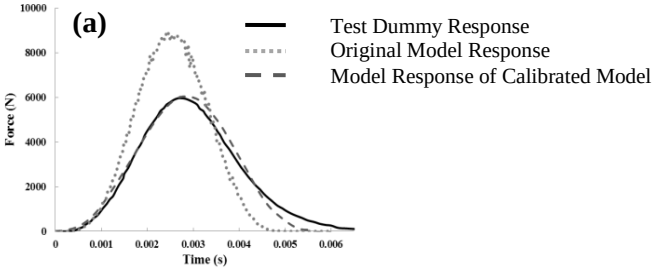

(b) 0.870 | 0.991

Figure 3-19**.** Head impact time history comparison: (a) head impact force (b) total CORA rating (original | calibrated).

3.4.2 Model Validation

3.4.2.1 Frontal Validation: NBDL Flexion Simulation

The fully calibrated head-neck complex of the THOR-k dummy model shows similar response to the dummy in the NBDL frontal test (Fig. 3-20). The model CORA rating from this validation test is 0.948. A high correlation is shown in the vertical forces and sagittal moments in the neck between the head displacement of the model and dummy. Test to simulation discrepancies remain in the lower neck vertical load as well as the rotation angle of the OC-joint. Head kinematics are similar though there is a slight under rotation in the model along with increased vertical and decreased horizontal displacement.

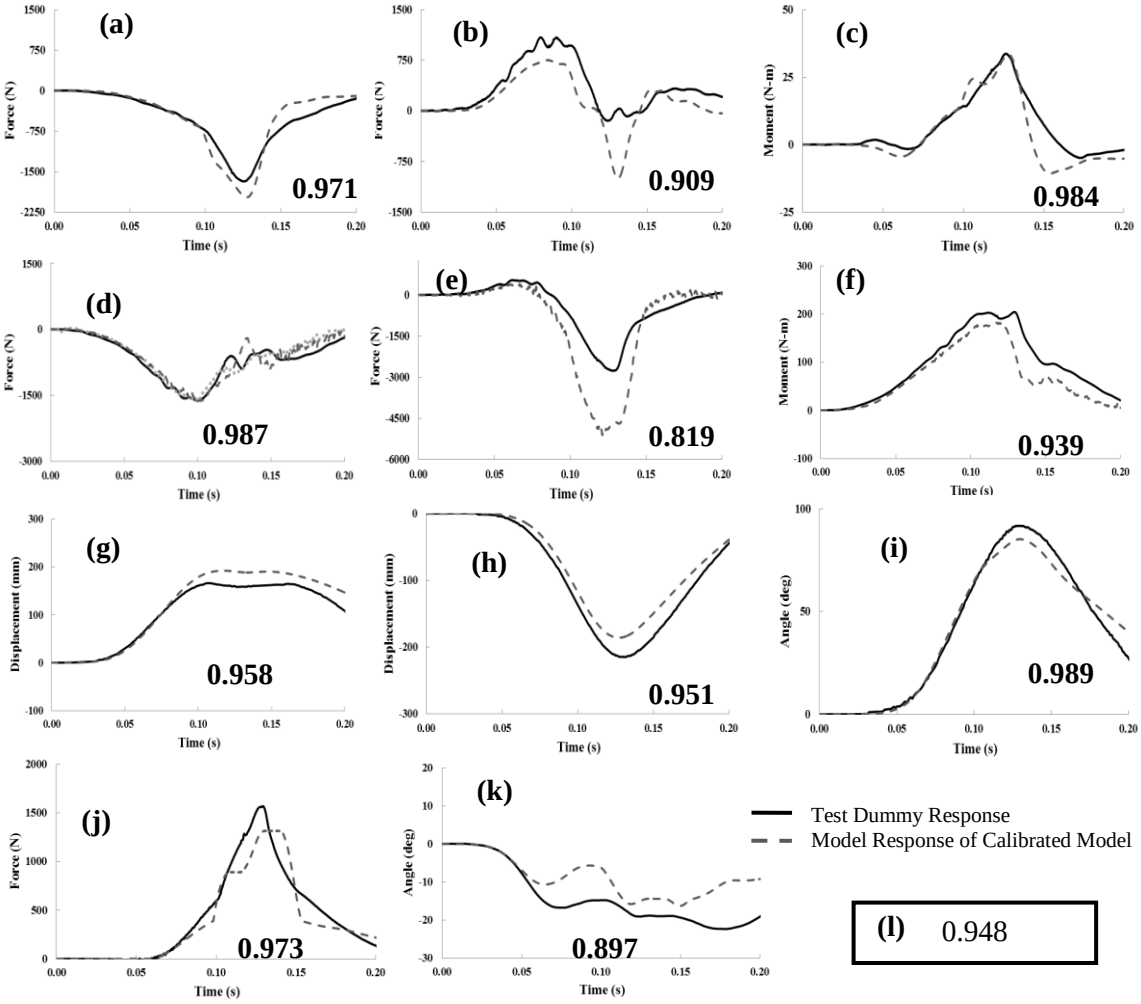

Figure 3-20. Model Validation: NBDL frontal time history comparison: (a) upper neck horizontal force, (b) upper neck vertical force, (c) upper neck sagittal moment, (d) lower neck lateral force, (e) lower neck vertical force, (f) lower neck sagittal moment, (g) head lateral displacement, (h) head vertical displacement, (i) head sagittal l rotation angle, (j) rear spring force, (k) OC-joint rotation angle, (l) total CORA rating.

3.4.2.2 Lateral Validation: Pendulum Lateral Simulation

The FE model closely predicts the response of the head-neck complex of the THOR-k dummy in the lateral pendulum test (Fig. 3-21). The model scored a total CORA rating of 0.936. The model most accurately predicts dummy response in upper neck vertical load and coronal moment. The lateral force time history in the upper neck exhibits close overall shape, though a slight under prediction of force for the majority of simulation. This changes to an over prediction

after peak force is reached. A similar trend is observed in the neck moment, though to a lesser degree.

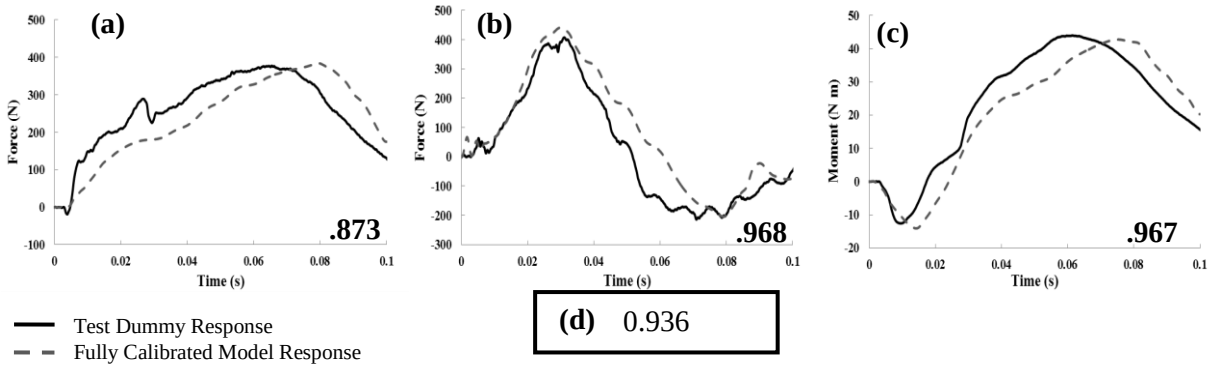

Figure 3-21. Model Validation: Pendulum lateral time history comparison: (a) upper neck lateral force, (b) upper neck vertical force, (c) upper neck coronal moment, (d) CORA score.

3.4.3 Sensitivity Analysis

In the frontal sled impact, sobol sensitivity analysis performed on the DOE results indicate upper body pre-impact rotation in the sagittal plane to have a larger influence on head neck model response than belt translation (Fig. 3-22a) within the variation ranges chosen. HIC_{36} values are shown to be the most sensitive to upper body rotation. Peak HIC_{36} values are observed at no belt translation while peak N_{IJ} values are observed at belt translation of approximately 3 mm to the right (Fig. 3-22 b,c). Body rotation causes a uniform decrease in both HIC_{36} and N_{IJ} values. Pure rotation of the thorax pre-test is shown to decrease HIC_{36} and N_{IJ} values a maximum 6.0% and 8.2% respectively. The maximum change in head-neck injury criteria predictions, HIC_{36} and N_{IJ} values, due to pure belt translation is 4.4% and 6.2% percent respectively. The maximum variation due to both of these variables is 10% HIC_{36} and 14.5% N_{IJ}.

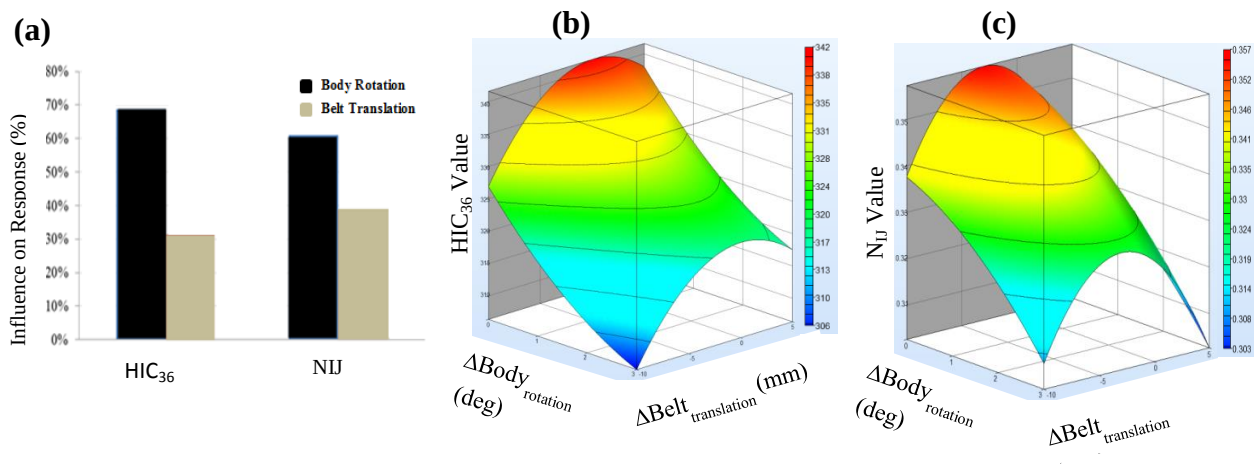

Figure 3-22. Sensitivity Results: (a) Sobol global sensitivities, (b) HIC_{36} response surface, (c) N_{IJ} response surface.

3.5 Discussion

A series of modifications have been recently made to the THOR dummy to improve its durability, operability, and biofidelity [13]. In this study, the head-neck region of THOR FE model has been updated to reflect these dummy modifications. Additional modifications were applied to both improve the computational performance and the ease of use of the THOR FE-model.

To calibrate the FE-model of the THOR-k dummy head-neck complex, rating system-based calibration approach has been developed and implemented. The CORA rating system was utilized to calibrate the FE model in both kinetic and kinematic response over its whole response phase. The material properties were optimized based on values previously implemented in the model. This approach resulted in an optimized parameter set that improved the ability of the FE model to predict the response of the physical dummy. However, specific component and material testing is recommended in the future to better characterize the properties of dummy components. For example, the head spring models used are a simplified representation of a much more complex system found in the dummy. The force-deformation responses of the neck spring towers

used in the dummy are dependent on not only the spring response but are also affected by internal damping and part friction within the tower. The original spring models were calibrated assuming a simplified stiffness curve shape that may not be optimal for representing this system. Non-physical artifacts in the model response, such as the force plateau peaks observed in the springs during simulation, which were not observed in testing, may be caused by the assumed spring stiffness shape. In addition, it is difficult to determine if the material model optimization better characterize the actual part material or are improving response by compensating for other parts. Though the largest material change in this study, the head skin bulk modulus, provided a much more realistic bulk modulus of 8 MPa opposed to the original 160 MPa, compared to head skin part models found in the literature[15]. To ensure individual part model accuracy future component and material testing at various loading rates would provide data to improve both spring models and the polymeric material part models (e.g. neck pucks and skin foams) that are strain-rate dependent. This would further increase the confidence in the response of dummy parts over a larger range of impact scenarios. Though exact material model parameter specification may not be possible, the calibration approach presented in this study may be used in conjunction with future material testing data to further improve the model. Potential application of the current calibration approach also exists in the calibration of other FE models.

Overall, the final calibrated head-neck model developed in this study is shown to respond with high similarity to the dummy in both NBDL frontal and pendulum lateral validation tests. This indicates that that the optimization performed during calibration is not test specific. Confidence is provided in the head-neck model for use in predicting dummy response in tests not performed in this study.

Though a high validation score is given and significant improvement is shown in optimization tests, there are a few differences seen between model response and dummy response. OC-joint rotational response is shown to significantly improve in flexion with the calibration of the rear spring, yet its response continues to diverge from the dummy response in extension. Though calibration of an added unloading curve showed to be more detrimental then positive, there may be room for improvement in the OC-joint model. One possibility is inadequate stiffness/damping characterization of this joint. Further implementation of rate-dependent properties of OC-joint, which is currently defined based on quasi-static testing, may improve its response. In the frontal NBDL validation test the predicted peak of the vertical lower neck force demonstrates the most significant divergence from the test dummy response. Because no lower neck data was available in the pendulum tests this region was not able to be properly calibrated while also used in validation. Therefore, further pendulum testing of the head-neck dummy parts with lower neck load cell instrumentation is suggested in future tests to better calibrate the model response in this region. It is also suggested that injury criteria (e.g. N_{IJ}, HIC etc.) implemented within the formulation of the model rating scores in future calibration studies may further improve model predictability of injury risk.

The simulation of the calibrated head-neck model in the full body crash test scenario demonstrated total model stability and its applicability for use in crash safety analysis. Though simulation results cannot be compared to the physical dummy, as this crash test scenario has not been performed on the THOR-k, the sensitivity analysis performed allows some insight into the effects of pre-test positioning discrepancies on the THOR response. It was shown that upper body rotation around the pelvis rotation point within a range of 0 to 3 degrees forward rotation moderately decreases the predicted head-neck injury risk. The belt translation from its original

location, within a total range of 15 mm, is shown to be less influential, although the significance of this is limited as the effect is not normalized to the range each parameter. Both variables have a similar overall effect on both head and neck injury predictions. Overall these pre-test position variations are shown to have only a slight effect on predicted injury levels. The maximum change in HIC_{36} value amounts to 3.5% of the maximum injury threshold (1000). The maximum change in N_{IJ} represents a 0.67% difference in estimated risk of an AIS 2 or greater injury at the upper neck. After full validation of the FE model of the whole THOR-k dummy, more numerical studies, which would be difficult and expensive to perform experimentally, are expected. Comparison studies with dummy and human models may also be performed in order to contribute to future changes in THOR dummy design in an effort of improving its biofidelity, which has been traditionally based on PMHS testing and designer experience.

3.6 Conclusions

The head-neck region of the THOR model was successfully updated to the specifications of the latest THOR dummy mod-kit, and then calibrated to replicate the response of the THOR-k dummy. The model calibration was performed using a novel rating-based optimization approach to identify the optimal parameter values that best match the model response to the dummy in a series of dummy certification tests. This numerical calibration approach was shown to be effective. The final head-neck model was validated in frontal and lateral testing directions, so it is recommended for use in both frontal and side impact simulations. The application of the calibrated head-neck model for use in the crash safety field is demonstrated in an evaluation of the sensitivity of its response to pre-test positioning variability during a frontal crash test simulation. It was found that both belt position and body rotation have a slight effect on predicted head and neck injury criteria values. To further improve the effectiveness of this model

it is suggested that component testing of the neck spring towers of the dummy is necessary to provide more consistent spring models and thus further improve the performance of the THOR head-neck model. Material testing of polymeric materials of the dummy at various loading rates may further improve model response through more accurate strain rate dependent material models. The results shown in this study indicate the potential of the optimization technique developed for use in later model improvements (e.g., calibration of material models with material test data). This technique maintains additional potential in the calibration of other models (human or alternative dummy models) for crash test simulation.

3.7 Acknowledgments

Funding for this study was provided by the National Aeronautics and Space Administration (NASA). The authors would like to thank Dassault Systèmes Simulia Corp. for providing Isight™ software. The authors would also like to thank to Dr. Koshiro Ono of Japan Automotive Research Institute (JARI) for providing the THOR-k pendulum test data and Mr. Dan Parent (NHTSA) for his support given to this work. All findings and views reported in this manuscript are based on the opinions of the authors and do not necessarily represent the consensus or views of the funding organization.

3.8 References

1. WHO, *World Health Organization: Global status report on road safety: time for action*, 2009.
2. Forman, J., et al., *Thoracic response of belted PMHS, the Hybrid III, and the THOR-NT mid-sized male surrogates in low speed, frontal crashes.* Stapp Car Crash J, 2006. **50**: p. 191-215.
3. Sherwood, C.P., et al., *Development of a frontal small overlap crashworthiness evaluation test.* Traffic Inj Prev, 2013. **14 Suppl**: p. S128-35.
4. Barbat, S., X. Li, and P. Prasad, *Bumper and Grille Airbags Concept for Enhanced Vehicle Compatibility in Side Impact: Phase II.* Traffic Inj Prev, 2013. **14 Suppl**: p. S30-9.
5. Hu, J., et al., *Development and validation of a modified Hybrid-III six-year-old dummy model for simulating submarining in motor-vehicle crashes.* Med Eng Phys, 2012. **34**(5): p. 541-51.
6. Untaroiu, C.D., et al., *A study of the pedestrian impact kinematics using finite element dummy models: the corridors and dimensional analysis scaling of upper-body trajectories.* International Journal of Crashworthiness, 2008. **13**(5): p. 469-478.

7. Fredriksson, R., J. Shin, and C.D. Untaroiu, *Potential of pedestrian protection systems--a parameter study using finite element models of pedestrian dummy and generic passenger vehicles.* Traffic Inj Prev, 2011. **12**(4): p. 398-411.
8. Kerrigan, J., C. Arregui-Dalmases, and J. Crandall, *Assessment of pedestrian head impact dynamics in small sedan and large SUV collisions.* International Journal of Crashworthiness, 2012. **17**(3): p. 243-258.
9. Shaw, G., J. Crandall, and J. Butcher, *Comparative evaluation of the THOR advanced frontal crash test dummy.* International Journal of Crashworthiness, 2002. **7**(3): p. 239-253.
10. Untaroiu, C.D., J. Shin, and J.R. Crandall, *A design optimization approach of vehicle hood for pedestrian protection.* International Journal of Crashworthiness, 2007. **12**(6): p. 581-589.
11. Adam, T. and C.D. Untaroiu, *Identification of occupant posture using a Bayesian classification methodology to reduce the risk of injury in a collision.* Transportation Research Part C-Emerging Technologies, 2011. **19**(6): p. 1078-1094.
12. Bose, D., et al., *Influence of pre-collision occupant parameters on injury outcome in a frontal collision.* Accid Anal Prev, 2010. **42**(4): p. 1398-407.
13. Ridella, S.A. and D.P. Parent, *Modifications to improve the durability, usability and biofidelity of the THOR-NT dummy*, in *The 22nd ESV Conference*2011: Washington, D.C., USA.
14. Parent, D.P., et al., *Thoracic Biofidelity Assesment of the THOR Mod Kit ATD*, in *The 23nd ESV Conference*2013: Seoul, Korea.
15. Untaroiu, C. and Y.-C. Lu, *A Simulation-Based Calibration and Sensitivity Analysis of a Finite Element Model of THOR Head-Neck Complex*, in *SAE 2011 World Congress & Exhibition*, SAE, Editor 2011: Detroit, USA.
16. LS-Dyna, *Keyword User's Manual*, 2007, LSTC.
17. Yu, H., et al., *Head-neck finite element model of the crash test dummy THOR.* International Journal of Crashworthiness, 2004. **9**(2): p. 175-186.
18. Jacob, C., et al., *Mathematical models integral rating.* International Journal of Crashworthiness 2000. **5**(4): p. 417-432.
19. Hovenga, P.E., H.H. Spit, and M. Uijldert, *Rated facet Hybrid-III 50th model with improved user-friendliness introduced*, in *10th International MADYMO Users Meeting*2004.
20. Gehre, C., H. Gades, and P. Wernicke, *Objective Rating of Signals using Test and Simulation Responses*, in *ESV Conference*2009: Stuttgart, Germany.
21. Sarin, H., et al., *A Comprehensive metric for comparing time histories in validation of simulation models with emphasis on vehicle safety applications*, in *ASME International Design Engineering Technical Conference and Computers and Information in Engineering Conference (DETC' 08)*2008: New York, USA.
22. Sarin, H., et al., *A Comprehensive Metric for Comparing Time Histories in Validation of Simulation Models with Emphasis on Vehicle Safety Applications.* Detc 2008: Proceedings of the Asme International Design Engineering Technical Conferences and Computers and Information in Engineering Conference, Vol 1, Pts a and B, 2009: p. 1275-1286.
23. Untaroiu, C.D., J. Shin, and Y.C. Lu, *Assessment of a dummy model in crash simulations using rating methods.* International Journal of Automotive Technology, 2013. **14**(3): p. 395-405.
24. Thunert, C., *CORA Release 3.6, User's Manual*, 2012, PDB.
25. Isight, *Isight 5.0 User's guide*, 2011, Dassault Systèmes Simulia Corp. Cary, North Carolina, USA (http://www.3ds.com/products-services/simulia/portfolio/isight-simulia-execution-engine/overview/).
26. Tiwari, S., et al. *AMGA: an archive-based micro-genetic algorithm for multi-objective optimization*. in *The genetic and evolutionary computation conference, GECCO*. 2008.

27. Untaroiu, C.D., et al., *Crash reconstruction of pedestrian accidents using optimization techniques.* International Journal of Impact Engineering, 2009. **36**(2): p. 210-219.
28. Untaroiu, C.D. and A. Untaroiu, *Constrained Design Optimization of Rotor-Tilting Pad Bearing Systems.* Journal of Engineering for Gas Turbines and Power-Transactions of the Asme, 2010. **132**(12).
29. Ewing, C.L., et al., *Dynamic Response of the Head and Neck of the Living Human to -Gx Impact Acceleration*, in *12th Stapp Car Crash Conference*, SAE, Editor 1968.
30. GESAC, *Biomechanical Response Requirements of the Thor NHTSA Advanced Frontal Dummy*, 2005.
31. ASM, *Handbook Vol. 18: Friction, Lubrification and Wear Technology*. 1992: ASM International.
32. Untaroiu, C., et al. *Evaluation of a Finite Element Model of the THOR-NT Dummy in Frontal Crash Environment*. in *Proceedings of 21st International Conference on Experimental Safety Vehicles (ESV)*. 2009.
33. Stander, N., et al., *LS-OPT® Version 4.3 User's Manual.* Livermore Software Technology Corporation, Livermore, 2012.

4. DEVELOPMENT AND EVALUATION OF A DUMMY FINITE ELEMENT MODEL FOR OCCUPANT PROTECTION OF SPACEFLIGHT CREWMEMBERS

Jacob B. Putnam, Jeff T. Somers, Costin D. Untaroiu

Manuscript to be submitted for publication to *Accident Analysis & Prevention*

4.1 Abstract

New vehicles are currently being developed to transport humans to space. A critical design driver for the vehicle is landing, where crewmembers are typically exposed to spinal and frontal loading. To reduce the risk of injuries during these common impact scenarios, the National Aeronautics and Space Administration (NASA) has begun research into the development of new safety standards for spaceflight. The THOR, an advanced multi-directional crash test dummy, was chosen to evaluate occupant spacecraft safety due to its improved biofidelity.

Recently, a series of modifications were completed by the National Highway Traffic Safety Administration (NHTSA) to improve the bio-fidelity of the THOR dummy. The updated THOR Modification Kit (THOR-k) dummy was tested at Wright-Patterson (WP) Air Base in various impact configurations, including frontal and spinal loading. A computational finite element (FE) model of the THOR-k was developed in LS-DYNA software to match the latest dummy modifications. The main goal of this study was to calibrate and validate the THOR-k FE model for use in future spacecraft safety studies.

An optimization-based method was developed to calibrate the material models of the lumbar joints and pelvic flesh. Data from a compression test of pelvic flesh was used to calibrate the quasi-static material properties of the pelvic flesh. The whole dummy kinematic and kinetic response under spinal and frontal loading conditions was used for dynamic calibration. The performance of the calibrated dummy model was evaluated by simulating separate dummy tests with different crash pulses along both spinal and frontal directions. The model response was compared with test data by calculating its correlation score using the CORA rating system. The biofidelity of the THOR dummy was then evaluated against tests recorded on human volunteers under three different frontal and spinal impact pulses.

The calibrated THOR-k dummy model responded similarly to the physical dummy in all validation tests. The THOR-k dummy showed good biofidelity relative to human volunteer data under spinal loading, but limited biofidelity under frontal loading, improvements in both THOR physical and model were suggested. Overall, results presented in this study provide confidence in the dummy model for use in predicting dummy responses for conditions such as those observed in spacecraft landing, and for use in evaluating THOR dummy biofidelity.

4.2 Introduction

With the advent of new space crew transport vehicles being developed by the National Aeronautics and Space Administration (NASA) and several commercial companies (e.g. Boeing, SpaceX, etc.), the number of spaceflight occupants is expected to increase dramatically. Learning from the trials of the automotive safety field, early development of occupant crash safety standards for these new spaceflight vehicles will be essential to prevention of injury. Though standards have been developed for the automotive field, spaceflight standards need to be developed separately due to unique considerations. An automobile impact is a low occurrence-high risk event with a crash impact risk of 1 in 1.3 million miles driven and 1 in 3.4 crashes resulting in injury. Therefore, automobile industry standards are focused on mitigating the risk of severe injuries. To achieve spaceflight, the human body is accelerated to over 11,200 m/s to escape earth's gravity, and in turn is decelerated back to rest during landing [1]. Though severe accelerations are mitigated as much as possible, there is still a large energy transfer into body during landing. Therefore, it is essential to develop spaceflight safety standards with a very conservative total injury risk, to ensure the continued health and safety of all human occupants traveling to and from space.

The majority of the space transport vehicles currently being developed are capsule-based [1]. During takeoff and landing the vehicles typically experience loads along the frontal (eyeballs in-out) and spinal (eyeballs up-down) directions. Though takeoff conditions can be highly controlled by engine thrust, landing is passively controlled by parachute and dependent on wind conditions, terrain, and parachute performance. This variability in landing conditions further adds to the necessity of conservative injury risk standards, requiring thorough crash safety analysis of these conditions.

Crash safety analysis is primarily performed through the testing of anthropometric test devices (ATDs), commonly referred to as crash test dummies. Currently NASA is investigating the Test Device for Human Occupant Restraint (THOR) ATD for use in the development of new spaceflight safety standards. The THOR, developed by the National Highway Traffic Safety Administration (NHTSA), was chosen for this investigation due to its improved biofidelity over other common ATDs [2]. The THOR dummy was tested in both spinal and frontal impacts aligning with spaceflight landing conditions. This test data was used to advance the development of the THOR computational model for future spaceflight analysis.

The increase in computational power over the last decade has enabled the use of a computational component complementary to experimental testing. The development of Finite Element (FE) modeling in the crash safety field presents many opportunities to increase the efficiency and capabilities of human safety analysis. An accurate and reliable ATD FE model provides a tool to increase testing efficiency, as test setup can easily be adjusted to assess response in a variety of conditions. In addition these models allow for the optimization of vehicle or restraint system design throughout the manufacturer's design process [3-5].

The goal of this study was to develop an accurate THOR FE model for computational spaceflight crash safety analysis. The effectiveness of the dummy model was ensured through comparison to physical tests in both frontal and spinal impacts. Once verified against the physical dummy, the THOR FE model was used assess the biofidelity of the THOR ATD against human volunteer test data. Based on these results, recommendations are made on the effectiveness of the THOR to predict human response in the spaceflight loading regime. The developed THOR FE model may be used to aid in the development of new spaceflight occupant safety standards, provide an effective tool in the optimization of new vehicle designs without the expense of testing and physical prototyping, and continuously improve of THOR dummy biofidelity.

4.3 Methods

4.3.1 Development/updating of THOR Dummy Model

The FE model of THOR [6] was updated according to recent modifications made to the THOR dummy (THOR-k) to improve its durability, usability, and biofidelity [7]. The FE models of updated dummy regions were developed [8] based on CAD drawings using Hypermesh software (Altair, Troy, MI, USA). The updated model components were calibrated and validated against component certification test data[8, 9], and then were assembled into the complete THOR-k FE model. The whole dummy FE model contains 222,292 nodes and 444,324 elements, and could be run in FE simulations, without mass scaling, with a time step of 0.22 μsec.

A positioning tree of the THOR-k model was developed in LS-Prepost (LSTC, Livermore, CA) to allow proper adjustment of the model posture to various test setups. The posture ranges were constrained to the positioning capabilities of physical dummy. Sensor definitions were also implemented into the model to match the instrumentation of the physical dummy.

4.3.2 Model Calibration

Material data for the updated THOR dummy was not publically available; therefore, to improve the response of the THOR FE model for typical spaceflight takeoff and landing impact conditions (frontal and spinal directions), material parameters of parts deemed essential to response in these conditions were calibrated from the baseline values assigned in the THOR-NT model[6]. It has been previously shown [10] that the overall response of the THOR model in vertical loading is significantly influenced by the properties assigned to the pelvic flesh. In addition, the rubber flex joints in the dummy spinal column showed to have a significant effect on the dummy response in both impact directions during several preliminary simulations. Therefore, the upper thoracic flex joint (UFJ), lower thoracic flex joint (LFJ), and pelvic flesh were chosen to be calibrated. The static and dynamic stiffness curves of the pelvic flesh material model (LS-DYNA Material Model 83, MAT_FU_CHANG_FOAM [11]) and the flex joints (LS-DYNA Material Model 183 MAT_SIMPLIFIED_RUBBER_WITH_DAMAGE [11]) were calibrated to optimize response to available dummy test data (Fig. 4-1). The robustness of this calibration was verified in two model validation tests unique from the calibration tests.

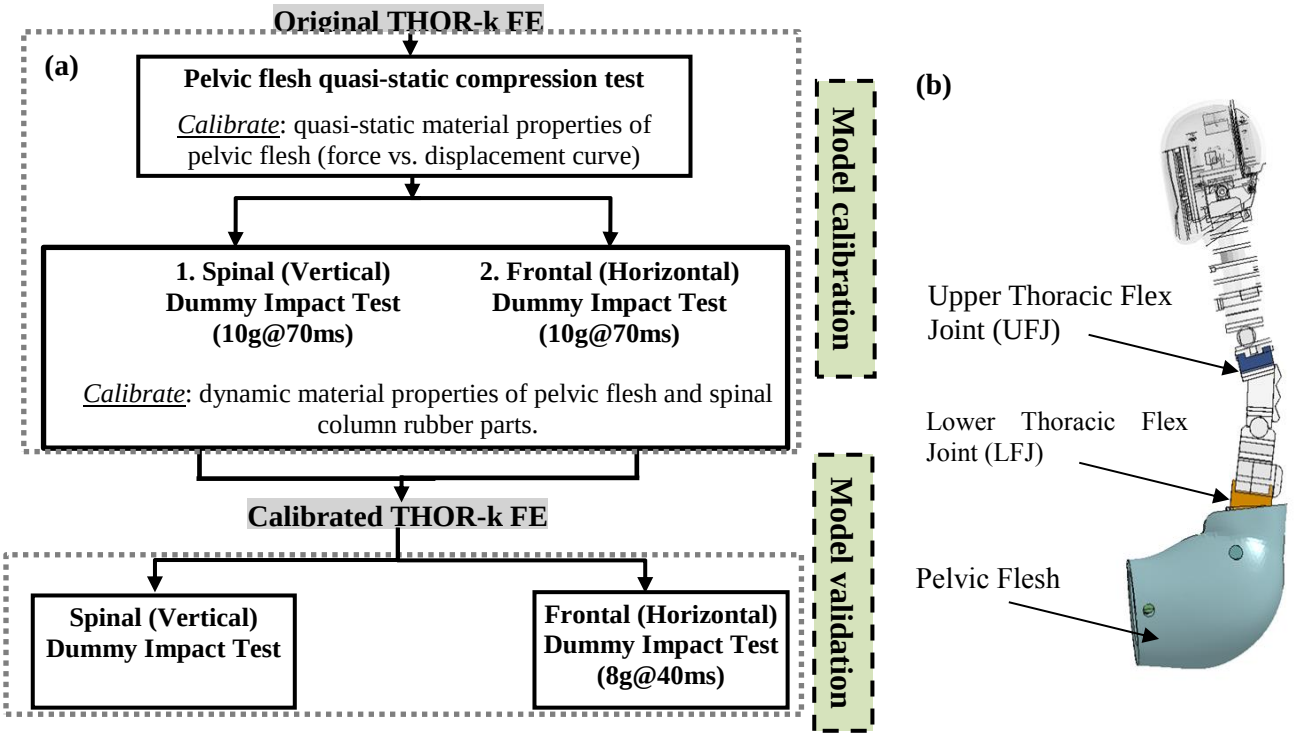

Figure 4-1. (a) Schematic of the calibration & validation of the THOR-k FE Model with (b) diagram of calibrated parts

4.3.2.1. The Calibration of Pelvic Flesh under Quasi-static Loading

The quasi-static stress strain curve defined in the THOR-k FE pelvic flesh material model was calibrated to match the force data recorded in a quasi-static compression test [12]. The test setup consisted of the pelvic flesh fitted onto a rigid metallic substructure (Fig. 4-2). A flat plate compressed the bottom of the pelvic flesh to 30 mm and then uncompressed it at a constant rate of 250 mm/min. This setup was simulated by constraining the interior nodes of the pelvic flesh model to a fixed rigid part. A flat shell plate was then simulated to compress the pelvic flesh as done in testing.

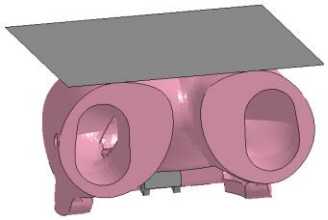

Figure 4-2**.** Pelvis flesh quasi-static compression setup: FE simulation.

Using this simulation the scale factor of the quasi-static strain-stress curve was determined by attempting to match the force-displacement time history between the pelvic flesh and rigid plate, in an optimization process carried out in LS-Opt (vers. 4). A successive response methodology (SRSM) with linear approximation was used with the objective function set to curve mapping between simulation and test data. The pelvic stiffness scale factor was the only defined variable and was ranged between .5 and .01, based on the results of several preliminary simulations. Two iterations with a total of 40 simulations were run with an explicit solver in Multi Parallel Processing (MPP) on the Argonne National Labs Transportation Research and Analysis Computing Center (TRACC). The total run time per simulation was approximately 10 hours with 8 CPU per run.

4.3.2.2 The Calibration of Dummy FE Model under Spinal and Frontal Loading

A series of frontal and spinal impact tests were performed on the THOR-K dummy at the Wright Patterson Air Force Base (WPAFB) by NASA to assess dummy response in spaceflight landing conditions[1]. A THOR dummy with all mod kit upgrades, excluding the SD-3 shoulder, and a generic test seat with rigid back and seat pan were used in testing [7]. A small layer of felt padding was placed over the head plate. The dummy was restrained to the seat with a five point belt system consisting of a double shoulder strap, lap belt, and negative-g strap, each pretensioned to (89±22 N) (Fig. 4-3a). In addition dummy hands and feet were restrained to the dummy legs and chair, respectively, to prevent excessive flailing. Acceleration conditions were

driven by the Horizontal Impulse Accelerator (HIA) [13] which has demonstrated a uniform 5% reproducibility on peak acceleration and velocity profile[14].

A seat model was developed based on the test seat dimensions recorded using a FARO arm system (FARO, Lake Mary, FL). The THOR-K dummy model was positioned within the seat model with appropriate contacts defined between test setup and dummy model (Fig. 4-3b). Initialization was performed by a pre-test simulation in which gravitational acceleration was applied to the dummy model until a steady state of compression state against the fixed seat was reached. The original nodal positions of the compressed parts were output and used to define the model's initial stress state for the impact scenario. Since the dummy was positioned upright to gravity in the frontal test and lying on its back in the spinal test, pre-simulation initialization was performed individually for each test condition. The material properties of the restraint system used in testing were determined through quasi-static tensile tests of each belt part. A material model (LS-Dyna Material Model B01, MAT_SEATBELT [11]) was then used to assign the determined material properties to each belt model part (Fig. 4-3b-c). A second pre-test simulation was run to pretension the belt around the dummy model to 22 N. In addition, springs models were used to restrain the hands and feet of the dummy model as in testing.

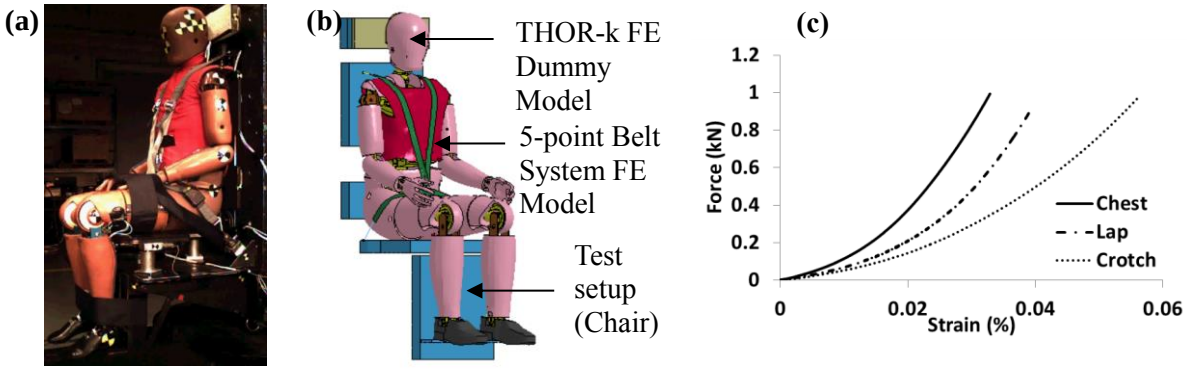

Figure 4-3**.** THOR-k dummy and test setup: (a) physical, (b) FE-Models, (c) belt stiffness curves.

The calibration of the whole THOR-k FE model was performed using test data recorded in one spinal and one frontal impact condition, both with nominal 10*g* peak acceleration at 70 ms. Acceleration pulses measured during testing were applied to the seat model. Acceleration pulses were applied along the upward (+z) (Fig. 4-4a) and the backward (-x) directions (Fig. 4-4b), respectively. The seat was constrained in all other directions. The minimum cpu run time required for the calibration process was 100 ms for the spinal simulation and 150 ms for the frontal simulation. In baseline simulations, it was shown that these reduced pulse lengths encompassed the peak response of all analyzed signals.

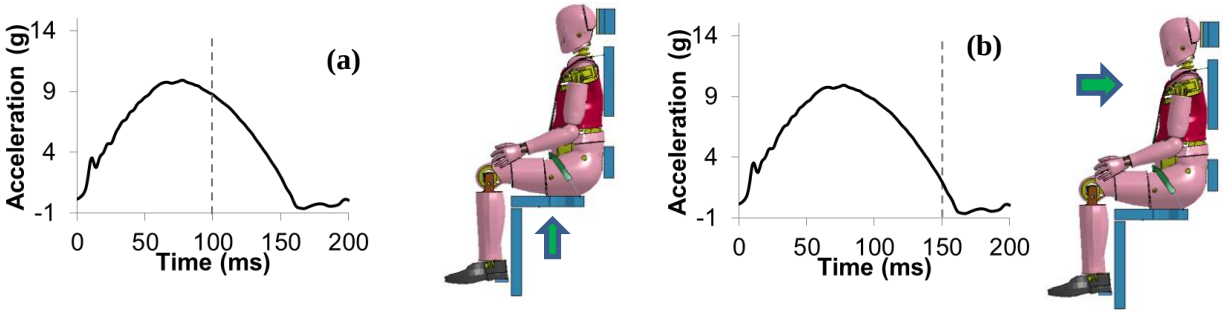

Figure 4-4**.** Model Calibration: Acceleration pulses used in the THOR-k simulations. (a) The spinal (vertical) direction, (b) the frontal (horizontal) direction.

The overall response of the THOR-k dummy model was quantitatively rated against test data to provide an objective metric for model calibration. The quality of a model's response in safety application has traditionally been evaluated by qualitative comparison of peak values to test data, curve shape, and injury indices. None of these techniques provide a quantitative means for grading the total response of a model based off the entire time history of its response. Recently there has been a focus to develop new curve-to-curve analysis techniques [15-19]. From this effort the CORrelation and Analysis (CORA) signal rating software has been developed [20]. The CORA rating method is made up of two independent rating methods, a corridor rating and a cross-correlation rating (Fig. 4-5). The corridor method scores the simulation curve based on its

position within inner and outer corridors developed around the test curve. Each evaluated curve is split into finite intervals which are scored individually. A score of 1 is given if the simulation is within the inner corridor, a score of 0 is given outside of the outer corridor, and a score between 0 and 1 is calculated by interpolation for the region between inner and outer corridors. The interval scores are averaged to calculate the total corridor score (S_{co}). The cross-correlation method rates the simulation curve, between 1 (perfect match) and 0 (no correlation) based on three characteristics with respect to the test curve (Fig. 4-5). Phase shift score (S_{ps}), size score (S_s) and shape score (S_{sh}) are measures of curve position, peak value, and curve shape, respectively (Fig. 4.5).

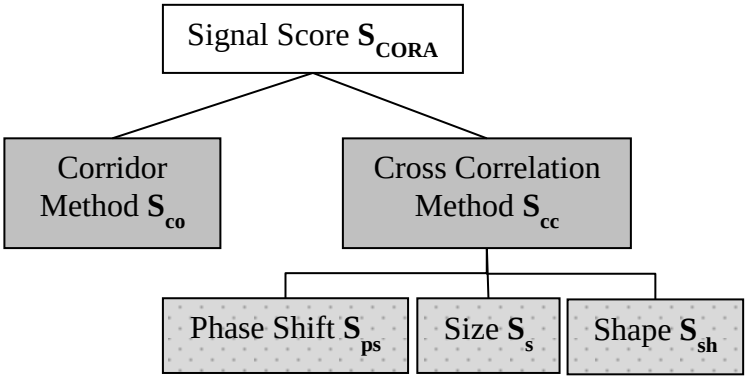

Figure 4-5**.** Schematic of CORA rating methodology.

The CORA rating of a curve (signal) is calculated as a linear combination of the corridor and the cross-correlation scores:

$$S_{cora} = w_{co}\ S_{co}\ + w_{cc}\ S_{cc} \tag{1}$$

where the cross correlation score is calculated:

$$S_{cc} = w_{ps}\ S_{ps}\ + w_s\ S_s\ + w_{sh}\ S_{sh} \tag{2}$$

The values of weighting factors were evenly set: $w_{co} = w_{cc} = 1/2$, and $w_{ps} = w_s = w_{sh} = 1/3$

The CORA model rating, defined as the average of all signals evaluated, was used to provide an objective model score for the dynamic material model calibration. To perform the model

calibration, both frontal and spinal simulations were run simultaneously in LS-Dyna with model material parameters iteratively selected using a Design of Experiments (DOE) scheme and successive response methodology (SRSM) with elliptic approximation optimization algorithm implemented in LS-OPT (LSTC, Livermore, CA, USA) (Fig. 4-6). Model response signals were chosen for CORA comparison based on relevance to typical injury criteria for the given impact direction and to encompass whole dummy response. Both dummy and model response data were post filtered using SAE 108. The average CORA model rating for both directions was set as the objective function which was maximized during the optimization process. Constraints on predicted injury criteria were set to be within ±15% of the test values for the peak lumbar load in the spinal simulation, the neck injury criteria and maximum chest deflection in the horizontal simulation. The optimization algorithm and all simulations were run on the TRACC cluster using an explicit solver in MPP with 8 CPU per run with an approximate run time of 6 hours per simulation. 128 simulations were run in both test directions over 4 iterations.

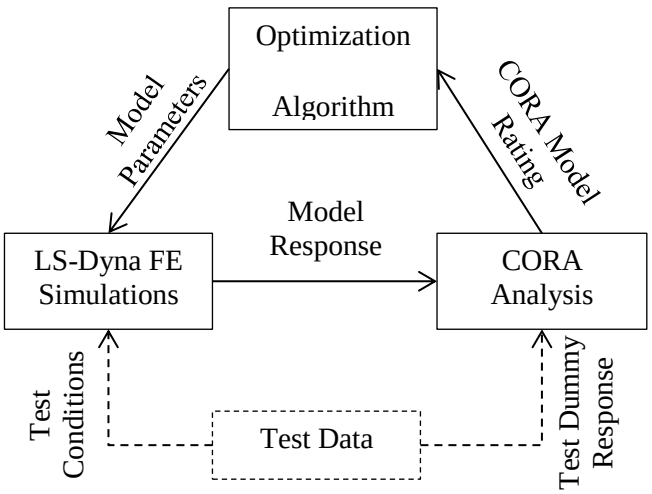

Figure 4-6. Schematic of the calibration method.

To calibrate the dynamic stress-strain properties of the pelvic flesh, each rate-dependent stress-strain curve defined in the pelvic flesh material model was scaled individually [11] (Fig. 4-

7a). To prevent the curves from overlapping the scale factor of each curve was calculated by the formula: $SF_n = SF_{n-1} + X_n$ (where SF is the scale factor, X is the optimization variable, and n represents each strain rate). SF_0 was assigned as the quasi-static scale factor previously determined. X_n was calibrated over a range of 0 to .5. The unloading properties of the pelvic flesh were calibrated by adjusting the hysteric unloading factor (HU) and shape parameter (SH) defined in the material model. HU was ranged between .1 and .9 while SH was ranged between -1 and 6. The force-displacement curves of the UFJ and LFJ were scaled in both loading and unloading (Fig. 4-7b-c) between .1 and 10. To simplify the total number of parameters used in optimization all loading rate curves for these parts were scaled using a single scale factor. All 10 variable ranges used in optimization were chosen based on pre-test simulations.

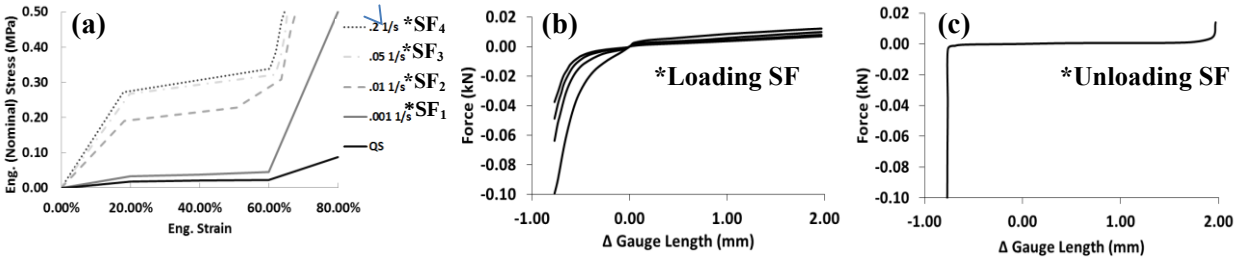

Figure 4-7**.** (a) Stress-strain curves of pelvis flesh model. Force displacement curves of spinal column rubber: (b) loading and (c) unloading.

4.3.3 Model Validation

The calibrated THOR-k FE dummy model was simulated under different spinal/frontal impact pulses to ensure calibration improvements were not test specific. A 10*g* at 40 ms and 8*g* at 100ms acceleration pulses were used respectively for the spinal and frontal validation simulations (Fig. 4-8 a,b). The same response signals used during the calibration phase were evaluated using the CORA rating system in the validation phase.

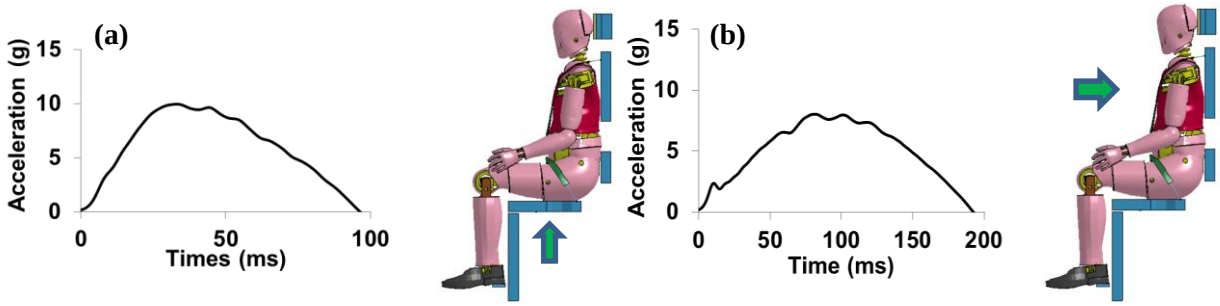

Figure 4-8**.** Model Validation: Acceleration pulses used in the THOR-k simulations. (a) The spinal (vertical) direction and (b) the frontal (horizontal) direction.

4.3.4 Comparison of Dummy-to-Human responses under Spinal and Frontal Impact Loadings

The THOR-k FE model, validated under frontal and spinal loading conditions, was used to evaluate the bio-fidelity of the THOR-k against historical human volunteer test data performed at WPAFB. The model response at nominal impact accelerations of 6, 8, and 10 g's in both frontal and spinal test directions was compared to human male volunteer data recorded in a horizontal test series (study #200301) and a spinal impact series (study #199906) [21, 22]. Although the dataset contained both male and female subjects, the comparison was limited to only the unscaled data recorded in male subjects, since the THOR-K is a representation of a 50th percentile male. The number of WPAFB volunteer tests performed with each impact pulse and the age/anthropometric data of male subjects are reported in Table 1.1.

Table 4-1. The Age and Anthropometric Information of WPAFB Male Volunteer subjects

Test	Frontal Test: #200301			Spinal Test: #199906		
Pulse	6*g*	8*g*	10*g*	6*g*	8*g*	10*g*
# of subjects	55	46	21	25	22	76
Age	30.8±4.7	30.5±4.5	31.7±4.7	31.7±6.3	32.5±6.9	32.5±3.6
Height (mm)	180±17	182±5.5	182±5.3	180±6.7	182±6.6	181±6.9
Weight (kg)	89.6±17.2	88.6±18.3	90.9±17	86.7±13.1	91.8±13.1	86.6±15.0

g- gravitational acceleration

The human volunteer horizontal impact study was performed on the WPAFB HIA similar to the THOR tests (Fig. 4-9a). A 40 G seat fixture was used in this test, the chair model used in

calibration and validation was adjusted accordingly. The back plate was extended, foot plate was added, and then the dummy model was positioned according to these test conditions. A generic HGU helmet model was developed to approximate the geometry and inertial properties (mass, center of gravity, and moment of inertia) of the helmet used in testing. An oxygen mask was additionally modeled to represent the equipment worn by human subjects. The previously developed 5-point belt model was fit to the new seat model and pretensioned to 89 N according to the test setup.

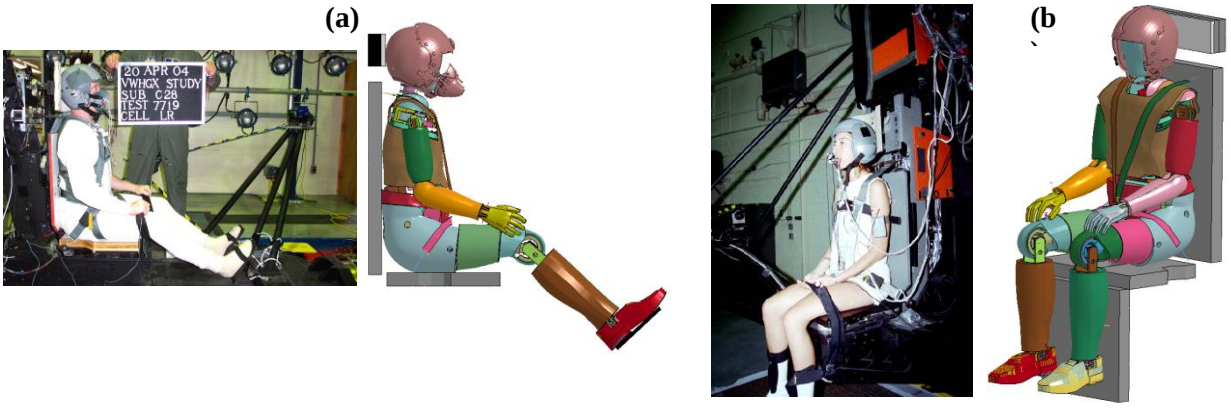

Figure 4-9**.** Physical test vs. FE model: (a) frontal test setup (test # 200301) and (b) spinal test setup (test #199906).

The spinal impact study was performed on the WPAFB Vertical Deceleration Tower (VDT) (Fig. 4-9b). The THOR-K FE model was positioned into a generic seat model as in testing. This study used a similar belt setup to the HIA tests, with the exception of the negative-g strap, which was removed from the model. In both frontal and spinal tests, subject head acceleration was measured within a bite block and the chest acceleration was measured using Velcro strapped accelerometers on the subject's chest center. In the FE model, chest acceleration was calculated at the dummy mid-sternal accelerometer location. Head acceleration was calculated at a point defined on the head casting approximate of the posterior jaw. Both human and THOR-K FE model response data was post filtered with an SAE 108 class filter. An additional SAE 60 class

filter was applied to the chest acceleration of the dummy model to reduce excessive noise caused by interaction between the accelerometer and non-rigid chest piece model.

The THOR-k simulation data was compared to human volunteer data using both the normal CORA rating system as a well as a built in biofidelity rating based on ISO 9790. The ISO 9790 biofidelity score is calculated based on the position of the model time history response relative to a test corridor developed from the human volunteer data. If the curve is completely within the assigned corridor it receives a score of 10. If it is outside the assigned corridor but within an outer corridor, automatically calculated twice the width of the assigned corridor, it receives a score of 5. Curves which pass outside the outer corridor receive a score of 0. The total biofidelity score is calculated as the average of all signal scores, and its values greater than 2.6 are considered acceptable for human analysis [20]. Though the test conditions evaluated in this study do not reflect the specific ISO 9790 test regime the rating system is used to provide an approximate bio-fidelity evaluation which encompasses the variation in human test data. To perform the CORA evaluation, elliptical test corridors [23] were developed for the acceleration responses of chest and head. The characteristic average curve from each instrumented region was used in the base CORA analysis while the 1 SD (Standard Deviation) elliptic corridors were used in the CORA biofidelity rating.

4.4 Results and Discussion

4.4.1 Model Calibration

4.4.1.1 Pelvic Flesh under Quasi-static Loading

The original pelvis part material model (approximated based on the material properties defined in THOR-NT model), showed a higher stiffness under quasi-static compression loading than the physical THOR-k part (Fig. 4-10a). The optimal scale factor found for the quasi-static

stress strain curve was 0.112, a significant decrease in part stiffness (Table 4-2). Comparing the pelvic model quasi-static stress-strain curve before and after calibration to generic foam testing, gives an approximate Young's modulus of 108 KPa and 12.175 KPa compared to 37 KPa [24].

Table 4-2. Pelvis Flesh Quasi-Static Stiffness

Variable	Original Values	Optimized Values
Pelvis Loading QS-SF	1.00	0.11

By scaling down the stress values in the quasi-static stress-strain curve, the pelvic model closely predicts the response of the physical part during the loading phase (Fig. 4-10b).

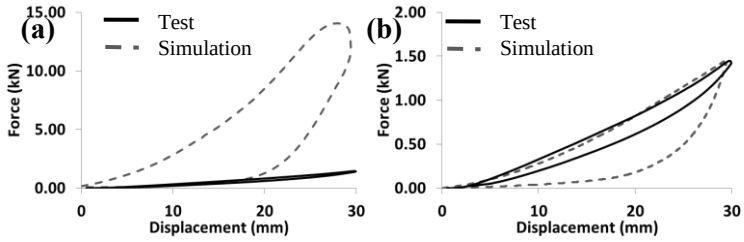

Figure 4-10. Pelvis flesh quasi static force vs. displacement response: (a) pre optimization, (b) post optimization.

4.4.1.2 Calibration of Dummy FE Model under Spinal (Vertical) Loading

The UFJ calibration resulted in an increased loading stiffness with decreased unloading stiffness (Table 4-3). The LFJ stiffness increased dramatically in both loading and unloading. The calibration of the dynamic stiffness curves of the pelvis flesh material model resulted in an increase in stiffness at the highest strain rate followed by a gradual decrease in the model stiffness with decreasing strain rate. The energy dissipation was increased in pelvis unloading with increased hysteretic unloading factor and the decreased shape value.

Table 4-3. The parameters of Calibrated Material Models

Part	Variable	Original Values	Optimized Values
UFJ	Loading SF	0.4	0.85
	Unloading SF	0.4	0.11
LFJ	Loading SF	0.4	6.40
	Unloading SF	0.4	9.84
Pelvis	Loading SF1	1.0	0.37
	Loading SF2	1.0	0.54
	Loading SF3	1.0	0.85
	Loading SF4	1.0	1.02
	Shape Parameter (SH)	3.0	6.00
	Hysteretic unloading factor (HU)	0.1	0.12

During spinal loading, an improved overall dummy response is observed in the calibrated dummy model. The CORA rating of the dummy model increased from 0.777 to 0.959 during the calibration process (Fig. 4-11). Good kinematic predictions of the calibrated dummy model are proven by the CORA scores of head, chest and pelvis acceleration which were above 0.97. Improvements were observed in the dummy kinetics as well. The average CORA rating scores of neck and lumbar forces increased from under 0.77 to above 0.934.

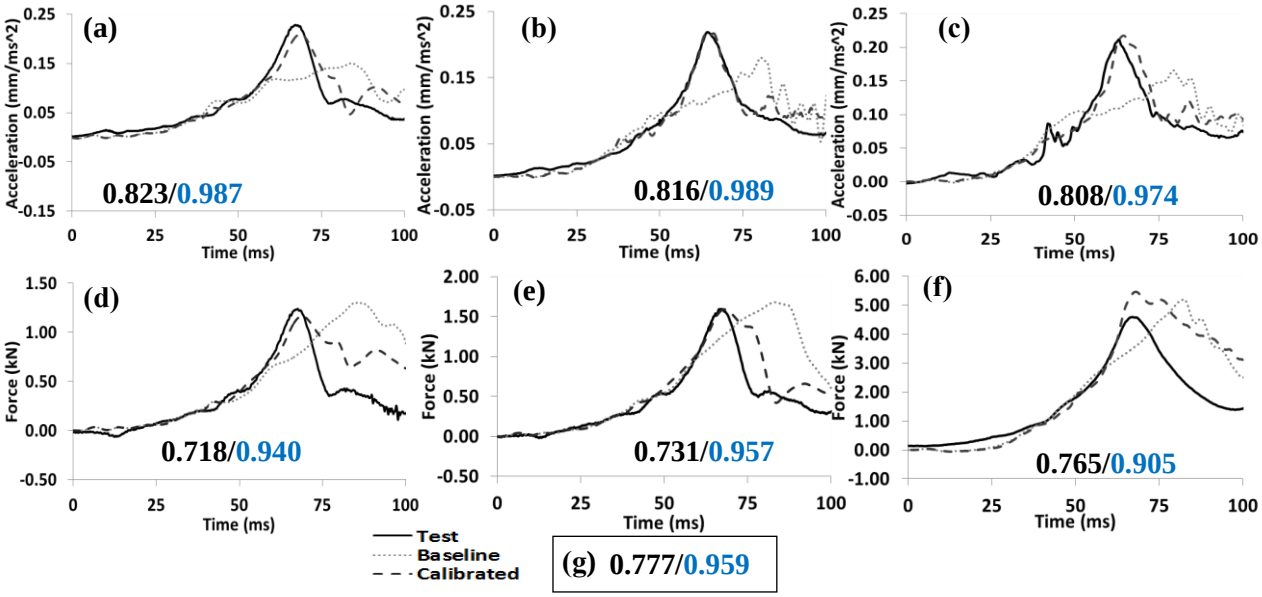

Figure 4-11. Model Spinal Calibration – pulse 10g @ 70 ms impact time history comparison in vertical direction: (a) head CG acceleration, (b) chest acceleration, (c) pelvis acceleration, (d) upper neck force, (e) lower neck force, (f) lumbar spine force, (g) total CORA rating.

An improvement of the calibrated model response in frontal loading was observed as well. However, the overall CORA model rating increased only slightly from .858 to .883 during the calibration process (Fig. 4-12). While the majority of dummy responses were improved with scores above 0.97 in the calibrated model (4 from 7 signals), the pelvis acceleration and lower neck force response ratings decreased. Oscillations in pelvis horizontal acceleration and the continuous increase of the horizontal neck lower force continued to be predicted by the model, but were not observed in testing.

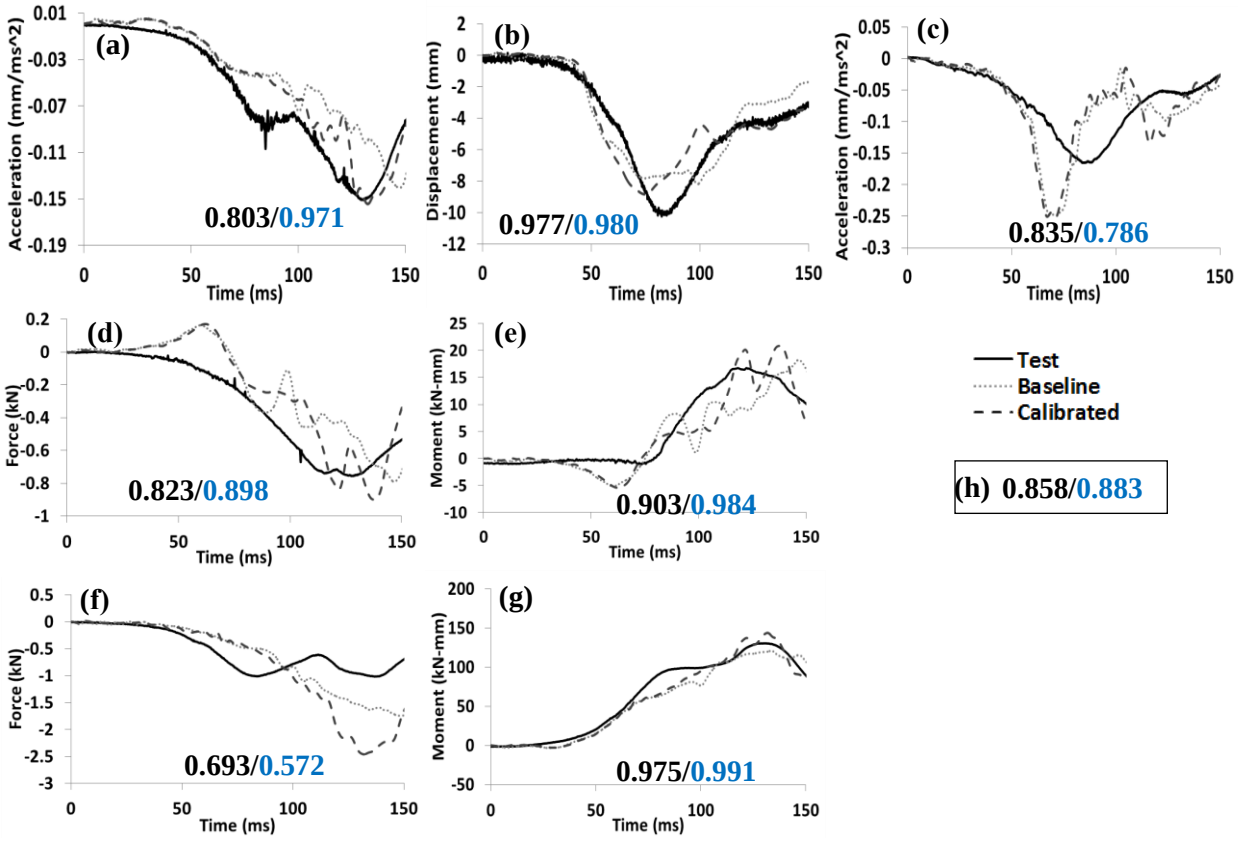

Figure 4-12**.** Model Frontal Calibration – pulse 10g @ 70 ms impact time history comparison in horizontal direction: (a) head CG acceleration, (b) chest TRACC displacement, (c) pelvis acceleration, (d) upper neck force, (e) upper neck moment, (f) lower neck force, (g) lower neck moment, (h) total CORA rating.

4.4.2 Validation of Dummy FE Model

4.4.2.1 Validation of Dummy FE Model under Spinal (Vertical) Loading

The calibrated THOR-k FE model closely predicts dummy response under spinal loading, receiving an overall CORA rating of .969 (Fig. 4-13). As in the calibration, there are some slight differences in lumbar spine and upper neck kinetics between FE simulations and test data. The lumbar load force is slightly higher than the test data and the upper neck unloading rate is slightly lower. Otherwise, the dummy response time history is very well predicted by the FE model in all instrumented areas.

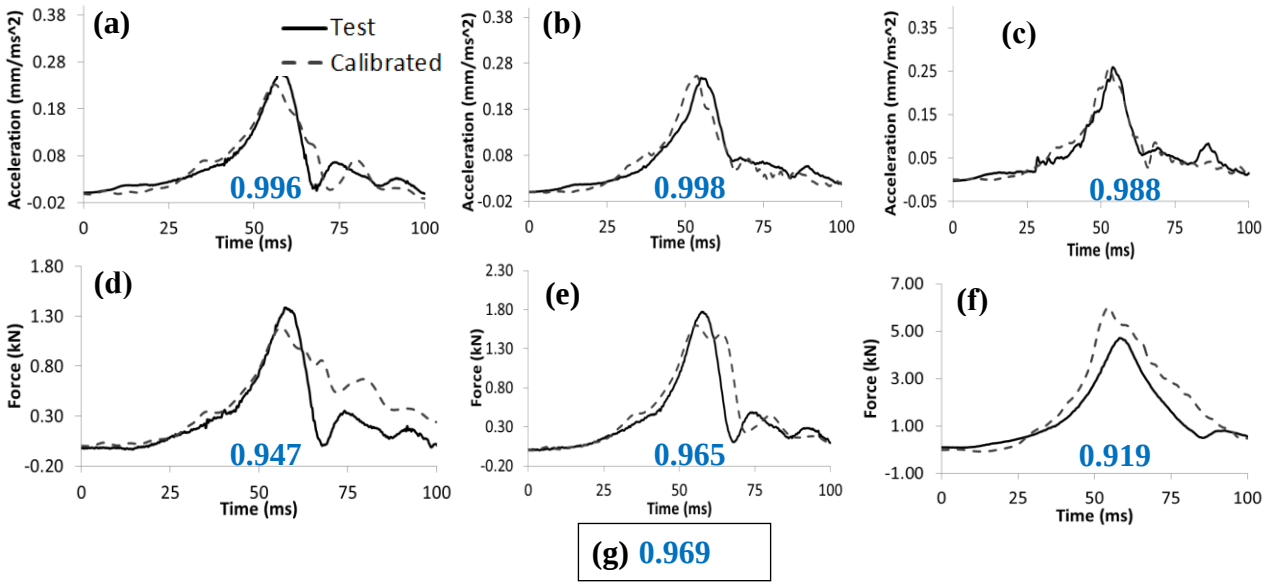

Figure 4-13. Model Spinal Validation – pulse 10g @ 40 ms impact time history comparison in spinal direction: (a) head CG acceleration, (b) chest acceleration, (c) pelvis acceleration, (d) upper neck force, (e) lower neck force, (f) lumbar spine force, (g) total CORA rating.

4.4.2.2 Validation of Dummy FE Model under Frontal Loading

During validation, the THOR-k FE model reasonably predicts the response of the ATD in an independent frontal loading test case (Fig. 4-14). The model response received a total CORA score of 0.89. As in calibration, the horizontal pelvis acceleration and lower neck force predicted by the model showed the same trends (not observed in testing) and consequently resulted in the lowest CORA scores (around 0.77).

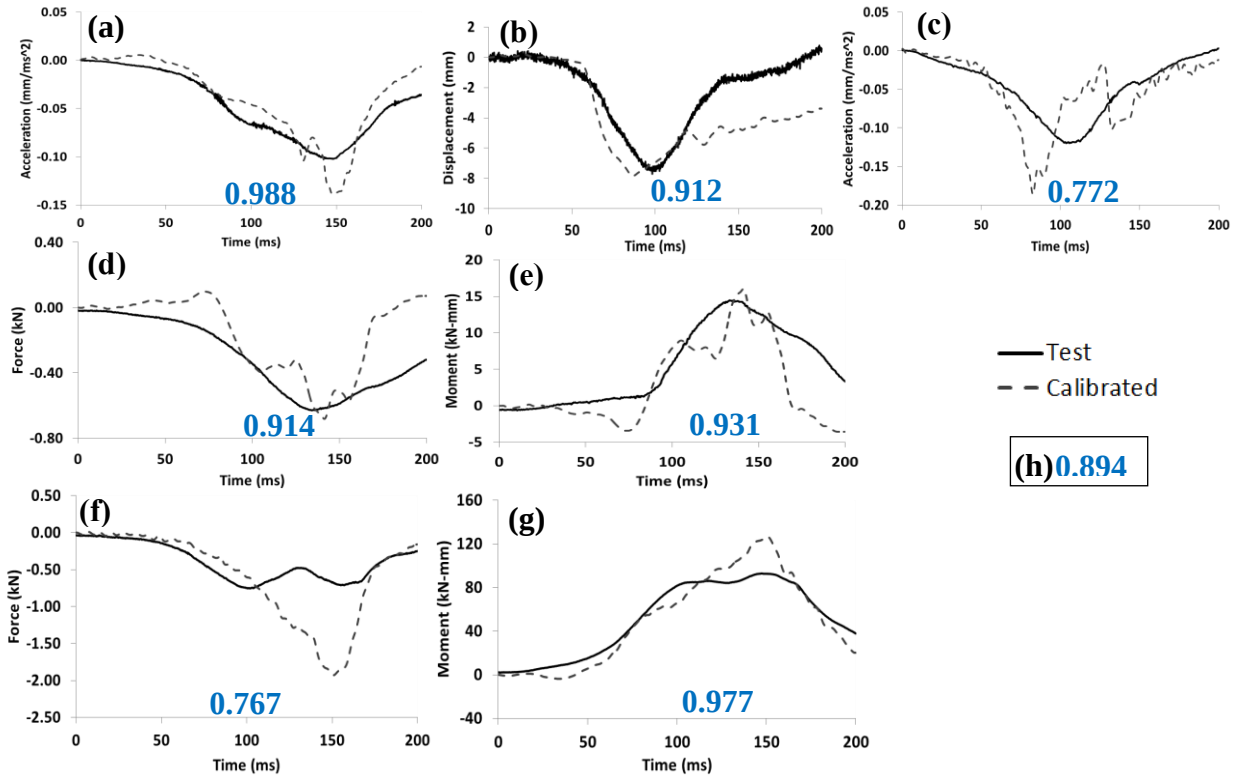

Figure 4-14. Model Frontal Validation – pulse 8g @ 100 ms impact time history comparison in horizontal direction: (a) head CG acceleration, (b) chest TRACC displacement, (c) pelvis acceleration, (d) upper neck force, (e) upper neck moment, (f) lower neck force, (g) lower neck moment, (h) total CORA rating.

4.4.3 Comparison to human response

4.4.3.1 Spinal Loading

When comparing the THOR-k responses to human responses in spinal loading, the acceleration response of the THOR-k FE model generally falls within the range of human response in each spinal impact test condition evaluated (Fig. 4-15). Head acceleration unloads faster in the THOR model than average human response, in the 8 and 10g pulse tests. A total average CORA score of 0.95 was achieved over all three impact conditions, indicating a good prediction of average human volunteer response. In addition, the total biofidelity rating of 4.2 indicates an acceptable rating for use in predicting human response in these test conditions.

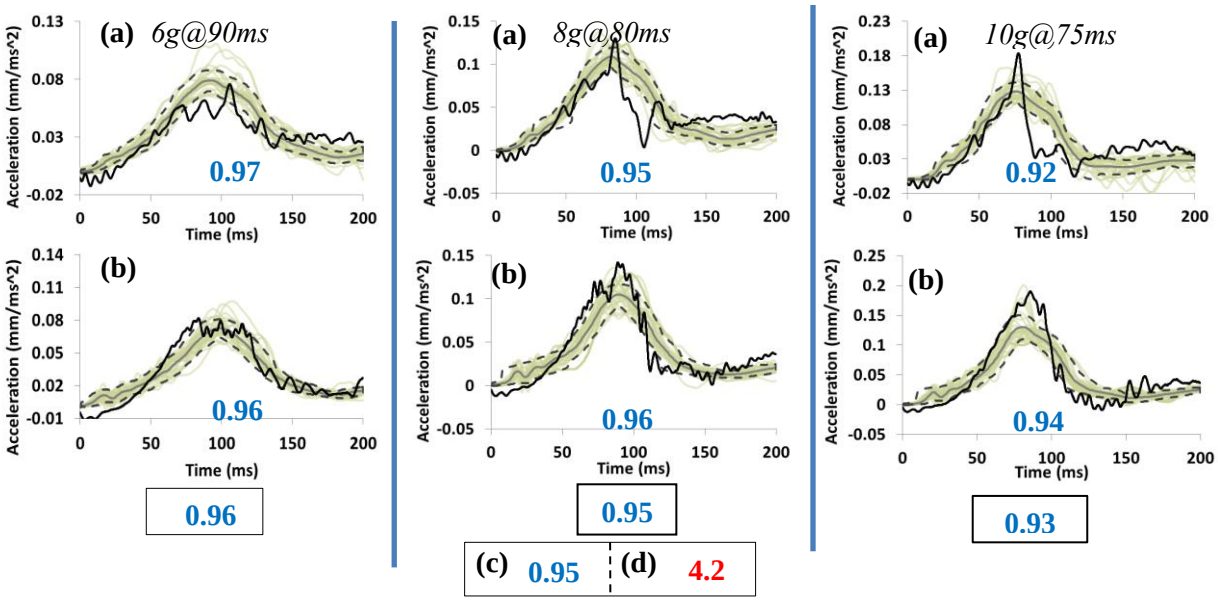

Figure 4-15. Dummy FE model vs. Human volunteer Comparison: Kinematic responses under spinal loading: (a) head acceleration, (b) chest acceleration, (c) total CORA rating, (d) total bio-fidelity rating.

4.4.3.2 Frontal Loading

A lower response correlation between THOR-K FE data and human volunteer test data is observed in the horizontal direction compared to the spinal direction (Fig 4.16). Over all three impacts, there is a delay in the THOR-K head acceleration compared to the characteristic human response; this difference decreases slightly with increasing pulse acceleration. The total average CORA score calculated relative to the average human horizontal responses was 0.91. The overall chest acceleration time history exhibits a better shape compared to the test data, although the response is much noisier. Towards after initial peak response both dummy model head and chest exhibit spikes not observed in human response. The total biofidelity rating is 2.5, just under the score for an acceptable prediction of human like response.

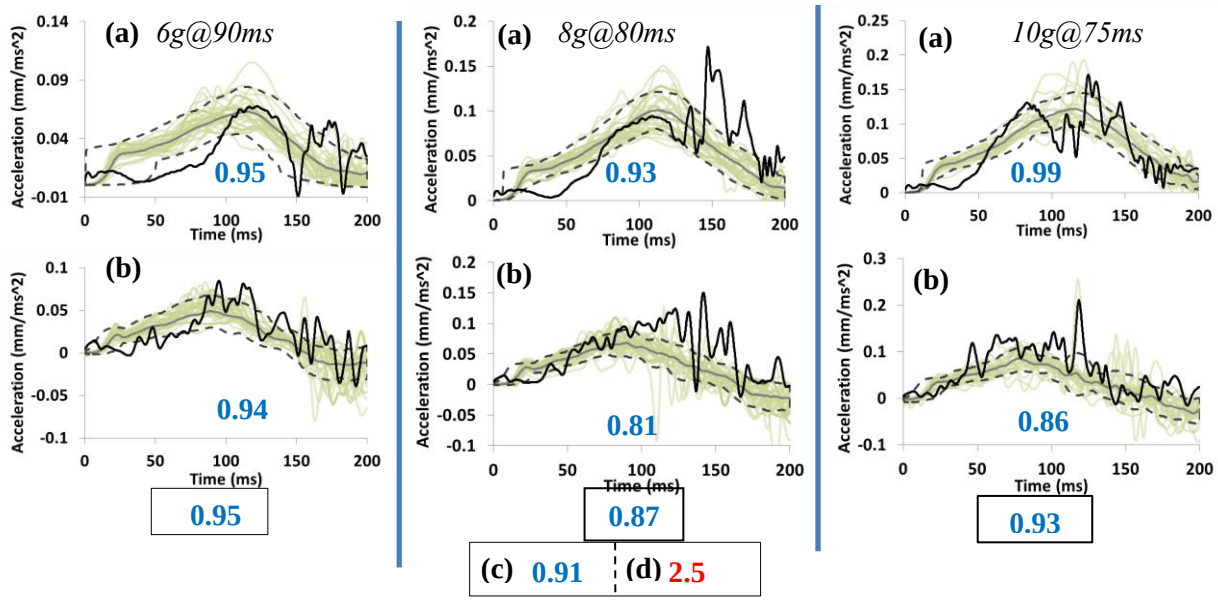

Figure 4-16**.** Dummy FE model vs. Human volunteer Comparison: Kinematic responses under frontal loading: (a) head acceleration, (b) chest acceleration, (c) total CORA rating, (d) total bio-fidelity rating.

4.5 Discussion

In the field of spaceflight occupant protection it is essential to acquire a test device which accurately mimics human response under impact conditions that crewmembers may be typically subjected to. The 50th percentile THOR ATD was chosen by a team of experts as the primary ATD to be evaluated for new NASA standards and requirements [25]. In the current study, a finite element model was developed, calibrated, and validated to accurately predict the response of the THOR-k ATD in complex impact events. Previous work on the THOR FE model has been primarily geared towards automotive crash analysis which is mostly focused on the dummy response under frontal impact loading [6, 26]. In this study, for the first time, key components to the THOR model's response in both spinal and horizontal impacts were identified and calibrated to accurately predict dummy response under loads characteristic of spaceflight impacts. Calibration was performed using a unique optimization protocol based on quantitative comparisons of simulation response to test time-history data. The time-history signals used in the calibration process were carefully chosen to evenly calibrate the full spectrum of dummy kinetic

and kinematic responses (head, thorax, and pelvis regions). In addition, constraints were added in the calibration protocol to ensure the model matched the dummy response in terms of current injury criteria standards. This calibration protocol has been shown to be effective, as the prediction of dummy responses in both spinal and frontal simulations were improved. Furthermore, validation simulations proved the robustness of the calibration process, so the model responses could be trusted beyond the test conditions used in the calibration process.

Finally, the THOR-k FE model was used to evaluate the dummy's biofidelity in spaceflight conditions based on previously collected human volunteer test data. FE modeling provides the unique ability to re-create these testing conditions for new dummy's, such as the THOR-k, without the expense of extensive physical testing. In the future human FE models [27, 28] may be used in conjunction with the developed THOR model to develop new injury criteria specific to spaceflight loading conditions.

4.5.1 THOR-k FE Model Calibration and Validation

The THOR-k model calibration resulted in large changes to the stiffness characteristics of the material models corresponding to the lumbar joints and pelvis flesh. A decreased stiffness in the pelvis paired with an increased stiffness in the spinal column led to a more accurate transfer of energy through the dummy FE-Model, along the spinal direction. This resulted in a sharper acceleration response throughout the model, better predicting the dummy kinematics. In addition to the improved kinematic response, an improved response shape of the neck loading was observed. Lumbar spine load also exhibited an improved shape, although the calibration was unable to bring the peak load down to match the test data. This difference may be caused by some model inaccuracies in terms of the loading path and energy dissipation in pelvic and abdomen regions. For example, the abdomen modeling (e.g. the gap between the foam parts)

should be further investigated, as this plays a role in offloading the spine when the foam parts come in contact.

The material model calibration improved the predicted shapes of head acceleration and chest deflection by stiffening the head response and allowing for greater chest deflection. However, the most significant model discrepancies were not improved with the updated material models. The change in pelvis stiffness had little effect on pelvis acceleration in the horizontal direction; therefore, other mechanisms such as the contact friction defined between seat and model should be further examined. Although the calibration improved the upper neck loading no improvements were observed in the lower neck loading and pelvis acceleration. As the source of these inaccuracies was not clearly determined in this study it is suggested that a future review of the THOR-k updates in these regions and their implementation in the model be performed. In addition the stress-strain response of the part material models were changed significantly from their original state in this optimization. Because no specific part material information is publically available for the THOR-K it is hard to determine the accuracy of these materials models and if optimization is improving part characterization or compensating for other inaccuracies in the model. Specific material testing is necessary to make this determination.

4.5.2 Biofidelity Analysis

The comparison of the THOR-k FE model and human volunteers under spinal loading, showed good biofidelity of the THOR-k in terms of the head and chest acceleration. One difference that is observed though, is head acceleration predicted by the dummy model was shown to fall more rapidly after peak response then human as the test pulse increased. As this was not observed in chest this may be an indication of a stiffer unloading response in the upper spine/neck region of the dummy. The part materials used in this region may be re-assessed to

improve the dummies dynamic unloading properties in the vertical direction. Though analysis of head and neck response provides a decent assessment of dummy biofidelity in the spinal direction, future analysis of remaining body regions should be performed to give a concrete determination.

The horizontal response of the THOR-k FE model, compared to the human volunteer test data, indicates some inaccuracies in the ATD response under frontal loading. Head acceleration predicted by the THOR-k FE model exhibits an initial lag in compared to the human test data, with this lag increasing with increasing input pulse. After this lag model head acceleration does rise quickly to decently approximate the point of average peak human acceleration. Since the THOR-k FE model approximated relatively well the physical ATD in these regions under frontal loading, the FE model vs. human volunteer differences observed in frontal impact indicate biofidelity limitations of THOR-k in this impact condition. The delayed peak acceleration present in the head acceleration is an indication of a slower transfer of energy through the upper spine and neck region, compared to human response. This may be due to the upper spine region being too soft in tension. The THOR-k modification reduced the neck stiffness to better match post mortem human subject (PMHS) test data [7] and the FE head neck model was calibrated to this response [8]. PMHS testing does not account for the resting muscle tone and possible active bracing in human volunteers [29] which would lead to a stiffer the neck response, possibly explaining the softer initial response of the THOR-k model compared to the active human volunteers. Thorax differences between the THOR and human volunteer may also play a role in the differences observed in frontal loading. Although, general thorax acceleration response is similar, there also exists a slight delay in response at the onset of the impact. Initial PMHS corridors of thoracic force-deflection, for thoracic ATD certification were generated using a hub-

impact test condition[30, 31]. It has been shown that the thoracic mechanical response depends strongly on the load distribution [32] and the geometrical characteristics of the ribcage and on its biological material properties [33]. Difference in thorax biofidelity may be explained by the different thorax loading in the examined condition, due to belt loading, compared to the hub-impact tests used in biofidelic cerification. These possible limitations should be examined further in future development of the THOR dummy to improve its biofidelity in this condition.

The two CORA rating systems used to provide a quantitative evaluation of the THOR biofidelity in these loading conditions demonstrate the need for rating standardization. When compared to average human response using the basic CORA rating system, with no adjusted parameters the FE model scores above .9/1 in both loading directions. From this score alone if may be judged that the model and thus THOR is very biofidelic receiving close to a perfect match based on this score. On the other hand when using the corridor method, defined for the ISO biofidelity rating system the model scores a 4.1/10 the spinal direction and 2.5/10 in the frontal direction. Looking at these scores alone one may conclude that the model barely if at all exhibits acceptable levels of biofidelity in these testing directions. The reason for the low biofidellity corridor rating is the noise exhibited by the model causes portions of the response to fall outside the defined 1 SD corridor in every comparison; reducing the rating score although the response shape may generally be accurate. On the other hand the corridor automatically generated by CORA in the average curve comparison is much larger resulting in a much less conservative score. Without standardized criteria these scores are currently effective only in providing a quantitative means of comparison between different test conditions or the effect of model improvements and should not be used to conclude the degree of dummy biofidelity.

Overall the THOR-k FE model developed in this study has shown to effectively predict dummy response in both spinal and frontal loading. In frontal loading a few regions could use further improvement, with this known the FE model can be used as an effective tool for performing crew crash safety analysis of future spaceflight vehicles in their typical loading environments. In addition the THOR FE model has been used to demonstrate the ATD's biofidelity in spinal loading, closely matching average human response and demonstrating acceptable biofidelity within the range of human variability. Differences observed between dummy and human response in the horizontal direction may be used to improve upon its design in the future to increase its effectiveness as a tool to predict human injury in these conditions.

4.6 Acknowledgments

This work was funded by the NASA Human Research Program through the Bioastronautics Contract (NAS9-02078). The authors would also like to thank to Toyota for meshing the updated pelvis FE model, and NHTSA for providing the THOR ATD for testing and the pelvic test data. All findings and views reported in this manuscript are based on the opinions of the authors and do not necessarily represent the consensus or views of the funding organization.

4.7 References

1. Newby, N., et al., *Assessing Biofidelity of the Test Device for Human Occupant Restraint (THOR) Against Historic Human Volunteer Data.* Stapp Car Crash J, 2013. **57**: p. 469-505.
2. Shaw, G., J. Crandall, and J. Butcher, *Comparative evaluation of the THOR advanced frontal crash test dummy.* International Journal of Crashworthiness, 2002. **7**(3): p. 239-253.
3. Untaroiu, C.D., J. Shin, and J.R. Crandall, *A design optimization approach of vehicle hood for pedestrian protection.* International Journal of Crashworthiness, 2007. **12**(6): p. 581-589.
4. Bose, D., et al., *Influence of pre-collision occupant parameters on injury outcome in a frontal collision.* Accid Anal Prev, 2010. **42**(4): p. 1398-407.
5. Adam, T. and C.D. Untaroiu, *Identification of occupant posture using a Bayesian classification methodology to reduce the risk of injury in a collision.* Transportation Research Part C-Emerging Technologies, 2011. **19**(6): p. 1078-1094.
6. Untaroiu, C., et al., *Evaluation of a finite element of the Thor-NT dummy in frontal crash environment*, in *ESV Conference*2009: Stuttgart, Germany.

7. Ridella, S.A. and D.P. Parent, *Modifications to improve the durability, usability and biofidelity of the THOR-NT dummy*, in *The 22nd ESV Conference*2011: Washington, D.C., USA.
8. Putnam, J.B., J.T. Somers, and C.D. Untaroiu, *Development, Calibration, and Validation of a Head-Neck Complex of THOR Mod Kit Finite Element Model.* Traffic Inj Prev, 2014.
9. Yue, N., et al., *Updates of the lower extremity of THOR-NT 50th finite element dummy to Mod Kit Specification*, in *23rd Enhanced Safety of Vehicles (ESV)*, ESV, Editor 2013: Seoul, Korea.
10. Putnam, J.B., et al. *Validation and sensitivity analysis of a finite element model of THOR-NT ATD for injury prediction under vertical impact loading* in *AHS International 69th Annual Forum*. 2013. Phoenix, AZ, USA: AHS International.
11. LS-Dyna, *Keyword User's Manual*, 2007, LSTC.
12. Mike Beebe, P.D., *THOR-NT Pelvis, Femur, Knee Revisions*, 2010, NHTSA.
13. Sakuma, I., et al., *In vitro Measurement of Mechanical Properties of Liver Tissue under Compression and Elongation Using a New Test Piece Holding Method with Surgical Glue*, in *Surgery Simulation and Soft Tissue Modeling*, N. Ayache and H. Delingette, Editors. 2003, Springer Berlin Heidelberg. p. 284-292.
14. Strzelecki, J.P., *Characterization of Horizontal Impulse Accelerator Pin Profiles, (AFRL-HE-WP-SR-2006-0057)*, 2005.
15. Jacob, C., et al., *Mathematical models integral rating.* International Journal of Crashworthiness 2000. **5**(4): p. 417-432.
16. Gehre, C., H. Gades, and P. Wernicke, *Objective Rating of Signals using Test and Simulation Responses*, in *ESV Conference*2009: Stuttgart, Germany.
17. Pellettiere, J. and D. Moorcroft, *Occupant calibration and validation methods*, in *Advances in Applied Human Modeling and Simulation*, V.G. Duffy, Editor. 2012, CRC Press: Boca Raton, FL. p. 307-316.
18. Untaroiu, C.D., J. Shin, and Y.C. Lu, *Assessment of a dummy model in crash simulations using rating methods.* International Journal of Automotive Technology, 2013. **14**(3): p. 395-405.
19. Sarin, H., et al., *A Comprehensive metric for comparing time histories in validation of simulation models with emphasis on vehicle safety applications*, in *ASME International Design Engineering Technical Conference and Computers and Information in Engineering Conference (DETC' 08)*2008: New York, USA.
20. Thunert, C., *CORA Release 3.6, User's Manual*, 2012, PDB.
21. Buhrman, J., *The AFRL Biodynamics Data Bank and Modeling Applications*, 1998: Dayton, OH.
22. Cheng, H. and J. Buhrman, *Development of the AFRL Biodynamics Data Bank and Web User Interface*, in *SAE Technical Paper 2000-01-0162*, SAE, Editor 2000: Detroit, MI.
23. Untaroiu, C.D. and Y.C. Lu, *Material characterization of liver parenchyma using specimen-specific finite element models.* J Mech Behav Biomed Mater, 2013. **26**: p. 11-22.
24. Moore, B., et al., *On the bulk modulus of open cell foams.* Cellular Polymers, 2007. **26**(1): p. 1-10.
25. Somers, J.T., et al., *Investigation of the THOR Anthropomorphic Test Device for Predicting Occupant Injuries during Spacecraft Launch Abort and Landing.* Frontiers in Bioengineering and Biotechnology, 2014. **2**.
26. Putnam, J.B., et al., *Finite Element Model of the THOR-NT Dummy under Vertical Impact Loading for Aerospace Injury Prediction: Model Evaluation and Sensitivity Analysis.* Journal of the American Helicopter Society, 2014. **(in press)**.
27. Danelson, K.A., J.H. Bolte, and J.D. Stitzel, *Assessing astronaut injury potential from suit connectors using a human body finite element model.* Aviation, space, and environmental medicine, 2011. **82**(2): p. 79-86.
28. Thompson, A., et al., *A paradigm for human body finite element model integration from a set of regional models.* Biomedical sciences instrumentation, 2011. **48**: p. 423-430.

29. Beeman, S.M., et al., *Occupant kinematics in low-speed frontal sled tests: Human volunteers, Hybrid III ATD, and PMHS.* Accid Anal Prev, 2012. **47**: p. 128-39.
30. Kroell, C.K. and D.C. Schneider. *Impact tolerance and response of the human thorax biomechanics of impact injury and injury tolerances of the thorax-shoulder complex*. in *15th Stapp Car Crash Conference*. 1971.
31. Lobdell, T.E., et al., *Impact Response of the Human Thorax*, in *Human Impact Response*, W. King and H. Mertz, Editors. 1973, Springer US. p. 201-245.
32. Kent, R., D. Lessley, and C. Sherwood, *Thoracic response to dynamic, non-impact loading from a hub, distributed belt, diagonal belt, and double diagonal belts.* Stapp Car Crash Journal, 2004. **48**: p. 495.
33. Gayzik, F.S., et al., *Quantification of age-related shape change of the human rib cage through geometric morphometrics.* Journal of Biomechanics, 2008. **41**(7): p. 1545–1554.

5. CONCLUSION

The work presented in this thesis represents one effort of many others to develop and improve occupant safety standards for the fields of aerospace and spaceflight transportation. This particular effort was to develop a reliable and accurate FE model of the THOR crash dummy, to be used to analyze the effectiveness of THOR as a test device for these fields. In this work the THOR-NT FE model was initially simulated in a series of drop tests to evaluate its performance under spinal loading, a subsection of the desired loading regime. Results demonstrated the model effectiveness in predicting the initial dummy response to impact; however, further calibration was required to have full confidence in total response accuracy. Sensitivity analysis of dummy position within this test setup indicated slight changes in both head and thorax positioning to have an effect on resulting injury criteria predictions. To account for recent modifications made to the THOR dummy (called THOR Mod Kit), updated parts in the head-neck region were meshed and integrated back into the THOR FE head-neck region model. A calibration method was then developed and used to ensure the updated head-neck model accurately reflected dummy response. Validation of this model region indicated successful part development and calibration approach. The developed THOR FE model regions were integrated into the full body THOR-k FE model. After integration, the model was calibrated and subsequently validated in frontal and spinal loading scenarios simultaneously, with remaining regions of inaccuracy identified. The developed THOR-k FE model was then simulated under conditions of human volunteer tests performed in both frontal and spinal directions. The THOR-k was shown to accurately predict the kinematic response of human volunteers to spinal impacts, but is less effective at predicting response during frontal impacts in these conditions. Overall, the results of this work indicate good potential for THOR-k as a tool to accurately predict occupant safety in multidirectional

impacts. Though to improve its viability effort may be made to better tune the dummy parts to match live volunteer test data rather than PMHS.

5.1 Future Work

An FE model is an approximation of a real object, its development and improvement is a continuous process. The THOR FE model developed in this work demonstrated good prediction of dummy response but there is still room for improvement. Future studies may focus to identify the cause of inaccuracy observed in the lower neck and pelvis response in the frontal impact setup. In addition material testing of deformable parts used in the latest THOR dummy could be used to more accurately define the part material models.

The developed THOR-k FE model will be used by NASA to further asses the biofidelity of the THOR dummy under a broad range of impact conditions. In this future work the THOR model will be assessed against a large number of additional human volunteer tests. The developed model may also be used to assess dummy response in full scale crash simulations. Injury assessment reference values (IARV's) will need to be developed for the THOR dummy in these loading conditions to relate dummy output to actual prediction of human injury risk. The THOR FE model should be used in conjunction with injury predictive human body models (THUMS, GHBMC) to develop these IARV's through extensive simulation of various aerospace and spaceflight impacts. This will lead to improved safety standards which will affect superior occupant vehicle design to reduce risk of injury and fatalities in these emerging transportation fields.